

BULLETIN 54

Volcanic Rocks of the Cienega Area,
Santa Fe County, New Mexico

*by MING-SHAN SUN
and BREWSTER BALDWIN*

*Sequence and geochemistry of Cenozoic
volcanic rock units, with a discussion of
the norm classification*

1958

**STATE BUREAU OF MINES AND MINERAL RESOURCES
NEW MEXICO INSTITUTE OF MINING & TECHNOLOGY
CAMPUS STATION SOCORRO, NEW MEXICO**

NEW MEXICO INSTITUTE OF MINING & TECHNOLOGY E.
J. Workman, *President*

STATE BUREAU OF MINES AND MINERAL RESOURCES
Alvin J. Thompson, *Director*

THE REGENTS

MEMBERS EX OFFICIO

The Honorable Edwin L. Mechem *Governor of New Mexico*
Mrs. Georgia L. Lusk *Superintendent of Public Instruction*

APPOINTED MEMBERS

Robert W. Botts Albuquerque
Holm O. Bursum, Jr. Socorro
Thomas M. Cramer Carlsbad
John N. Mathews, Jr. Socorro
Richard A. Matuszeski Albuquerque

Contents

	<i>Page</i>
ABSTRACT	1
INTRODUCTION	3
Purpose	3
Setting	3
Previous work	5
Method of work	5
Acknowledgments	6
FIELD RELATIONSHIPS (by Brewster Baldwin)	7
Stratigraphy	7
Cretaceous mudstone	8
Galisteo formation	8
Andesite breccia	10
Augite monzonite	11
Calcic latite	12
Glassy latite	13
Units of uncertain stratigraphic position	14
Volcanic conglomerate	14
Augite basalt	14
Hornblende andesite dike	14
Vent breccia	15
Felsite dike	15
Cieneguilla limburgite	15
Ancha formation	18
Basalt	18
Terrace gravel	19
Alluvium	19
Cover	19
Age and correlation	19
Structure	23
LABORATORY STUDIES (by Ming-Shan Sun)	26
Petrography	26
Introduction	26
The term "monzonite"	26
Andesite breccia	27

	<i>Page</i>
Augite monzonite	29
Calcic latite	30
Hornblende andesite	31
Glassy latite	31
Felsite	32
Vent breccia	33
Cieneguilla limburgite	33
Olivine basalt	34
Limburgite	34
Basalt	35
Petrology	36
Norm classification	38
Weight norm	40
Molecular norm.....	41
Norms of the Cienega rocks	45
Geochemical aspects	45
Index of refraction	45
General discussion	45
Artificial glasses	48
Chemical composition	51
Minor constituents	51
Major constituents	54
APPENDIX I	59
Rules for the calculation of norms.....	59
Weight norm	60
Molecular norm	64
APPENDIX II	69
Summary of data from rock samples, Cienega area, New Mexico	69
REFERENCES	74
INDEX	77

Illustrations

TABLES

1. Rock units of the Cienega area, New Mexico	7
2. Orthoclase-plagioclase ratios of the Cienega monzonite, latite, and andesite, in comparison with those of Daly's average monzonite, andesite, and diorite	27

	<i>Page</i>
3. Grain-size analysis of disintegrated andesite breccia	28
4. The C.I.P.W. weight norms of seven volcanic rocks, Cienega area, New Mexico	43
5. The molecular norms of seven volcanic rocks, Cienega area, New Mexico	44
6. Effect of various oxides on the index of refraction of glasses of binary or ternary system with silica	46
7. The ionic density of the cations which occur as modifiers in silicate glass	47
8. Lower limits of spectrographic detection	51
9. Minor constituents of the Cienega volcanic rocks	53
10. Chemical composition of seven volcanic rocks, Cienega area, New Mexico	54
11. Modified Holmquist formulae	55
12. Calculation of standard rock cell of olivine basalt of the Cienega area	56
13. Calculation of the ionic volume percentage of the average igneous rock of Clarke and Washington (H ₂ O included)	57
14. Ionic (elementary) composition by volume of the volcanic rocks of the Cienega area, New Mexico	58

FIGURES

1. Sketch map and section of the Cienega area, New Mexico	4
2. Columnar section of the Galisteo formation	9
3. Columnar section of the Cieneguilla limburgite	17
4. Oxide variation diagram	36
5. Cation variation diagram	37
6. Variation diagram of total oxygen versus cations	39
7. Index of refraction versus SiO ₂	49
8. Classification of the volcanic rocks of the Cienega area, New Mexico, according to the indices of refraction of their artificial glasses	50

PLATES

1. Geologic map and sections of the Cienega area, Santa Fe County, New Mexico	In pocket
2. Setting of the Cienega area	Frontispiece
3. Features of volcanic rocks	Following 26
4. Photomicrographs of volcanic rocks	Following 26
5. Photomicrographs of volcanic rocks	Following 26
6. Photomicrographs of volcanic rocks	Following 26

Abstract

Detailed mapping of the Cienega area, which is 5 miles square and is situated 14 miles southwest of Santa Fe, New Mexico, indicates the following sequence of volcanic and sedimentary units of Cenozoic age: The Eocene and Oligocene(?) Galisteo formation, of sandstone and red mudstone, is overlain conformably by andesite breccia. Those units were domed by intrusion of augite monzonite. The andesite breccia is correlative with the second igneous period of the Cerrillos area, 5 miles to the southwest (Disbrow and Stoll, 1957); the monzonite is correlative with the fourth igneous period.

Erosion exposed the monzonite. Extrusion of calcic latite flows and breccia, glassy latite breccia, and the Cieneguilla limburgite followed in sequence. The Cieneguilla limburgite (Stearns, 1953-b) consists of flows and tuff-breccia of limburgite and olivine basalt, possibly of Miocene age. Augite basalt, a conglomerate of volcanic pebbles, a hornblende andesite dike, a vent breccia, and a felsite dike are probably older than the limburgite, but their position in the sequence is uncertain. During the making of the Rio Grande trough, rocks of the Cienega area were faulted and tilted 10 degrees northeastward. The rocks were then eroded.

In late Pliocene or Pleistocene time, the area was covered by at least 100 feet of sand and gravel of the Ancha formation. Basalt flowed over the western part of the area, diverting the ancestral Santa Fe River. Hills of monzonite and of limburgite stood above the gravel- and basalt-covered plain. In Quaternary time, the Santa Fe River cut as much as 400 feet below this plain, revealing the Tertiary sedimentary and volcanic units. The geologic map of the area, scale of 1:15,840, indicates the places where samples were collected for laboratory study.

Petrographic descriptions are given for each of the volcanic rock types noted above. The definition of "monzonite" is discussed on the basis of the molecular norm of various rocks. The approximately equal amounts of (modal) orthoclase and (modal) plagioclase in the definition of monzonite and latite are here considered to be the equivalent of a normative orthoclase-plagioclase ratio of 30:70. Six spectrographic analyses show that the minor constituents — vanadium, chromium, cobalt, and nickel — are inversely proportional to the silica content of the rocks. Vanadium is stored in pyroxene, instead of in olivine, which is rich in basic rocks. In basic rocks, the amount of nickel exceeds that of cobalt. The cobalt-nickel ratio of calcic latite is 2.67; the cobalt-nickel ratio of glassy latite and monzonite is 1.

About 80 rock samples were powdered and fused to form artificial glasses, and the index of refraction was determined for each glass. Complete chemical analyses were made for seven of these samples, and the silica content only was determined for 14 additional samples. Of the

21 points on the curve of silica content versus index of refraction, 19 are within 2½ percent silica, or 0.010 in index, and 2 points are within 5 percent, or 0.020 in index. The index of refraction aided in assigning some samples to their proper geologic units and in approximating the silica content of the samples. The index depends on silica content and on other constituents and factors.

Chemical analyses of glassy latite, andesite breccia, monzonite, calcic latite, basalt, and olivine basalt (a flow of Cieneguilla limburgite) are given. An analysis of limburgite, reported by Stearns (1953-b), is also used. Variation diagrams of these seven rock types illustrate oxides versus silica, cations versus silicon, and total oxygen versus cations. The seven rock types are presented in terms of molecular and weight norms. Both kinds of norm are described, and rules for calculation are stated. The molecular norm has several advantages over the weight norm. The major constituents of the seven rock types are calculated in terms of the Holmquist formula, which represents the "standard rock cell." The total cations in each standard cell is taken as 100, and the oxygen number of the cells varies from 162 for glassy latite to 139 for limburgite. The oxygen number decreases from the acidic rocks to the basic rocks. The total volume of the ions of each rock is calculated. Discounting the empty spaces between ions and between mineral grains, oxygen forms 92 percent by volume of the "average igneous rock" of Clarke and Washington (1924).

The main volcanic units, with approximate percentage of silica, are given in stratigraphic sequence: Andesite breccia of Oligocene age, 55-61; hiatus, during which there was one period of monzonitic intrusion and extrusion in the Cerrillos area; augite monzonite, 58-61; calcic latite, 55-60; glassy latite, 62-69; hiatus, with erosion and possibly tilting; Cieneguilla limburgite (including olivine basalt), 39-46; hiatus, with erosion and then deposition of the Ancha formation; basalt of Pleistocene(?) age, 50. Thus, subcrustal disturbances must have shifted the parent basaltic magma, permitting the differentiates to reach the surface in a sequence independent of their composition.

Introduction

PURPOSE

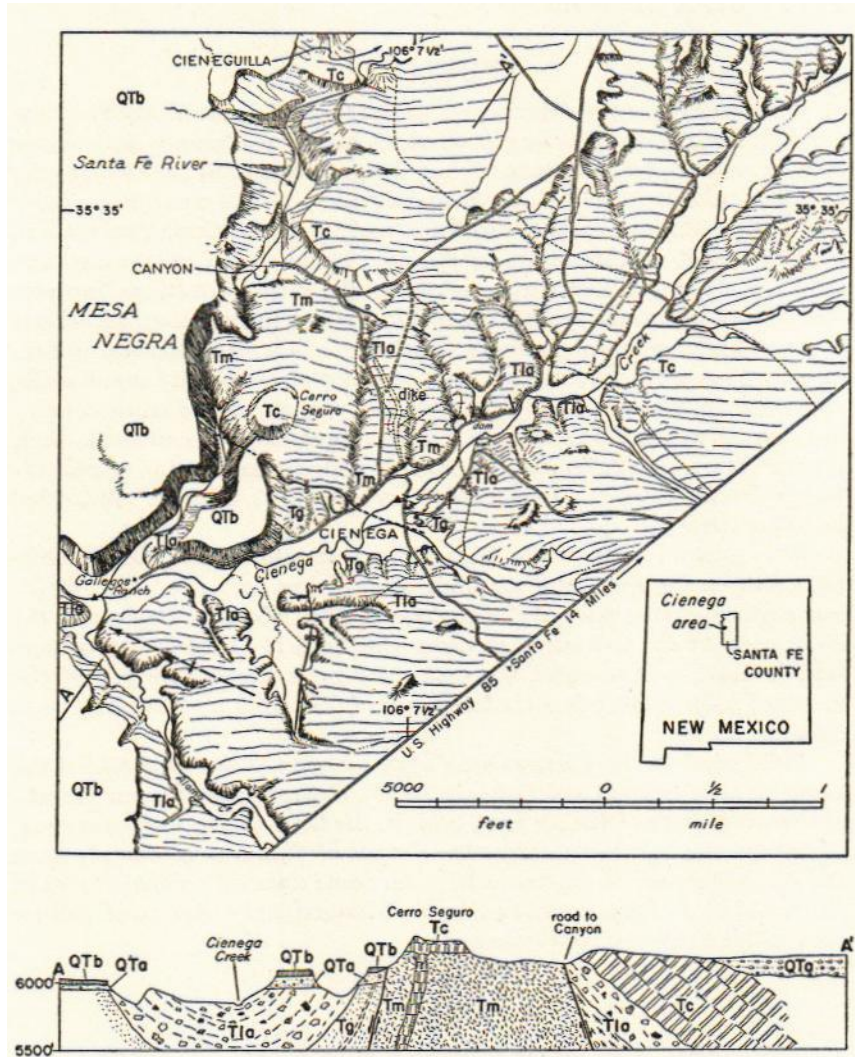
This report presents the results of field and laboratory study of the volcanic rocks of the Cienega area, which have a moderately wide range in composition and a sequence that is significant both in stratigraphy and in petrology. Field study is summarized by a large-scale geologic map (pl. 1), showing sample localities, and by description of rock units, with emphasis on the nature of geologic contacts and on the inferred sequence of units. Laboratory study of the field collections includes microscopic examination of hand specimens and thinsections, and chemical and spectrographic analyses of selected rocks. In addition, indices of refraction were determined for a number of artificially fused rocks, and these indices not only gave a clearer picture of the silica content but also were of considerable aid in assigning particular samples to their proper rock units. Breccias and flows of andesite and latite, previously lumped in the Espinaso formation (Stearns, 1953-b), are here subdivided into three units.

The present study of the Cienega area should be valuable in indicating the techniques and methods of studying volcanic rocks, which form an important part of the geology of New Mexico. Therefore, the evaluation of the technique of measuring indices of refraction of artificially fused rock samples, the molecular norm classification, and the modified Holmquist formulae for standard rock cells are treated in some detail.

Field work in the Cienega area began as part of the mapping of the Santa Fe area (Spiegel and Baldwin, 1957). However, preliminary results of the work on the Cienega area, both in the field and in the laboratory, prompted the decision to treat the details of this area separately from the general report of the Santa Fe area. Some data on volcanic rocks in the remainder of the Santa Fe area and immediately adjacent localities are included here for convenience.

SETTING

The Cienega area, which is about 5 miles square, is 14 miles southwest of Santa Fe, New Mexico, and includes parts of Tetilla Peak and Turquoise Hill 7½-minute quadrangles. The area is situated where the Santa Fe River and its main tributary, Cienega Creek, join to flow westward toward the Rio Grande through a canyon cutting into Mesa Negra (fig. 1). U. S. Highway 85 is arbitrarily taken as the southeast border of the area, and several secondary roads provide ready access to the communities within the area: La Cienega, Cieneguilla, and Canyon. The southern, western, and northern limits are the blanketing basalt flows and gravel. Hills stand above the gravel- and basalt-covered surface, and



SKETCH MAP AND SECTION OF THE CIENEGA AREA, NEW MEXICO

QTb, basalt flow; QTa, Ancha formation (not shown on map); Tc, Cieneguilla limburgite; Tla, latitic to andesitic flows and breccias; Tm, augite monzonite; Tg, Galisteo formation.

Figure 1

the Santa Fe River and its tributaries have cut as much as 400 feet below the surface (pl. 2A, B).

The dissection here has locally removed late Pliocene or early Pleistocene gravels and basalt flows to reveal the "bedrock floor" of Eocene sedimentary rocks and Oligocene-Miocene(?) volcanic rocks. These rocks, and the Cerrillos ("little hills") several miles to the south, are part of La Bajada constriction, an upfaulted element of the Rio Grande structural trough (Kelley, 1952, 1954). A fault on the southwest side of La Bajada constriction forms the abrupt northeast limit of the Santo Domingo structural basin, and geophysical studies in the Santa Fe area (Spiegel and Baldwin, 1957) suggest that a fault on the northeast side of the constriction similarly separates this element from the Santa Fe embayment of the Espanola basin to the north and east.

The "bedrock floor" is thus at the surface at Cienega. To the east, water from heavy local precipitation and from mountain runoff seeps down into the sand and gravel underlying the plain. This water seeps westward through the sand and gravel, but at the Cienega area it comes to the surface as seeps and springs because of the ground-water barrier formed by the volcanic rocks. "Cienega" means "marsh" or "miry place." The perennial flow of the Santa Fe River and Cienega Creek has for many years been diverted to irrigate crops, both on the alluvial terrace of Cienega Creek and at Cieneguilla, situated at the upper end of the canyon of the Santa Fe River, northwest of Cienega. The moist green valley of Cienega Creek is in marked contrast with the sandy arroyos farther east and north.

The Oligocene-Miocene(?) igneous rocks of the Cienega area represent the northernmost volcanic center known in the north-trending chain of centers of monzonitic-latic activity that includes the Cerrillos, the Ortiz Mountains, and others.

PREVIOUS WORK

Stratigraphic and structural features of the region have been set forth by Stearns (1943, 1953-a, 1953-b). Disbrow and Stoll (1957) made a fairly detailed study of the intrusive and extrusive rocks of the Cerrillos area, which includes the Cienega area.

METHOD OF WORK

Field mapping was carried on by Baldwin, and the laboratory study was performed by Sun. Aerial photographs on a scale of 1:28,000 served as a base for field mapping, which began in 1951 and continued intermittently until 1954. Critical contacts were remapped on enlargements to 1:20,000. Parts of the new topographic sheets of the Tetilla Peak and Turquoise Hill 7½-minute quadrangles were enlarged to 1:10,000. Field

data were transferred to this base map by means of a focalmatic reflecting projector (Reed 513), manufactured by Reed Research, Inc., of Washington, D. C. Field work was concerned with mapping the distribution of the rock units and with determining their sequence. In this connection preliminary results from laboratory study of the field collections were of aid in assigning some of the rock outcrops to their proper units.

Laboratory study of the volcanic rocks involved several techniques. Although 43 thinsections were examined, the fine-grained groundmass of most of the rocks prevented accurate estimates of composition. Seven rocks are represented by complete chemical analyses (including an analysis of limburgite [Stearns, 1953-b]) and by spectrographic analyses. Fourteen additional samples were analyzed for silica only. Refractive-index determinations of artificial glasses made of these and 59 other samples served to supplement the understanding of composition. X-ray diffraction was employed to identify some of the minerals in the rock.

Data for the rock samples are summarized in Appendix II.

ACKNOWLEDGMENTS

Eugene Callaghan drew attention to some of the problems of the Cienega area and pointed out the fundamental difference between the two latitic units. Field and office conferences with him have been most useful. W. M. Bundy assisted in the earlier mapping, and W. M. Burand prepared some of the rocks for fusion. Appreciation is also due the people of the Cienega area for their help and information. Discussions with C. E. Stearns and with A. E. Disbrow have been most stimulating, and contributed to a better understanding of the geology. C. S. Treseder prepared the photographs of Plates 2 and 3 from Kodachrome transparencies.

Field Relationships

By BREWSTER BALDWIN

STRATIGRAPHY

The principal rock units of the Cienega area (table 1) fall into four groups. The first group includes Cretaceous mudstone, the Galisteo formation of Eocene age, and andesite breccia. Augite monzonite, the only unit of the second group, has intruded and domed rocks of the first group. The third group consists of calcic latite flows and breccias, glassy latite breccias, and the flows and breccias of the Cieneguilla limburgite, each resting with at least erosional unconformity on the preceding unit. Rocks of the first three groups are faulted, tilted, and eroded. In late Pliocene or early Pleistocene time, sand and gravel of the Ancha formation and basalt flows, constituting the fourth group, buried most of the older rocks.

This sequence of units has been established on the basis of field relationships that are in part indirect, and so the following description

TABLE 1. ROCK UNITS OF THE CIENEGA AREA, NEW MEXICO

Basalt flows	In part, olivine-bearing	LATE(?) PLIOCENE TO EARLY(?) PLEISTOCENE
Ancha formation	Sand and gravel; 0-300 ft	
————— angular unconformity —————		OLIGOCENE TO MIDDLE(?) MIOCENE
Cieneguilla limburgite	Flows of olivine-augite limburgite and some olivine basalt; interbedded with tuff-breccia; 700 ft	
Glassy latite	Flow breccia; gray; 400 ft	
Calcic latite	Flows and flow breccias; brownish-gray; 400 ft	
Augite monzonite	Stock of brownish-gray porphyritic monzonite	
Andesite breccia	Flow breccia; gray, brownish-gray, and reddish-orange; 600 ft	
Galisteo formation	Yellow sandstone, red mudstone, and minor conglomerate; 1,300 ft	
Undifferentiated sedimentary rocks	Dark-gray, red, and white mudstone, in fault slivers	CRETA- EOCENE CEOUS

of the units is concerned both with the nature of each unit and with the nature of the contacts between units. Most of the units, sedimentary, volcanic, and intrusive alike, are treated in what is believed to be the chronologic order, but several outcrops with uncertain position in the sequence are described separately. Petrography and petrology of these units are described in subsequent parts of the report. Data from rock samples are given in Appendix II; sample localities are shown in Plate 1.

CRETACEOUS MUDSTONE

Three outcrops of mudstone are interpreted as fault slivers of Cretaceous rocks. The first, by the bridge near the Cienega school, is intruded by a dike of hornblende andesite. The Cretaceous rock here consists of laminated dark-gray mudstone that resembles Mancos shale 6 miles to the southwest and also 4 miles down the Santa Fe River. At the second outcrop, at the junction of the road toward the Gallegos ranch with the road toward Canyon, red laminated siltstone and shale dip 27° N., toward the monzonite. These sedimentary rocks are more thin bedded and fine grained than is usual for the Galisteo formation and so are interpreted as being Cretaceous, and their red color is ascribed to the effect of the intrusive monzonite. The third outcrop, in the gully 4,300 feet northeast of the Gallegos ranch, is a fault sliver between the Galisteo formation and the monzonite. The material here is a white conchoidally fractured siltstone showing a few prints of a ribbed shell that resembles the clam *Inoceramus*. Similar material occurs as float 1,200 feet farther southeast along the fault between the Galisteo formation and the monzonite. Although Mesozoic formations are well exposed in the vicinity of the Cerrillos (Stearns, 1953-a, pl. 1), the outcrops of Cretaceous mudstone at Cienega cannot be assigned with certainty to a particular formation.

GALISTEO FORMATION

In the Cienega area, the Galisteo formation crops out southeast, south, and southwest of the monzonite, and the beds commonly dip 25° - 40° away from the intrusion. Fragments of petrified wood represent the only fossils found, and the formation was recognized by its lithology and general stratigraphic position. Nowhere in the area was the stratigraphic base of the Galisteo observed. The uppermost strata of Galisteo lithology are interbedded with the lowest beds of the andesite breccia.

About 1,300 feet of Galisteo was measured on the north side of Cienega Creek (fig. 2). The lower 500 feet is fairly well exposed in the gully 4,200 feet northeast of the Gallegos ranch, just east of a nearly isolated basalt-capped mesa. In this gully, the Galisteo formation consists predominantly of fine- to coarse-grained, yellow to red, well-sorted sandstone, interbedded with red siltstone and silty fine-grained sandstone. A few red clayey beds were noted, but the clay content of the beds is less in the Cienega area than elsewhere in the region (C. E.

Stearns, oral communication). The covered intervals in the lower part of the section are probably represented by silty fine sandstone and mudstone. The upper part of the section, as measured along the talus-covered southern slope of the basalt-capped mesa, is about 800 feet thick. This interval is probably represented by the sandstone, conglomeratic sandstone, and red mudstone that crop out on the south side of Cienega Creek. Conglomerates, which occur in several parts of the section, contain a variety of rock types, including chert, limestone, granite, and schist.

The gradational upper contact can be studied most readily in the roadcut 2,700 feet east of the Gallegos ranch (pl. 3A). Just north of the road at the east end of the outcrop, red mudstone is overlain by a 20-foot ledge of crossbedded conglomeratic sandstone containing pebbles of Precambrian granite. This ledge is overlain by 16 feet of red silty clay and soft sandstone. The sandstone grades upward (west along the road) into soft-weathering volcanic conglomerate or tuff-breccia that contains scattered grains of quartz and pink feldspar. At the west end of the roadcut, a ledge-forming conglomeratic sandstone, containing pebbles of chert, quartz, and minor Precambrian granite, is in fault contact with the volcanic breccia to the east.

The transitional nature of the contact between the Galisteo formation and the andesite breccia is still better demonstrated in the tributary valley southeast of Cienega Creek. About 1,000 feet east of where the felsite dike crosses this tributary valley, red sandstone and mudstone lie on top of stream-bedded soft-weathering volcanic tuff-breccia and are overlain by similar tuff-breccia. Also, pebbles of volcanic rocks form a few layers half a foot thick interbedded with layers of Galisteo lithology.

The fault that trends southward from the felsite dike is bordered on one or both sides by the transitional beds immediately above the Galisteo formation. In the structure sections the top of the Galisteo formation is arbitrarily taken as the base of the lowest layer of tuff-breccia, but on the geologic map the individual outcrops near the fault are shown according to lithology.

ANDESITE BRECCIA

Andesite breccia, which is exposed south and southwest of the monzonite, is estimated to be 600 feet thick. The lowest 50 to 100 feet consists of soft, locally disintegrated, crudely bedded tuff. The lower part of the andesite breccia is gray to brownish gray and it is covered on many slopes by gravel from the overlying Ancha formation and by rubble from the breccia itself. The upper part, a welded breccia with a reddish-orange matrix, forms a cliff on the south side of the Santa Fe River, just downstream from the mouth of Cienega Creek.

Above the basal "soft zone" the andesite breccia is poorly bedded, poorly sorted, and contains blocks up to a foot across. Both boulders

and matrix are characterized by needles of hornblende, white crystals of feldspar, and aggregates of ferromagnesian minerals. Most of the rock fragments in the andesite breccia appear to be composed of hornblende monzonite or hornblende andesite.

The andesite breccia rests with gradational contact on the Galisteo formation, but it is not found in contact with any of the other volcanic units, except for the crosscutting dikes of limburgite and felsite. However, blocks of hornblende-bearing volcanic rock are present in the fault breccia in the valley 1,800 feet due south from the west end of the dam. Also, sample 119, which was collected from a small outcrop southeast of the dam, is evidently a hornblende monzonite of uncertain relationship.

AUGITE MONZONITE

The intrusive monzonite, which forms the core of the domelike structure of the Cienega area, is 4,600 feet by 11,600 feet in known horizontal dimension. The northwest half of this intrusion is represented by Las Tetillitas, an island of monzonite surrounded by the several Pleistocene(?) basalt flows. The monzonite of Las Tetillitas is inferred to be continuous with the mass of monzonite that crops out between the Santa Fe River and Cienega Creek (pl. 1, section D-D').

The monzonite is medium gray on fresh fractures but it is stained yellow to brown on the surface and along joints. Phenocrysts of feldspar and some augite can be seen in hand specimen, although most of the augite crystals have been removed by weathering. In some outcrops, a banded flow structure is so pronounced that, from a distance, the rock has the appearance of parallel-bedded sediments. This effect is due, megascopically at least, to differential weathering and staining along parallel joints. Brecciated zones, which can be seen on some weathered surfaces of the monzonite, are possibly intrusion breccias, formed as the pasty magma congealed locally and then was shattered by further intrusive movement. In general, however, the monzonite is homogeneous. It is resistant to weathering, for it stands above the main erosion surface that underlies the gravel and basalt flows.

In the vicinity of Canyon several outcrops indicate a "fossil" weathered mantle. Where the monzonite crosses the road leading to Canyon, monzonite blocks rest on a weathered surface of the monzonite and are interpreted as an ancient talus. This talus breccia can also be *seen* along the east side of the tributary gully east of the road (shown as Tm² on pl. 1), and again on the south side of the valley at Canyon.

The southwest and probably the northeast boundaries of the monzonite in the Cienega area are faults. The monzonite intrusion domed the Galisteo formation and the andesite breccia; the calcic latite appears to rest on the monzonite with erosional unconformity.

Only two outcrops of stratigraphic contact between the monzonite and the calcic latite are known. One outcrop is in a gully 600 feet S. 70°

W. from the west end of the dam. The contact zone is only about 2 inches wide, and monzonite fragments occur in the calcic latite breccia. It is not certain whether the contact dips steeply or gently. The other outcrop is on the north side of a gully 3,000 feet N. 70° W. from the west end of the dam. Here, the contact dips about 10° NE. It is believed that the breccia, which has an orange matrix and contains fragments of both monzonite (sample 185) and calcic latite, is a basal part of the calcic latite unit.

CALCIC LATITE

Flows and breccias of calcic latite are exposed east and northeast of the monzonite. The calcic latite appears to lie with erosional unconformity on the monzonite and is overlain with erosional unconformity by the glassy latite. The thickness is estimated at 400 feet, although exposures and structure within the unit are such that a reliable section could not be measured. In general, the calcic latite can be divided into three parts. The lowest part, which is well exposed in the reentrant on the northeast side of the monzonite, includes a remarkably angular breccia. Flows predominate in the central portion of the unit, and flow breccia is predominant in the upper part. Tuff and tuff-breccia may form much of the calcic latite unit, but they are generally covered.

The angular breccia, which occurs in the lower part of the calcic latite, is either a fault breccia or a flow breccia. The fragments forming the breccia are etched out by weathering, and range from a fraction of an inch to as much as a foot in diameter. They consist of only one rock type; namely, that of the calcic latite in the flows. The masses of breccia have an inferred stratigraphic thickness of about 30 feet, if indeed they are part of a stratigraphic unit. The field distribution is anomalous, for the breccia does not occur in a narrow band suggestive of a fault breccia, nor does it occur uniformly adjacent to the monzonite. On the other hand, the breccia apparently does not occupy the definite stratigraphic position that would suggest a flow breccia.

Angular breccia near the base of the calcic latite unit also crops out south of Cienega Creek 1,100 feet S. 20° E. from the west end of the dam. Here, as in several places north of the creek, the breccia is cemented in part by manganese oxide.

The flows are gray to brownish-gray, dense-grained rocks. Phenocrysts of feldspar measure 1 mm or less, and in some specimens of more granular rock, augite is also visible. On the west side of the dam (sample 74), vesicles form 5-10 percent of the rock; these vesicles are elongated north-south and are locally lined or filled with chalcedony. In the saddle 900 feet N. 25° W. from the west end of the dam (sample 13), vesicles form about a third of the rock.

The flow breccias, which are commonly marked by abundant small feldspar phenocrysts, are apparently restricted to the upper part of the calcic latite unit, where they occur as the broken crust of the uppermost

few flows. The best exposures are in the first cliff east of the dam (sample 72a). These breccias are brownish gray, and they grade downward into flows (sample 72b) that faintly show coarse brecciation. The breccia fragments contrast only slightly with the somewhat lighter colored matrix.

Southeast of Cienega Creek, the upper half of the calcic latite unit consists of a variable tuff-breccia, containing angular fragments of calcic latite. Samples 122 and 125 are composed of tuff with less than 10 percent of small included fragments; but sample 18 has less matrix and larger fragments, and in places the included fragments are 2 feet in maximum dimension. The tuff matrix commonly is readily weathered, leaving a veneer of angular blocks of calcic latite over the surface. Along the gully between samples 120 and 122, both matrix and fragments are weathered to a clay.

Northwest of Cienega Creek the tuff-breccia may form much of the middle part of the calcic latite unit. However, tuff-breccia here is poorly exposed and is perhaps represented only by weathered breccia north and northwest of the dam.

The two exposures of calcic latite on monzonite have been noted. Although the calcic latite is not seen in stratigraphic contact with the premonzonite units, it is inferred in the structure sections (pl. 1) to rest with angular unconformity on the Galisteo formation and the andesite breccia. On the southwest side of the gully that is 1,800 feet south from the west end of the dam, blocks of calcic latite and of hornblende andesite or hornblende monzonite occur in a matrix of red sandstone, and this outcrop is interpreted as a fault breccia between the Galisteo formation to the west and the calcic latite to the east.

Northeast of the monzonite, calcic latite flow breccia is overlain with erosional unconformity by the glassy latite unit (pl. 3C). In the only exposure of the contact, on the hill just east of the dam (by sample 92), the surface has several feet of relief. Considerably greater relief is indicated by the occurrence of glassy latite (1,800 feet east of the dam) some 80 feet below the knob of calcic latite tuff-breccia (1,600 feet southeast of the dam).

GLASSY LATITE

The sequence of glassy latite breccias is fairly well exposed along the road northeast of the dam, and again southeast of Cienega Creek. Northeast of the dam are two cliff-forming units: a lower series of unsorted welded breccias with a grayish-orange-pink matrix, and an upper series of crudely layered gray breccias (pl. 3B, C). The included fragments are light gray and light brownish gray to medium dark gray, and they occur in blocks up to 10 feet in maximum dimension. The glassy latite can be distinguished from the other volcanic units by the predominance of glass in the matrix and by the somewhat larger size of the feldspar phenocrysts.

The contact of the glassy latite on the calcic latite has been described. The glassy latite is not seen in contact with the monzonite, and in the vicinity of Canyon these units are probably separated by a northwest-trending fault.

Although the contact itself is not seen, limburgite may rest on the glassy latite with angular unconformity (pl. 1, sections A-A', B-B', C-C'). Northeast of the dam, the limburgite overlies a fairly thick sequence of the gray, upper part of the glassy latite, but near the road junction southeast of Canyon there appears to be little room for the gray breccias between the calcic latite and the limburgite (pl. 1, section A-A').

UNITS OF UNCERTAIN STRATIGRAPHIC POSITION

Five minor rock units which have been recognized in the Cienega area are difficult to assign accurately to the sequence of volcanic events. Therefore these units are described separately. On the geologic map (pl. 1) these units are given in their inferred order of formation.

Volcanic Conglomerate

The conglomerate of volcanic boulders exposed on the northwest bank of the Santa Fe River, north of the Gallegos ranch, contains a variety of prelimburgite rocks. Rocks possibly derived from andesite breccia (samples 173, 174), calcic latite (samples 176, 177), augite basalt (sample 182), vent breccia (sample 180), and glassy latite (sample 181) were collected. Limburgite and Pleistocene(?) basalt are not represented in the conglomerate. The conglomerate is crudely bedded and may represent a stream gravel that was deposited after extrusion of the glassy latite but before the Cieneguilla limburgite. On the geologic map (pl. 1) the volcanic conglomerate is not differentiated from the andesite breccia, because the assignment of pebbles to the major volcanic units is not certain.

Augite Basalt

Augite basalt, a brownish-gray granular rock with distinct augite phenocrysts, occurs at half a dozen localities within the limits of the calcic latite unit. At all these localities the rock is altered and in part brecciated. Contacts with adjacent rocks are not exposed and therefore relationships are uncertain. Because of field distribution and because of similarity to some parts of the calcic latite, the augite basalt is tentatively assigned to the calcic latite unit. However, samples 83 and 118, which are less altered than samples 20 and 123, resemble the Cieneguilla limburgite.

Hornblende Andesite Dike

The most prominent dike of the Cienega area is about 40 feet thick and is composed of brownish-gray andesite with conspicuous needles of

hornblende. Inclusions or "pods" of rock fragments and ferromagnesian minerals are fairly common. From the schoolhouse, where it forms two prominent knobs, the dike was traced N. 15° W. for about 4,300 feet. The dike is somewhat irregular in trend, owing, at least in part, to offsetting faults, and the observed dip in two outcrops is 85° W. and 30° E., respectively. North of Cienega Creek, the dike does not crop out boldly, and most of its length is marked only by a float of small particles of rock from which the hornblende crystals have been weathered.

Near the school, the dike occurs on the inferred contact between the monzonite and the Galisteo formation, (pl. 1, sections C-C', D-D'), and it intrudes what may be a fault sliver of Cretaceous mudstone. Farther north, the dike cuts both the monzonite and the calcic latite. It is not seen in contact with the glassy latite, but east of the dam a few small pieces of rock (sample 70) similar to the hornblende andesite were found near the base of the gray glassy latite breccia. If these pieces indeed represent the hornblende andesite dike, rather than the andesite breccia, the dike was intruded after the calcic latite but before the glassy latite.

Vent Breccia

Glassy gray-black rock fragments (samples 187, 189, 190) set in a gray-white ashy matrix form an outcrop about 200 feet across, about 1,500 feet N. 35° W. from the west end of the dam. The fragments are commonly about one inch across, but one block measured 3 feet in length. The outcrop is interpreted as a vent breccia (pl. 1, section B-B').

Felsite Dike

Grayish-pink felsite, with scarcely visible feldspar grains, forms a dike about 20 feet wide southwest of the monzonite. The dike crops out on the road to the Gallegos ranch (sample 3) and again on the south side of Cienega Creek, where it trends S. 40° E. The total length, including the intervals covered by alluvium, is about 2,400 feet. In the valley south of Cienega Creek, the felsite contains about 10 percent of flattened vesicles that are several millimeters long. Within a foot or two of the borders of the dike, the vesicles are minute or absent. What may be a faulted portion of the dike crops out about 600 feet northeast from the south end of the dike. The dike cuts across the Galisteo formation and the lower part of the andesite breccia and it is buried by the Ancha formation at both ends. If the dike is part of one of the recognized volcanic units, it is probably part of the glassy latite stage.

CIENEGUILLA LIMBURGITE

The Cieneguilla limburgite, named by Stearns (1953-b, p. 445) for the community of Cieneguilla, consists of flows of limburgite and olivine basalt interbedded with tuff and breccia. The type section is along the Santa Fe River, in the canyon between the villages of Cieneguilla and

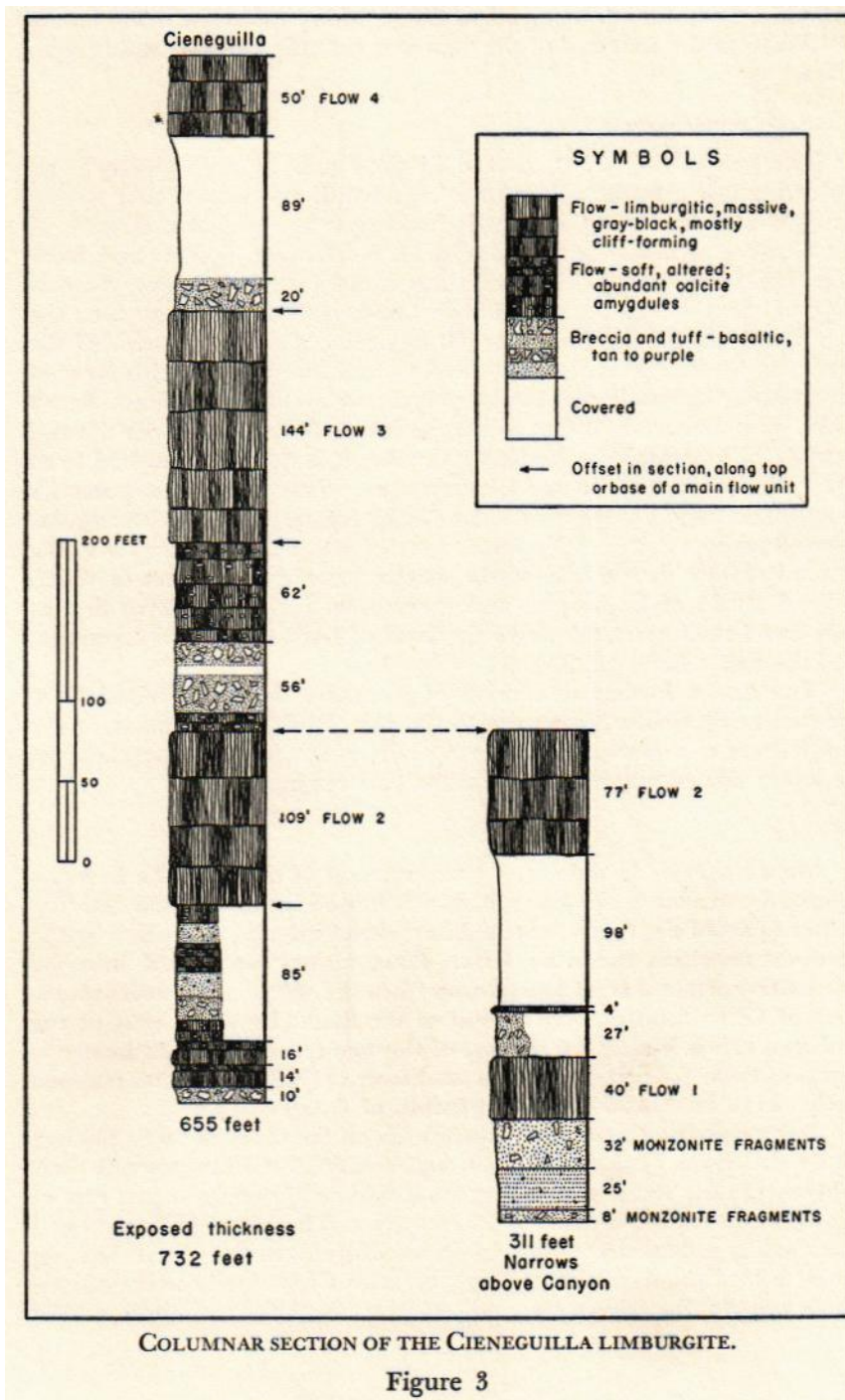
Canyon. The formation dips northeastward about 10° . The walls of the canyon are formed by four massive cliff-forming flows, which are separated by soft-weathering tuff, breccia, and vesicular to amygdaloidal flows. In one place (sample 141) there are two flows, each about 15 feet thick, and the upper third of each is abundantly amygdaloidal. Calcite commonly fills vesicles. The cliff-forming flow units, which range from 40 to 144 feet in measured thickness, are composed of gray-black dense-grained rock that contains small, brown olivine phenocrysts and exhibits a greasy luster on fresh surfaces. The main flows are not vesicular, but they are fractured by both vertical and horizontal joints.

Stearns (1953-b, p. 445-446) reports a total exposed thickness of 590 feet. The composite section measured by Baldwin and Bundy (fig. 3) totals 732 feet in thickness, but it was measured down the face of cliffs, with offsets along the top or bottom of a main flow unit, and so both the total thickness and the proportion of tuff and breccia to flows may be in moderate error.

The Cieneguilla limburgite crops out in the eastern part of the Cienega area and on the lava mesa near Las Tetillitas. Limburgite caps both Cerro de la Cruz and Cerro Seguro. Cerro de la Cruz, which was referred to as Calvary Butte by Stearns, is 3,500 feet S. 75° E. from the Turquoise Trading Post. Near the mouth of the Santa Fe River canyon (4 miles southwest of Cerro Seguro), two flows of limburgite dip westward, and Cieneguilla limburgite is exposed in two other localities farther to the southwest (Stearns, 1953-a, pl. 1; 1953-b).

Although the actual contact is not seen on Cerro Seguro, outcrops of limburgite and monzonite are separated only by narrow covered intervals. On the southwest side of the hill inclusions of monzonite (sample 49) occur in the limburgite. Stearns (1953-b, p. 447) states that the contact is nearly vertical and that the entire limburgite cap of Cerro Seguro represents a plug. A second interpretation (pl. I, section A-A') is that the capping limburgite is a flow, and that there may be a feeder under the southwest part of the hill. The absence of brecciated limburgite on Cerro Seguro is a point in favor of the latter interpretation.

Many thin grayish-black dikes, associated with the Cieneguilla limburgite, cut across the Galisteo formation, the andesite breccia, the monzonite, and the latitic flows and breccias. In hand specimen, the dike rocks are similar to the limburgite flows, although the former are altered in several localities. The dikes, which trend N. 12° W. to N. 27° E. through the Cienega area, are a few inches to 10 feet wide. Few dikes have continuous outcrops longer than 100 feet, although in several places a series of outcrops can reasonably be assigned to a single dike. The small black knob east of the road to Canyon (2,300 feet N. 70° W. from the west end of the dam; sample 109) is actually a dike about 10 feet wide, for it shows horizontal columnar jointing. Where this dike cuts across the hornblende andesite dike, the latter is offset about 10



feet. The two outcrops mapped as Cieneguilla limburgite 4,200 feet S. 70° W. from the west end of the dam may actually be dikes rather than flows.

ANCHA FORMATION

The Ancha formation, named in the Santa Fe area (Spiegel and Baldwin, 1957), forms a blanket of silt, sand, and gravel that is now being eroded from the Cieneguilla limburgite and earlier rock units of the Cienega area. Resistivity data by H. A. Winkler (Spiegel and Baldwin, 1957) suggest that the formation is 300 feet thick along the east edge of the Cienega area. However, throughout most of the area the formation is generally less than 100 feet thick. On the west side of the area, the Ancha formation is covered by and interbedded with flows of olivine-bearing basalt, and locally gravel rests on top of the flows. Basalt tuff is present about 20 feet below the lowest flow and though the tuff is mapped separately in the Santa Fe area, it is not distinguished from the Ancha formation in the Cienega area, where the tuff is generally intermixed with Ancha gravel. The Ancha formation rests with angular unconformity on the older rock units of the Cienega area, and the erosion surface at the base of the Ancha has about 500 feet of relief. Several knobs of limburgite and monzonite, including Cerro Seguro and Las Tetillitas, stand above the level of both the Ancha formation and the basalt flows (pl. 2A).

The Ancha formation consists of piedmont deposits derived from the Sangre de Cristo Mountains to the east. With the extrusion of the basalt flows, the westward drainage was diverted, and the ancestral Santa Fe River carried much gravel into the Cienega area.

BASALT

Mesa Negra de la Bajada, the upland west of the Santa Fe River, is capped by olivine-bearing basalt, which flowed southeastward into the western part of the Cienega area. After a brief interval of erosion by the diverted ancestral Santa Fe River, flows moved northward into the southwest corner of the Cienega area from the volcano 31/2 miles southwest of Cerro Seguro. The canyon of the Santa Fe River west of the Gallegos ranch is near the contact of the two sets of flows. At least two layers of flows are present in each set. Stearns (1953-a, pl. 1) has mapped both sets of flows as the Cuerbio basalt, of Quaternary age.

The aggregate thickness of the flows is on the order of 50 to 100 feet along the Santa Fe River canyon, and the flows thicken toward their sources. On the south side of the small basalt-capped mesa just east of the Gallegos ranch, the flow is 20 feet thick. The basalt cliffs are characterized by rude vertical jointing. In hand specimen the olivine-bearing basalt is medium to medium dark gray, with a few small olivine phenocrysts and smaller feldspar crystals set in an aphanitic groundmass; the

rock is characteristically fresh. Vesicles, some of which are filled with calcium carbonate, form only a few percent of the volume of basalt.

TERRACE GRAVEL

Many small patches of gravel form the ridgetops that flank Cienega Creek. These remnants rest on a surface that slopes towards Cienega Creek. Gravel was deposited by the ancestral Santa Fe River during its diversion in late Ancha time, and the terrace gravel was deposited by the tributaries of the Santa Fe River during the downcutting of the present canyon of the Santa Fe River. Not only are the field relationships of the Ancha gravel and the terrace gravel similar, but the terrace gravel consists of reworked Ancha material. Therefore, the terrace gravel is not distinguished on the map (pl. 1) from the Ancha formation.

ALLUVIUM

Alluvium, consisting of silt and sand, forms a narrow band along the Santa Fe River and it forms the broader valley of Cienega Creek. Cienega Creek has cut locally as much as 15 feet into its alluvial fill, and bedrock appears in the channel in only a few places. Therefore, the fill is probably 20 feet or more in thickness.

COVER

On the geologic map (pl. 1) "cover" is indicated in several ways. Covered areas of both the basalt and the Quaternary gravel are shown as a lighter value of the color used for the outcrop areas of these units. Soil- and rubble-covered areas of the other rock units are uncolored. In both instances no contact is shown between the outcrop areas and the covered areas of what is interpreted to be the same unit. In certain parts of the Cienega area, however, the symbol of "cover, undifferentiated," enclosed by a geologic contact, is used for the particular covered areas where reliable interpretation of the underlying rock unit is not possible. Such covered areas include the talus-covered slopes below the basalt cliffs and the lava mesa south of Las Tetillitas, where soil cover obscures the limits of the tongue of Ancha gravel between the two basalt flows.

AGE AND CORRELATION

Stearns' reconnaissance study (1943, 1953-a, 1953-b) and Disbrow and Stoll's study of the Cerrillos area (1957) included the Cienega area. The following comments are intended to clarify the different rock names and relationships of the Cienega area as they are treated in the several reports.

The outcrops mapped as Cretaceous mudstone in this report are shown as Mancos shale by both Stearns (1953-a, pl. 1) and Disbrow (Disbrow and Stoll, 1957, pl. 1).

The "Gallisteo [sic] sand group" was named for Galisteo Creek by

Hayden (1869). It was mentioned by later workers, but Stearns (1943) first described the Galisteo formation in detail.

The Galisteo formation is Eocene, and possibly lower Oligocene, in age. Robinson (1957) reports finding an upper molar of *Coryphodon* of Wasatchian age (lower Eocene) 700 feet above the base of the Galisteo formation, near Cerrillos. Titanotheres bones and teeth have been collected from Arroyo Pinovetito, 17 miles southeast of Cienega, both from the upper beds of the Galisteo formation and from the base of the conformably overlying volcanic sequence (Stearns, 1943, p. 310-311; Disbrow and Stoll, 1957). These fossils are essentially Duchesnean (late Eocene) in age.

According to Stearns (1943) the Galisteo formation consists mostly of sandstone, which is usually gray white or buff but which is locally yellow, brown, red, or pink. Lenses of fine conglomerate are abundant, and in many places one or two limestone conglomerates are found. Highly colored red, maroon, purple, green, brown, or gray clay, with sandy lenses, forms about a third of the formation. Limestone beds are found in a few places and tuffaceous beds are present in the upper part of the formation. Stearns measured 1,250 feet of Galisteo 2 miles west of the Cienega area in the canyon of the Santa Fe River and he reports a range of 900 to 4,300 feet in the area between Cienega, Lamy (16 miles to the east) and Hagan (16 miles to the south). The formation accumulated as an alluvial deposit in a basin formed by the Laramide orogeny. This area was at that time characterized by a warm and moderately or seasonally humid climate and by perennial streams that drained southwestward and southeastward from forested uplands. Petrified wood and a few collections of mammal bones represent the known life of that time. The Galisteo formation was deposited with angular unconformity on Upper Cretaceous beds and was buried with no appreciable break by volcanic materials of the Espinaso formation. (Stearns, 1943.)

In the Cienega area the Galisteo formation grades up into the andesite breccia. A similar transition zone is noted in Stearns' type section (1953-b, p. 422) of the Espinaso volcanics in Arroyo Pinovetito, and locally the volcanics of Disbrow's second period of igneous activity in the Cerrillos rest conformably on the Galisteo. Stearns (1953-b, p. 427-428) presents a reasonable interpretation of the ending of Galisteo deposition by the extrusion of the Espinaso volcanics. It is at least implicit in all three studies that, although the upper part of the Galisteo formation contains volcanic pebbles, the base of the volcanics is taken as the base of the lowest flow, tuff, or breccia. Thus, beds of Galisteo lithology are locally included as part of the volcanic sequence.

The following summaries of the report by Stearns (1953-b) on the Espinaso volcanism and the report by Disbrow and Stoll (1957) will simplify the comparison of the Espinaso volcanics and associated intrusive rocks in the three studies.

In an unpublished manuscript on the Santo Domingo Valley by Bryan and Upson, the Espinaso volcanics were named for Espinaso Ridge, 16 miles southwest of Cienega. The volcanics, which rest conformably on the late Eocene Galisteo formation and are overlain by the Cieneguilla limburgite, are of latest Eocene age. The formation consists largely of alluvial deposits radiating from volcanic centers. Water-laid material predominates in the type section, but in the Cienega area the volcanics include large blocks and were probably deposited as mud flows. A few lava flows are known. Although the Espinaso volcanics are not subdivided, the intrusive rocks of the Cerrillos are separated on a basis of "texture and habit of intrusion" into fine-grained porphyries and medium-grained equigranular rocks. The fine-grained porphyries are inferred to connect with vents of late Espinaso time, and the equigranular rocks were probably significantly later, but with no known extrusive equivalents. (Stearns, 1953-b.)

Disbrow distinguished four periods of igneous activity in the Cerrillos. The first period was marked by intrusion of hornblende monzonite porphyry, with no recognized extrusive equivalents. Rocks of the second period consist of an intrusive mass of hornblende-augite monzonite porphyry, with associated extrusive hornblende-augite latite porphyry. The extrusive rocks include a thin basal soft tuff and an overlying red, moderately bedded tuff-breccia with scattered quartz grains; locally, a flow of hornblende-augite latite porphyry forms the base of the section. The third period is represented by at least 1,370 feet of light-gray or light-pink tuff and breccia of hornblende-augite latite porphyry associated with a few minor intrusive masses of hornblende-augite monzonite porphyry. Rounded quartz grains are present in the lower 300 feet, and going upward in the section augite decreases with an increase in hornblende. Aggregates of hornblende crystals and phenocrysts of hornblende and plagioclase are visible in hand specimen. The fourth period of igneous activity in the Cerrillos is represented largely by irregular stocks of augite-biotite monzonite, with some extrusive equivalents. The Espinaso volcanism "may span Oligocene and early Miocene time." (Disbrow and Stoll, 1957.)

The type section of the Espinaso volcanics may represent only the earlier phases of volcanism, though Stearns does include in the Espinaso volcanism all of the intermediate rocks in the vicinity of the Cerrillos. Stearns' excellent photograph (1953-b, pl. 1, fig. 2) of Espinaso volcanics near Cienega is a view westward across the road toward a cliff of glassy latite. This cliff is viewed from another direction in Plate 3B. Stearns did not subdivide the Espinaso volcanics in the Cienega area, but he made a distinction between the equigranular monzonite of Las Tetillitas and the intrusive porphyry of augite quartz latite beneath Cerro Seguro. Disbrow mapped the monzonite of Las Tetillitas with the same symbol as that for the mass beneath Cerro Seguro, namely as an augite-

biotite monzonite porphyry. The monzonite is presumably correlative with the youngest (fourth) period of igneous activity in the Cerrillos. Although Disbrow did not subdivide the volcanics of the Cienega area, he did (oral communication) identify the volcanics southwest of the monzonite (andesite breccia of this report) as being equivalent to the "soft tuff" and red breccia of his second period of igneous activity. The abundance of hornblende crystals in the hornblende andesite dike led Disbrow (oral communication) to assign the dike to the second period of igneous activity, although it cuts across both the monzonite and the calcic latite. The calcic and glassy latite units of the Cienega area have not been recognized in the Cerrillos by Disbrow, and they probably are younger than any other known occurrences of the Espinaso volcanics.

The age of the Espinaso volcanics is given by Stearns (1953-b, p. 430) as latest Eocene, whereas Disbrow (Disbrow and Stoll, 1957) states that the age "may span Oligocene and early Miocene time." In the present report, the age is considered to be some or all of the time between and including the late Eocene and the middle Miocene. The Duchesnean fossils collected from the top of the Galisteo formation and from the base of the volcanic sequence in Arroyo Pinovetito indicate that volcanic activity began in the late Eocene or early Oligocene. The volcanism ended before extrusion of the Cieneguilla limburgite, which conceivably might be as young as late Miocene.

Stearns (1953-b, p. 448) infers that the Cieneguilla limburgite is Oligocene or earliest Miocene, and Disbrow (Disbrow and Stoll, 1957) infers an early Miocene age. However, the age of the Cieneguilla can be only approximated, for the evidence is indirect. Stearns (1953-a, p. 471-472) tentatively correlates the Abiquiu(?) formation, which rests on the Cieneguilla limburgite 1½ miles southeast of La Bajada, with the Abiquiu tuff some 60 miles to the north. The Abiquiu tuff grades up into the Santa Fe formation (Smith, 1939, p. 955), which is presumably equivalent to the beds near Espanola that have yielded the Santa Fe fauna of late Miocene-early Pliocene age. However, Kottlowski (Spiegel and Baldwin, 1957) describes basalt flows interbedded in the lower part (probably late Miocene in age) of the Tesuque formation less than five miles north of Santa Fe, and these flows are possibly correlative with the Cieneguilla limburgite. On the Bajada constriction, the limburgite is overlain unconformably by the Ancha formation, and the Tesuque formation is here absent, although it is present to the northeast and to the southwest. From these lines of evidence, it is fairly certain that the Cieneguilla limburgite is late Miocene or older. More specific dating is not warranted by the available data.

The Ancha formation and the basalt flows rest with angular unconformity on the Tesuque formation (Spiegel and Baldwin, 1957) and so are younger than early Pliocene. The Ancha formation and the basalt flows are tentatively dated as early Pleistocene. However, a number of volcanic and topographic features of the region were formed after ex-

trusion of the basalt flows. Moreover, the Pliocene is from 5 to 10 times longer than the Pleistocene. Therefore, the Ancha formation and basalt flows might be Pliocene in age.

STRUCTURE

The regional structures that affect the Cienega area include igneous intrusion, middle Tertiary warping, and late Tertiary to Quaternary normal faulting.

Monzonitic rocks were intruded along a north-trending belt that includes the Ortiz Mountains, the Cerrillos, and the Cienega area. According to Stearns (1953-a, fig. 7) the Cienega area is on the west limb of the Galisteo structural basin, which was formed by faulting and broad folding of middle Tertiary time.

In late Tertiary time, basins and uplifts of the Rio Grande trough were formed by normal faulting. The Cienega area is situated on La Bajada constriction (Kelley, 1952, 1954), which is the northern extension of the Cerrillos uplift. The Santo Domingo basin lies to the southwest and the Santa Fe embayment of the Espanola basin lies to the northeast of La Bajada constriction. La Bajada fault (Kelley, 1954), called the Rosario fault by Stearns (1953-a, pl. 1), separates the constriction from the Santo Domingo basin, and the Cienega fault (Spiegel and Baldwin, 1957, pl. 5) separates the constriction from the Santa Fe embayment. The Cienega fault is inferred from the distribution of springs, from distribution of pre-Santa Fe rocks, and from geophysical data; the position of the fault is uncertain.

Within the Cienega area, the structure is dominated by the eccentrically exposed intrusion of monzonite, which has faulted margins on the southwest and north. Sedimentary and volcanic rocks of pre-Santa Fe Tertiary age dip away from the monzonite. Certain structural relationships bear on the sequence as presented under "Stratigraphy."

The Galisteo formation dips away from the monzonite at angles from 4° to 54° , but commonly 25° - 40° . Dips are steepest near the fault north of Cienega Creek and again in the vicinity of the school, and it appears that where the beds dip more steeply than 40° the fault is within 500 feet. The direction of dip ranges from S. 65° E. to S. 65° W., an arc of 130 degrees. Thus the Galisteo was evidently domed by intrusion of the monzonite and was further deformed later by drag along the fault.

Structure of the andesite breccia is less evident because of the unreliability of "bedding planes." However, field data do indicate that the unit is gently folded into a syncline which plunges gently northwest near the Gallegos ranch. The southwest dips on the northeast side are compatible with the dips of the Galisteo formation and thus are ascribed to doming by the intrusion. The northeast dips are essentially parallel with the dips of the Galisteo formation a mile down the Santa

Fe River from the Gallegos ranch; these northeast dips are on the west limb of the Galisteo structural basin.

A fault striking N. 63° W. separates monzonite on the northeast from the downthrown block of Galisteo formation and andesite breccia on the southwest. In a gully 4,400 feet northeast of the Gallegos ranch, the fault plane dips 60° SW. Although the contact here between the monzonite and the Galisteo is sharp, the two units are separated in places by slivers of Cretaceous mudstone dragged up along the fault, and just southeast of the Santa Fe River the Galisteo is brecciated. Northwest of the river, volcanic breccia is adjacent to the monzonite, either because of the nature of the preceding doming by the intrusion or because the displacement is greater there than farther southeast. The lower of the Pleistocene(?) basalt flows northwest of the river is raised about 10 feet on the southwest side of the fault, indicating minor renewed movement in the opposite direction.

A fault exposed on the northeast corner of the monzonite probably extends northwest to Canyon, forming the northern limit of the monzonite. In the gully 3,500 feet N. 43° W. of the west end of the dam, angular breccia of calcic latite on the north and east is faulted down against monzonite, the latter being brecciated locally. Nearby the monzonite has a smooth, curved surface sloping 45° NE., and this may be the fault plane. No other exposures of the fault were found, but indirect evidence indicates that the fault continues toward Canyon. About 200 feet northwest of the gully, outcrops of calcic latite end and 100 feet farther west glassy latite is next to the monzonite. This is probably due to faulting (pl. 1, section A-A'). Along the road leading down to Canyon a fault breccia is suggested by a small outcrop of red sandstone resembling the Galisteo formation and by large blocks of limburgite (sample 96) in a scant matrix of red sand. Although no displacement was noted either northwest of Canyon or southeast of the gully, 1,100 feet N. 18° W. of the west end of the dam the calcic latite is completely altered to an orange, soft material, possibly by hydrothermal activity along the southeastward extension of the fault. Another occurrence of similarly altered calcic latite, 800 feet S. 45° E. from the west end of the dam is not, however, along the projection of this line.

Determination of the attitude of the latite units is difficult because of the poorly defined "bedding planes." Although the directions of dip are somewhat erratic (pl. 1), they appear to be discordant with the direction of dip of the Galisteo formation half a mile away. Inasmuch as the andesite breccia is not found in contact with the calcic or glassy latite, the indirect structural evidence is critical, for it helps to confirm stratigraphic evidence that the andesite breccia is a volcanic unit distinct from the latite units. Whereas the Galisteo formation, and presumably the gradationally overlying andesite breccia, were domed by intrusion of the monzonite, the latite units appear to dip northeastward with no marked change in strike.

The Cieneguilla limburgite dips northeast and crops out in a north-west-trending belt. The northeast dip of the latite units and of the Cieneguilla limburgite is probably the regional dip of the west limb of the Galisteo structural basin.

Along the road to the Gallegos ranch, the Galisteo formation is faulted against the soft-weathering basal zone of the andesite breccia (pl. 3A). The poorly exposed fault plane seems to dip 26° NW., with the ledge of conglomeratic sandstone of the Galisteo formation occurring on the hanging-wall side. The contact is at a marked angle with that of the bedding of the sandstone and volcanic breccia, and a layer of red mudstone is cut out along the fault. Movement on the fault is inferred to be strike-slip, with the hanging-wall block moving southwest; for dip-slip movement, or thrust faulting, is not likely in such open structure.

A fault trending east of north occurs at the east end of the basalt-capped isolated mesa half a mile west of the Gallegos ranch. The fault forms the western limit of the cliff of orange welded breccia which maintains the eastern step of the mesa. Renewed movement along this fault is indicated on aerial photographs by short straight gullies in the basalt.

In the notch 50 feet west of where the felsite dike crosses the ridge just south of Cienega Creek (5,700 feet S. 42° W. of the west end of the dam), Galisteo sandstone on the west side is faulted up against Galisteo sandstone interbedded with andesite breccia on the east. Where the fault cuts the south wall of the notch, Galisteo sandstone and mudstone are pushed up about a foot into gravel of the Ancha formation, evidently the result of renewed movement. The fault plane is also exposed in a gully on the south side of the ridge, and it can be traced 3,500 feet in a direction S. 7° W. from the notch. The fault separates the upper part of the Galisteo formation on the west from the lower part of the andesite breccia on the east. Vertical movement is on the order of 100 feet, with the eastern block downthrown.

On the south side of the northeast prong of the monzonite, calcic latite breccia is exposed at the mouth of the gully. This breccia is weathered and its contact with the monzonite is nearly vertical. The contact may be a minor fault.

The many dikes of the area have a northward trend. The limburgite dikes strike from N. 12° W. to N. 27° E. The hornblende andesite dike strikes N. 15° W., and the felsite dike strikes N. 40° W.

Laboratory Studies

By MING-SHAN SUN

PETROGRAPHY

INTRODUCTION

The descriptive treatment of each rock unit of the Cienega area is divided into two parts: first, the megascopic description of hand specimens, and second, the microscopic description of a thinsection of a representative sample of one rock unit. Special features of other thinsections of the same rock unit are mentioned. Ten rock units, including two types of the Cieneguilla limburgite, are described in ascending order, beginning with the oldest andesite breccia unit.

Ilmenite, which increases in amount in the more basic rocks, is not differentiated from magnetite in the microscopic description. The composition of plagioclase was determined by the immersion method.

THE TERM "MONZONITE"

On the basis of Daly's (1933) average composition of monzonite (table 2), three units of the Cienega area are monzonite or its extrusive equivalent, latite.

Iddings (1920, p. 369) classified diorite, andesite, monzonite, and latite as rocks composed chiefly of calcic-alkalic feldspar, with subordinate amounts of biotite, hornblende, or pyroxene. If the rocks are potash-rich, then they are monzonite or latite; if the rocks are soda-rich, then they are diorite or andesite. Iddings did not specify a division point between monzonite and diorite.

Monzonite has been defined as a granular igneous rock containing approximately equal amounts of orthoclase and plagioclase. Johannsen (1937, v. 3, p. 94) suggested 35 and 65 percent lines as the division points. According to these division points, if the orthoclase is in excess of 65 percent, the rock should be classified as syenite or trachyte; if the plagioclase is in excess of 65 percent the rock should be classified as diorite or andesite. Johannsen thought that it was better to omit the term monzonite entirely.

The orthoclase-plagioclase ratio of the Cienega rocks cannot be established by modal analysis, because of the predominance of fine-grained and glassy groundmass. However, a similar ratio can be established by normative analysis, as shown in Tables 4 and 5. The orthoclase-plagioclase ratios, based on normative analysis, of the Cienega monzonite or latite are very close to that of Daly's average monzonite. Daly's average diorite (table 2) has a silica content of 56.77 percent, and its normative orthoclase-plagioclase ratio is about 19:81. Daly's average andesite (table 2) has a silica content of 59.59 percent, and its normative orthoclase-plagioclase ratio is about 17:83.



Plate 2

SETTING OF THE CIENEGA AREA

- A. View northwest across the Cienega area from Cerro de la Cruz. Rounded black hill in middle distance is Cerro Seguro; Las Tetillitas are to left. Tetilla Peak is in left distance, and Jemez Mountains are on skyline. U. S. Highway 85 is in foreground.
- B. View southeast across the Cienega area from Cerro Seguro. Conical black hill is Cerro de la Cruz; Turquoise Hill is just to right, and Bonanza Hill is just to left. Cienega school is left of *center*. just beyond road that traverses the valley floor.



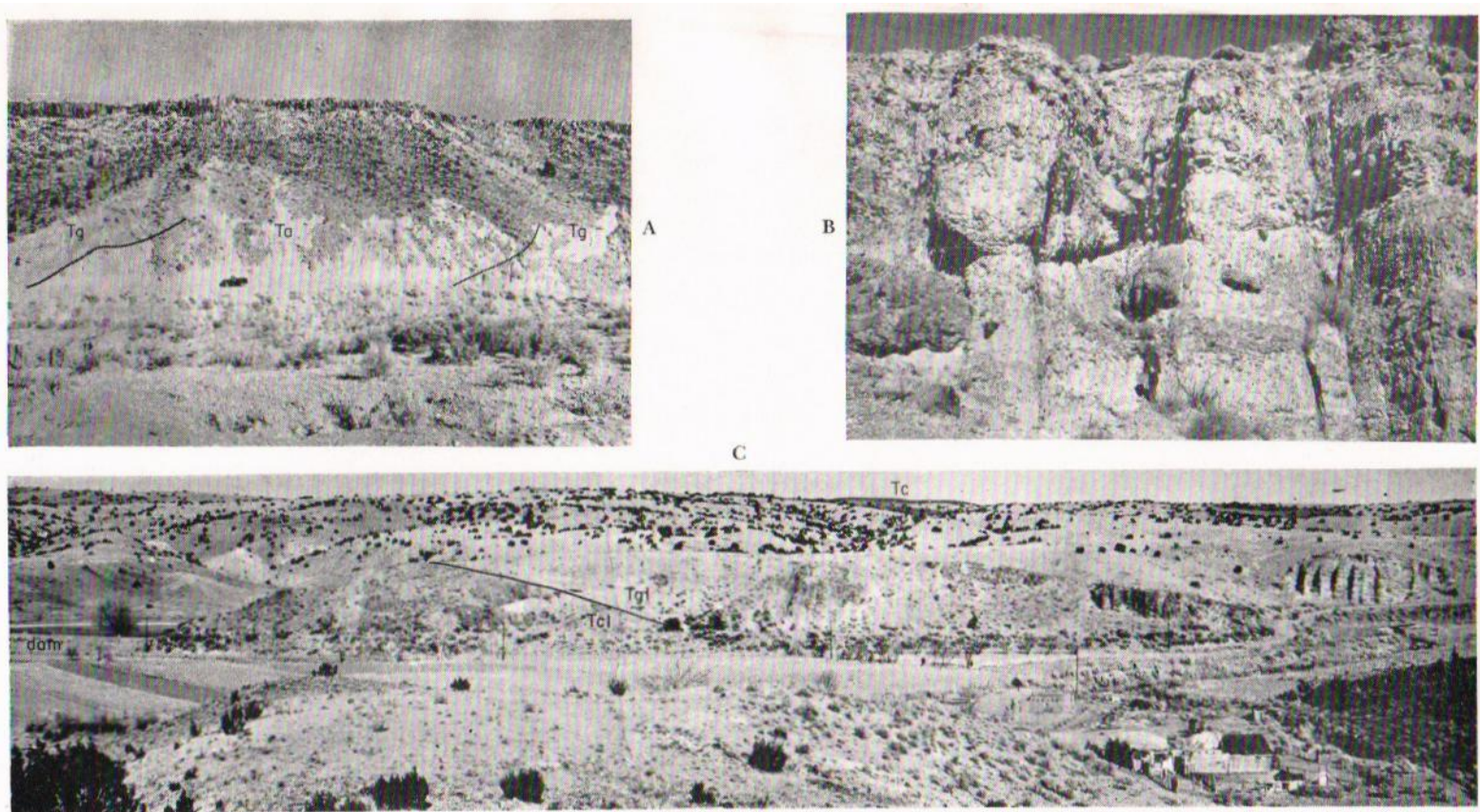


Plate 3

FEATURES OF VOLCANIC ROCKS

- A. Andesite tuff-breccia (Ta) resting conformably on Galisteo formation (Tg) to right. Galisteo formation to left is faulted toward observer. View north just east of Gallegos ranch.
- B. Detail of gray glassy latite breccia at sample locality 199. Note figure of boy, lower center.
- C. Contact between calcic latite (Tcl) and glassy latite (Tgl), east of the dam. Cieneguilla limburgite (Tc) on skyline. Fluted cliff to right is shown in (B). View northwest across Cienega Creek.

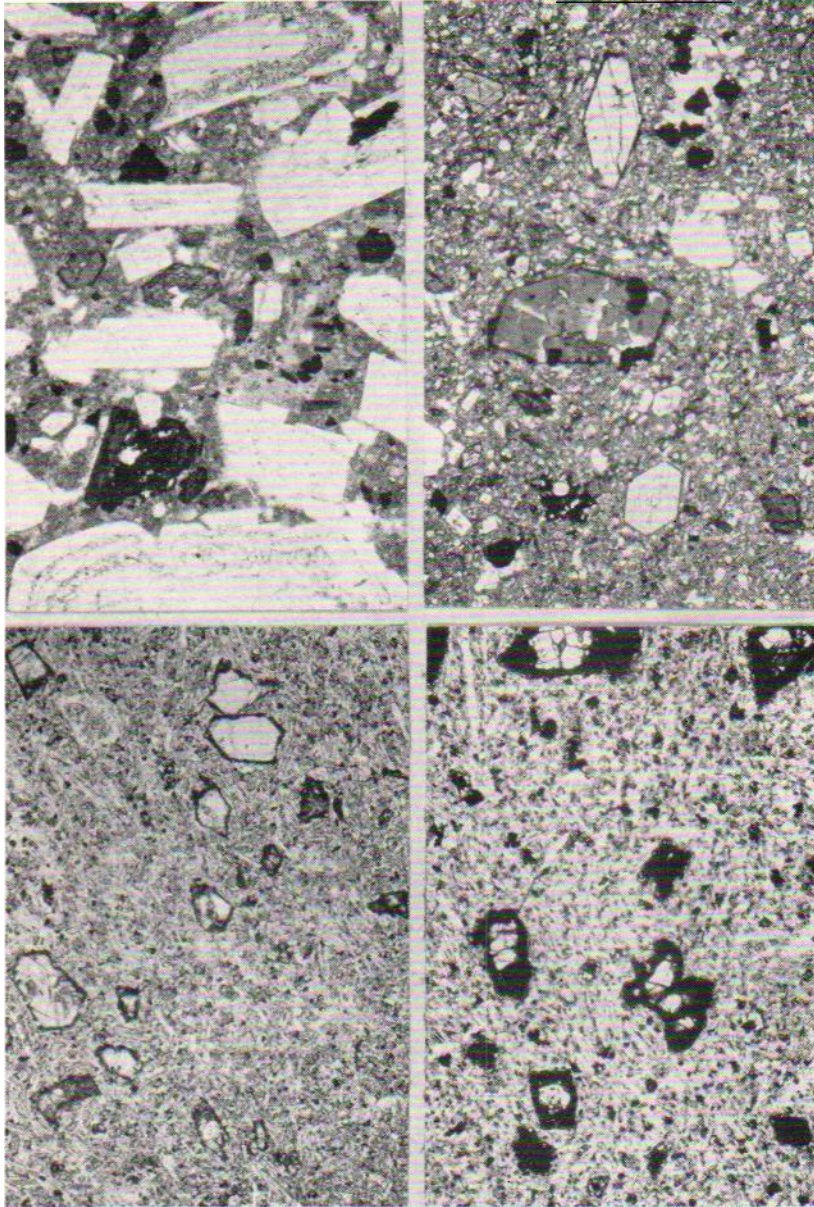


Plate 4

PHOTOMICROGRAPHS OF VOLCANIC ROCKS

- A. Andesite breccia (sample 162). Phenocrysts of andesine-labradorite, hornblende, and magnetite in fine-grained groundmass. Zoning structure and albite twinning are common in the plagioclase. x 15.
- B. Hornblende andesite (sample 8). Hornblende crystals in a fine-grained, felty, and partly glassy groundmass. x 15.
- C. Basalt (sample 85). Partly absorbed olivine crystals in felty groundmass. There is no olivine in the norm of this basalt. x 15.
- D. Olivine basalt (sample 142). The olivine crystals are partly or completely altered to iddingsite, which is shown as dark rims. x 15.

SUN-BALDWIN: CIENEGA AREA



Plate 5

PHOTOMICROGRAPHS OF VOLCANIC ROCKS

- A. Classy latite (sample 92). Oligoclase phenocrysts in glassy and partly fine-grained groundmass. x 15.
- R. Calcic latite (sample 72b). Andesine and augite phenocrysts in fine-grained ground-mass. x 15.
- C. Augite monzonite (sample 84). Large and abundant feldspar and some augite phenocrysts in fine-grained groundmass. x 15.
- U. Vent breccia (sample 189). Plagioclase microlites in brown glassy groundmass. There are a few large plagioclase and augite phenocrysts. x 15.



Plate 6

PHOTOMICROGRAPHS OF VOLCANIC ROCKS

- A. Limburgite (sample 27). Olivine phenocrysts in a fine-grained groundmass of olivine, augite, magnetite, nepheline, and glassy material. x 15.
- B. Monzonite inclusion in limburgite (sample 49). Glassy limburgite prevails along the contact. x 15.
- C. Calcic latite breccia (sample 6). Fragments of calcic latite are shown. x 15. U. Augite basalt (sample 20). Augite and some altered olivine in felty groundmass. This augite basalt may belong to the Cieneguilla limburgite. x 15.

TABLE 2. ORTHOCLASE-PLAGIOCLASE RATIOS OF THE CIENEGA MONZONITE, LATITE, AND ANDESITE, IN COMPARISON WITH THOSE OF DALY'S AVERAGE MONZONITE, ANDESITE, AND DIORITE

ROCK NAME	TOTAL FELDSPAR PERCENTAGE		NORMATIVE ORTHOCLASE-PLAGIOCLASE RATIO	
	WT. NORM	MOLECULAR NORM	WT. NORM	MOLECULAR NORM
Andesite breccia	71.46	73.95	18.71 : 81.29	18.17 : 81.83
Augite monzonite	72.32	74.99	32.16 : 67.84	31.27 : 68.73
Calcic latite	75.32	78.11	30.10 : 69.90	29.25 : 70.75
Glassy latite	75.15	77.75	30.13 : 69.87	28.10 : 71.90
Daly's average andesite	68.34	70.68	17.87 : 82.13	16.25 : 83.75
Daly's average diorite	66.24	68.13	19.20 : 80.80	18.71 : 81.29
Daly's average monzonite	72.73	74.67	30.86 : 69.14	30.07 : 69.93

Daly's average monzonite (table 2) has a silica content of 56.12 percent, and its normative orthoclase-plagioclase ratio is about 30:70. It is evident that the normative orthoclase-plagioclase ratios of the glassy latite, the augite monzonite, and the calcic latite of the Cienega area are very close to that of Daly's average monzonite, whereas the normative orthoclase-plagioclase ratio of the andesite breccia is very close to that of Daly's average andesite.

It is apparent that in a majority of the rocks which have been named monzonite or latite, the amount of normative plagioclase is about 40 percent more than the amount of normative orthoclase. It seems that the approximately equal amounts of (modal) orthoclase and (modal) plagioclase in the definition of monzonite and latite are the equivalent of a normative orthoclase-plagioclase ratio of 30:70. Therefore, the use of monzonite or latite for the Cienega rocks conforms with the customary use of these names in New Mexico and elsewhere. The amount of modal orthoclase is usually larger than that of the normative orthoclase, because the modal orthoclase may contain various amounts of albite and, sometimes, anorthite molecules. On the other hand, the amount of modal plagioclase is usually less than that of the normative plagioclase.

ANDESITE BRECCIA

The andesite breccia unit includes a basal soft-weathering tuff and breccia, overlain by breccia and welded tuff-breccia.

Megascopic description. Stratification is clearly shown in a few samples of tuff by the change in grain size. Fine-grained volcanic material commonly forms layers of grayish-brown mudstone that, according

to their muddy appearance, were probably deposited in water. Calcite veinlets or patches are found in some samples of mudstone.

The tuff is generally gray to brownish gray, although in some samples the matrix is reddish brown. The fragments, which are subrounded to subangular, range from minute to one inch in diameter. Crystals of hornblende, plagioclase, and minor augite and biotite are visible in hand specimen. The hornblende, which varies in amount from sample to sample, occurs in both the fragments and matrix. The crystals are about 4 mm in maximum length and are generally in random orientation. The plagioclase crystals, which have a maximum length of about 3 mm, are light gray and dull lustered; some crystals have a pinkish cast. Some biotite is found, and in the matrix of some weathered samples a few augite crystals have been recognized.

The results of grain-size analysis of sample 201, which represents the disintegrated basal tuff, are summarized in Table 3.

In *each* sieve fraction, the nature and relative abundance of grains were estimated under the binocular microscope. The quartile measurements of the sample, as determined from the cumulative curve plotted on the phi scale, are as follows: Q_3 0.38 mm; Q_1 , 0.17 mm; Md 0.25 mm; So (Frask) 1.50; Sk 1.03. Therefore, this disintegrated tuff is a well-sorted medium-grained sand. Plagioclase grains, which predominate in the finer size fractions, are rather fresh, although many have a dull luster. Magnetite and clayey particles are relatively more abundant in the finer size fractions, and andesite fragments are more abundant in the coarse fractions.

The breccia and welded tuff-breccia that form the bulk of the andesite breccia unit are gray to brownish gray, although samples from the

TABLE 3. GRAIN-SIZE ANALYSIS OF DISINTEGRATED ANDESITE BRECCIA

GRAIN SIZE (mm)	PERCENT	COMPOSITION
Above 2	0.29	Mainly porphyritic andesite fragments, with a few grains of quartz, plagioclase, and sandstone.
1-2	1.31	Andesite grains 94%; plagioclase 5%; biotite 1%.
0.5-1	11.05	Andesite grains 88%; plagioclase 10%; quartz and rock fragments 1%; magnetite and biotite 1%.
0.25-0.5	36.92	Andesite matrix, containing few or no phenocrysts 55%; plagioclase 30%; biotite and amphibole 10%; magnetite 3%; clayey particles 2%.
0.125-0.25	33.33	Andesite matrix 45%; plagioclase 40%; biotite and amphibole 10%; magnetite 3%; clayey particles 2%.
0.062-0.125	11.80	Andesite matrix 40%; plagioclase 48%; biotite and amphibole 2%; magnetite 7%; clayey particles 3%.
Below 0.062	5.30	Andesite matrix 30%; plagioclase 57%; biotite and amphibole 1%; magnetite 4%; clayey particles 8%.
Total	100.00	

upper part of the unit have a reddish-orange matrix. Visible mineral grains include plagioclase and hornblende. The plagioclase crystals, which exhibit considerable range in both size and abundance, have a maximum length of about 10 mm. Many of the plagioclase grains show parallel arrangement. Generally the plagioclase crystals in the matrix are in random orientation. The borders of the plagioclase grains are generally indistinct, and in some samples the grains show up only as white spots or streaks. Although hornblende crystals are characteristic of the rock, they are generally not abundant. Chlorite, formed as an alteration product of the ferromagnesian minerals, gives some samples a greenish cast.

Microscopic description. Sample 162 (pl. 4A).

MINERAL	PERCENT	SIZE
Plagioclase	39.9	Maximum 1.3 x 3.4 mm; average 0.7 x 1.5 mm.
Hornblende	6.7	From 0.1 mm across up to 0.9 x 1.3 mm.
Biotite	1.5	From 0.1 mm across up to 0.5 mm across.
Magnetite	1.2	Average 0.2 mm across.
Augite	0.2	0.4 mm across.
Groundmass	50.5	

The texture is porphyritic. The groundmass, which is fine grained, is composed mainly of plagioclase grains and ferromagnesian minerals, including magnetite; some glassy material is present. Plagioclase phenocrysts, which have a composition of Ab₄₆An₅₄, commonly show fairly distinct borders, and many of the crystals are broken. Zoning and albite twinning are common, and cloudy rings indicate an incipient alteration parallel to the zoning. The hornblende, which forms good crystals that show typical amphibole cleavage, has the dark pleochroism of basaltic hornblende. Augite is rare; magnetite is common and is without much alteration.

The andesite breccia is characterized by hornblende and minor biotite and by a small percentage of glass in the groundmass.

AUGITE MONZONITE

Megascopic description. The monzonite is medium gray on fresh fractures, but it weathers to brownish gray and to pale brown and pale red. Plagioclase crystals, which form about 90 percent of the phenocrysts, average about 1.6 X 2.6 mm in size, and the maximum length observed was 4 mm. Many of the feldspar phenocrysts appear as white spots in a brown medium-grained groundmass. Augite phenocrysts are commonly found, and hornblende and biotite have been observed. The phenocrysts, which commonly have indistinct boundaries, occur in random orientation.

Microscopic description. Sample 84 (pl. 5C).

MINERAL	PERCENT	SIZE
Plagioclase	31.2	From 1.3 x 2.2 mm up to 1.8 x 2.8 mm.
Augite	8.5	Average 0.9 x 2.3 mm.
Magnetite	1.6	Average 0.16 mm across.
Groundmass	58.7	

The texture is porphyritic. The groundmass is fine to medium grained. It is composed of orthoclase, plagioclase, magnetite, and a small amount of ferromagnesian minerals. Some of the orthoclase has carlsbad twinning. The plagioclase phenocrysts, which have a composition of $Ab_{58}An_{42}$, have irregular and indistinct borders. The augite is fairly fresh, but some grains have skeleton structure. Magnetite crystals usually cluster together. Biotite and hornblende are present in small amounts in some thinsections. The monzonite is generally characterized by large and abundant feldspar phenocrysts, and by the large amount of augite in a fine- to medium-grained groundmass.

CALCIC LATITE

The calcic latite unit is composed of flows and flow breccias.

Megascopic description. The rock of the flow breccia is generally porphyritic, light brown, and fine to medium grained. A few samples are greenish gray. The groundmass is fine grained and a little of it appears to be glassy. Plagioclase phenocrysts are generally small. The maximum length is about 2 mm. Most of the plagioclase grains do not have clear outlines in the fine-grained groundmass, and some simply appear as pinkish-white spots in a darker groundmass. Plagioclase phenocrysts are few in some samples and numerous in others. They do not show any orientation or flow lines.

Samples of the flows are generally dense to fine grained, with scarcely visible plagioclase phenocrysts and some small augite phenocrysts. Several samples are vesicular; vesicles in one sample average about 3 X 8 mm in size, with a maximum length of 20 mm. The openings in some samples are lined or filled with calcite or chalcedony.

A few of the calcic latite samples have a glassy appearance, and therefore it is rather difficult to distinguish them from glassy latite. The calcic latite flow breccias are somewhat more altered than the flows.

Microscopic description. Sample 72b (pl. 5B).

MINERAL	PERCENT	SIZE
Andesine	22.0	From 0.04 x 0.1 mm up to 0.7 x 1.6 mm.
Augite	7.9	From 0.08 mm across up to 0.66 x 2.0 mm.
Magnetite	2.5	Up to 0.3 mm across.
Groundmass	67.6	

The texture is porphyritic. The groundmass is fine grained. Several thinsections of this rock have been studied, and glassy groundmass was not found. The size of the plagioclase phenocrysts is fairly uniform. Most of the plagioclase is Ab50An50. Albite twinning is common. Many show absorption embayments or have skeletal structure. Zoning structure of the plagioclase is present but not common. Most of the plagioclase phenocrysts have a cloudy appearance, indicating slight alteration. Most of the augite crystals are fresh, although a few are partly altered. Minute magnetite crystals are common and many are altered into hematite, which is the ingredient of the brown color of the rock. There is no biotite or hornblende in the calcic latite. Apatite is common in both the plagioclase phenocrysts and the groundmass.

HORNBLLENDE ANDESITE

Megascopic description. This brownish-gray rock is characterized by its abundance of hornblende phenocrysts, some of which are more than 5 mm long. Most of the hornblende crystals are clearly shown in the groundmass. They show a vague parallel arrangement. Clusters of hornblende crystals are common. Some clusters are as big as 3 cm across. Most of the hornblende crystals are fresh, but a few are brownish, indicating slight alteration. In a few samples the hornblende crystals form an estimated 25 percent of the rock.

Microscopic description. Sample 8 (pl. 4B).

MINERAL	PERCENT	SIZE
Hornblende	20.7	From 0.1 mm across up to 1.2 x 2.3 mm.
Andesine	5.8	From 0.1 mm across up to 0.7 x 1.3 mm.
Magnetite	0.4	From 0.1 mm across up to 1.2 mm across.
Groundmass	73.1	

The texture is porphyritic, partly glomeroporphyritic, and felty. The groundmass is fine grained, felty, and partly glassy. It is composed of plagioclase, hornblende, and magnetite smaller than 0.1 mm across. Almost all the hornblende phenocrysts are euhedral crystals showing good cleavages and pleochroism. They are fresh, without noticeable alteration. A few have twinning, or zoning structure along the rims. Absorption edges and embayments are common in some of the hornblende. The amount of andesine crystals is much less than hornblende. Zoning structure is common in andesine. One cluster of hornblende and magnetite is found. One distinct rock fragment, 0.4 x 1.2 cm in size, is composed of biotite, epidote, augite, and small grains of feldspar.

GLASSY LATITE

The glassy latite unit is composed of breccia and minor tuff.

Megascopic description. The tuff is grayish white and medium grained. It is composed of grayish-white clayey matrix, small rock frag-

ments, and feldspar. A few large subangular fragments and some long (0.5 X 3.0 mm) hornblende crystals are found in the tuff.

The breccia is compact and appears rather coarse. The rock is porphyritic, and the groundmass is fine grained to glassy. Flow lines are seen in some samples. The phenocrysts are unevenly distributed in the rock. In some samples phenocrysts form about 80 percent of the rock, but in others subrounded rock fragments are predominant. The phenocrysts are mostly plagioclase, with a few hornblende crystals. In some samples having few plagioclase phenocrysts there is a slight increase in abundance of slender hornblende crystals. A few samples contain specks of biotite. Some plagioclase phenocrysts are as much as 4 mm in length. The plagioclase crystals may protrude from the weathered surface. Many plagioclase phenocrysts are not very distinct because they are much the same color as the groundmass. The glassy latite is characterized by conspicuous plagioclase phenocrysts and glassy groundmass.

Microscopic description. Sample 92 (pl. 5A).

MINERAL	PERCENT	SIZE
Plagioclase	31.6	From .02 mm across up to 1.8 x 2.5 mm; 1.8 x 6.8 mm.
Biotite	2.0	From 0.16 x 0.3 mm up to 0.36 x 0.46 mm.
Magnetite	1.4	From 0.02 mm to 0.2 mm across.
Hornblende	2.0	Average 0.4 x 0.7 mm.
Groundmass	63.0	

The texture is porphyritic. The groundmass is glassy to fine grained. It is composed mainly of glassy material, with some grains of plagioclase, ferromagnesian minerals, and magnetite. A few of the plagioclase (Ab₇₇An₂₃) phenocrysts are large. Albite twinning is common, and zoning structure is present in many crystals. Most of the plagioclase crystals have clear square outlines, although many have absorption embayments and indistinct borders. There are many small apatite crystals. A few magnetite crystals show skeleton structure. Only a few small magnetite crystals are partly altered into hematite. Biotite crystals are fresh and show strong pleochroism. Typical cleavages are shown in some of the hornblende crystals. All the hornblende crystals show strong pleochroism that resembles the pleochroism of biotite. The glassy latite is characterized by a predominance of glassy groundmass and by the few large rectangular plagioclase phenocrysts. As a whole, the rock shows only slight alteration. Augite is present in the glassy latite, although it is not present in this thinsection.

FELSITE

Megascopic description. The felsite dike which intrudes the Galisteo formation is light pinkish gray. Dendritic manganese oxides occur on the weathered surfaces.

Microscopic description. Sample 3. The texture is aphanitic and felty. Calcite, which forms about 20 percent of the rock, occurs in patches about 1.3 mm across. Microlites of albite, 0.1 X 0.2 mm in size, are numerous. No other minerals in this rock are recognized. Some grains which have low indices of refraction might be orthoclase. There are no quartz grains. Based on the presence of albite and possible orthoclase, sample 3 might be latitic in composition.

VENT BRECCIA

Megascopic description. The vent breccia consists of dark-gray glassy subangular fragments set in random orientation in a white ashy matrix. The fragments are generally less than 6 inches in diameter. Numerous tiny white spots give some fragments a salt-and-pepper appearance, but no crystals can be identified by naked eyes. One fragment (sample 187) shows some gray and brownish banding on its surface, but such banding does not extend clearly to its internal part. The dense glassy part of the rock is dark gray or black, but the parts with abundant white spots are light gray.

Microscopic description. Sample 189 (p1. 5D). The texture is fine grained and glassy. The brown glassy groundmass, which is full of microlites, forms about 72 percent of the rock. The gray bands are composed of plagioclase crystals, whereas the brownish bands are glassy ground-mass. The tiny white spots of the rock were revealed to be small plagioclase crystals. The average size of the plagioclase is 0.06 X 0.20 mm, but one large crystal measures 1.0 X 1.6 mm. Albite twinning is common. One large grain shows a biaxial positive interference figure. Plagioclase crystals amount to 35 percent of the rock. Augite, about 0.34 X 0.60 mm in size, amounts to about 1 percent. The shape of augite is irregular; it varies from tiny grains to long rods, and the elongated ones are roughly parallel to the flow lines. Usually a few grains occur together in clusters. Few crystals have twinning. The crystals are fresh, without any evidence of alteration. Magnetite amounts to about 1 percent. Its average size is 0.10 mm across. The rock is slightly vesicular. As revealed by the microscope, the white ashy material that cements the rock fragments together is the powdered material of the rock.

CIENEGUILLA LIMBURGITE

This volcanic unit includes limburgite flows, limburgite dikes, olivine basalt flows, and possibly some augite basalt.

Megascopic description. The limburgite is grayish black to black, massive and compact. It is fine grained, with visible grains of olivine and some augite. Some samples are slightly vesicular. Some of the limburgite, especially the limburgite of a dike on the east side of the monzonite, is coated with desert varnish of manganese and iron oxides. This desert varnish looks very black and greasy. The olivine basalt is slightly lighter

in color than limburgite. Olivine and some augite of the olivine basalt are visible.

Microscopic description. (1) Olivine basalt, sample 142 (pl. 4D).

MINERAL	PERCENT	SIZE
Olivine	12.6	From 0.2 mm across up to 1.2 x 2 mm.
Augite	1.9	Average 0.24 x 0.6 mm.
Plagioclase	0.6	About 0.2 mm long.
Magnetite	0.4	Average 0.15 mm across.
Groundmass	84.5	

The texture is porphyritic and partly glomeroporphyritic. The groundmass is fine grained. It is composed mainly of small grains of augite, magnetite, and plagioclase. One cluster of plagioclase and augite is present. The composition of the plagioclase is estimated to be $Ab_{42}An_{56}$ on the basis of its refractive indices. The augite has $n_x = 1.684$, and $n_z = 1.712$.

Olivine phenocrysts form 12.6 percent of the rock. Nearly one-half of this percentage is fresh and the remainder consists of a reddish-brown material surrounding the olivine phenocrysts. Some of the small olivine phenocrysts are completely altered to the reddish-brown material. This reddish-brown material has been identified as iddingsite, but recent study (Sun, 1957) shows it is not a true mineral but, rather, a complex alteration product of olivine. It is composed of cryptocrystalline goethite, and the other substances shown by chemical analysis to occur in iddingsite are largely amorphous.

(2) Limburgite, sample 27 (pl. 6A).

MINERAL	PERCENT	SIZE
Olivine	13.0	From 0.04 mm across up to 1.0 x 1.7 mm.
Nepheline	5.0	(Veinlets) from 0.04 mm across up to 0.5 x 1.4 mm.
Groundmass	82.0	
1. Olivine	22.5	
2. Augite	52.5	
3. Magnetite	3.0	
4. Nepheline	2.0	
5. Glassy material	2.0	

The texture is porphyritic. The groundmass is fine grained and partly glassy. It is composed of olivine, augite, magnetite, nepheline, and glassy material. Nepheline forms some large phenocrysts, but most of

the nepheline is present as short irregular veinlets. There are numerous prismatic crystals in the nepheline. Some olivine crystals are altered along their cracks to chlorite and magnetite. A few tiny euhedral crystals of apatite can be recognized.

Sample 49 (pl. 6B) shows a monzonite fragment included in fresh limburgite. Of the olivine phenocrysts, which make up 26 percent of the limburgite, only a few have brown rims. On the other hand, in sample 86 the olivine phenocrysts are partly to completely altered, and only a vague outline of the original olivine phenocrysts and the swarm of magnetite are left.

BASALT

Megascopic description. The basalt is fresh and fine grained. It is generally medium to dark gray. Some samples are slightly vesicular. The vesicles may form 5 percent of the rock. Many of the vesicles are filled with calcite. Partly altered ferromagnesian minerals, up to 2.5 mm long, are common. Many are altered to iron oxides and chlorite, appearing as brownish and greenish spots. Some white spots are either altered feldspar grains or introduced calcite. Olivine phenocrysts, although few in number, are found in several hand specimens. Such olivine and some feldspar crystals usually protrude on the weathered surface.

Microscopic description. Sample 85 (pl. 4C).

MINERAL	PERCENT	SIZE
Olivine	7.4	From 0.1 mm across up to 2.4 x 3.4 mm. Average 1.0 mm across.
Augite	0.2	0.4 mm across.
Groundmass	92.4	
Augite	13.8	Average 0.1 mm across.
Magnetite	1.5	0.04 mm across.
Plagioclase	72.1	0.04 x 0.24 mm.
Glassy material	5.0	

The texture is porphyritic. The groundmass is felty and is composed of plagioclase laths, augite, magnetite, and minor glassy material. All the olivine phenocrysts have absorption edges and embayments. The small ones are completely altered to a brown color, and the large ones have brown rims of varying width. There is no olivine in the ground-mass or norm. It is apparent that many crystals of olivine in the basaltic magma failed to react completely in the liquid during the crystallization of the magma, and therefore were left as partly absorbed phenocrysts. One augite phenocryst is present.

PETROLOGY

Igneous rocks can be classified into three groups according to their silica content: (1) basic rocks, which contain less than 45 percent of silica; (2) intermediate rocks, which contain 45 to 68 percent of silica; and (3) acidic rocks, which contain over 68 percent of silica. In the Cienega area limburgite belongs to the basic group; monzonite, andesite breccia, calcic latite, hornblende andesite, basalt, and olivine basalt belong to the intermediate group; and glassy latite, whose silica content ranges from 62 to 69 percent, belongs to both the intermediate and the acidic groups. The average silica content of the glassy latite is about 65 percent.

The change of composition of these rocks is illustrated in three variation diagrams. The oxide variation diagram in Figure 4 shows that

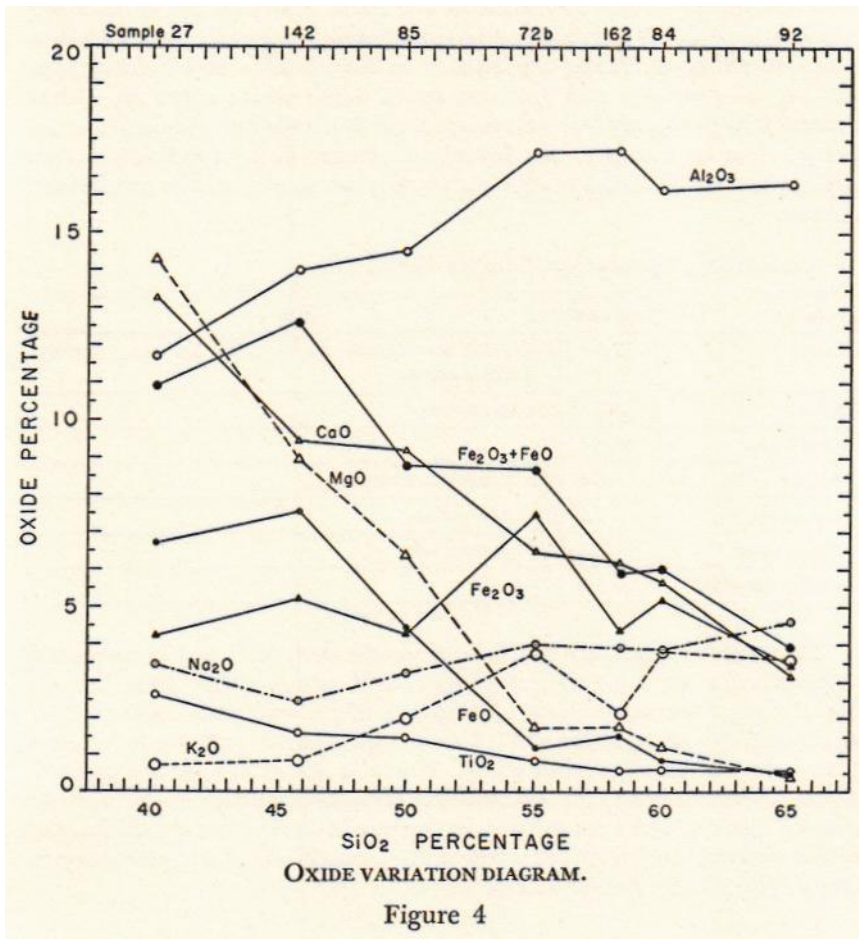


Figure 4

with a decrease of silica several changes are evident: (1) alumina tends to increase in the intermediate rock types and then it decreases toward the basic rocks; (2) calcium and magnesium oxides increase, indicating a change toward the more calcic plagioclase and an increase of ferromagnesian minerals; (3) iron oxides increase, reflecting an increase of olivine, augite, and magnetite. Sample 162 of the andesite breccia shows a certain amount of alteration of the groundmass of this rock unit: (1) the removal of about 2 percent of K_2O , and (2) the formation of some clay mineral, most likely montmorillonite. The phenocrysts of the andesite breccia are fairly fresh.

The cation variation diagram in Figure 5 is another way of showing the variation of composition of the volcanic rocks. It has several advantages over the oxide variation diagram. The curves are less crowded. It is better suited to the molecular norm classification and the modified Holmquist formulae for the study of the rock composition.

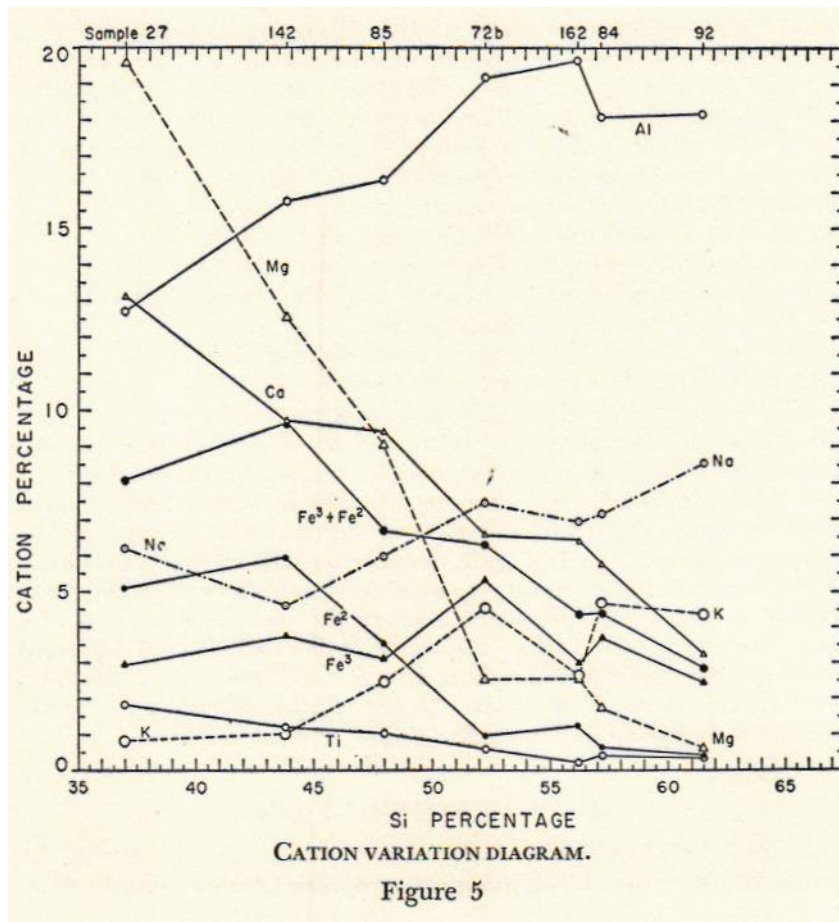


Figure 5

Figure 6 shows a variation diagram of total oxygen versus cations. The total oxygen increases with the silica content of the rocks. The total oxygen content of the Cienega rocks ranges from 139 to 162 per 100 cations, whereas the silicon content ranges from 37 to 62 percent. Total oxygen per 100 cations increases from the basic rocks to the acidic rocks. This increase of total oxygen is largely related to the increase of silicon and aluminum cations. Inasmuch as there is an increase of basic rocks from the surface of the earth toward its core, there must be a decrease of oxygen content of the rocks toward the core of the earth.

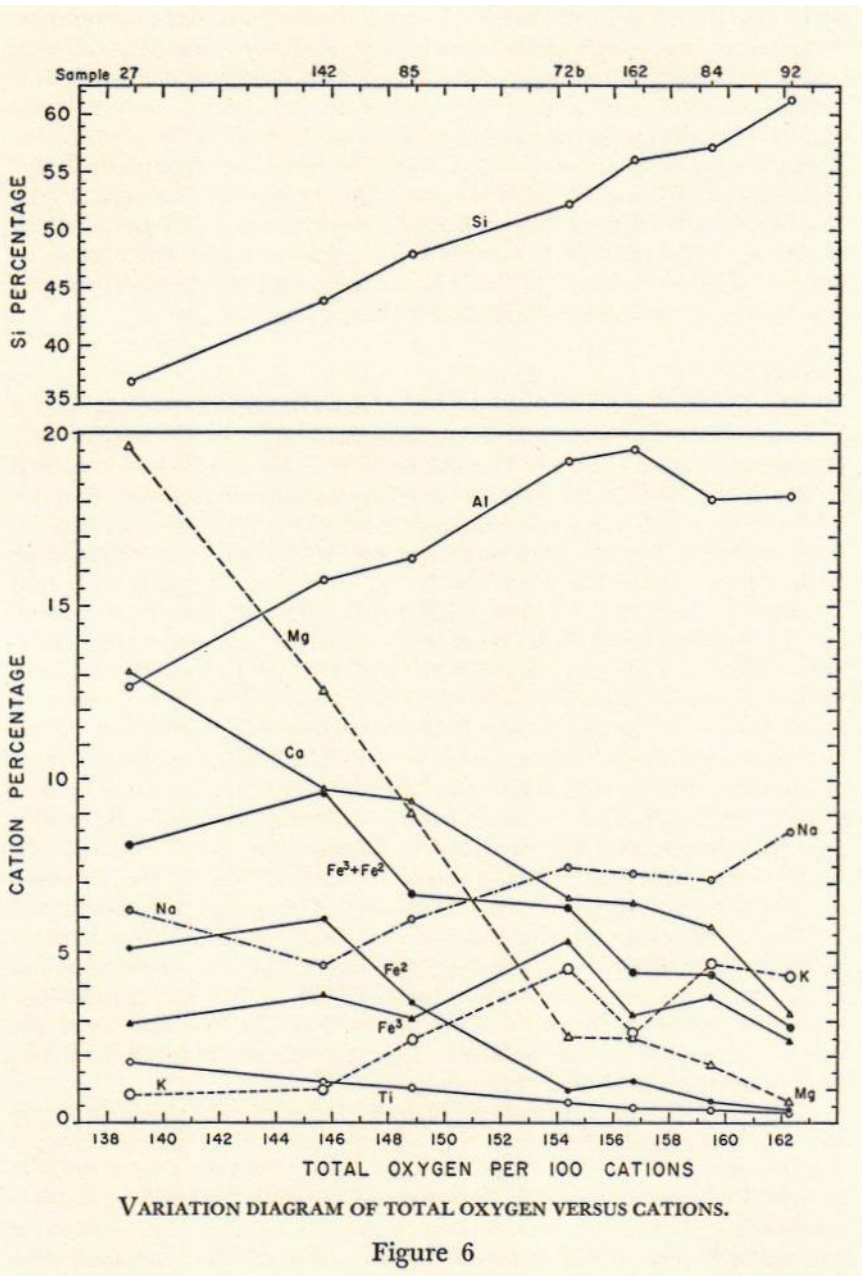
It is probable that the various rocks of the Cienega area were formed from magmas that were differentiated from a large body of parent basaltic magma. It is generally assumed that in a large chamber of basaltic magma the acidic components of the magma through the same or adjacent vents may not follow a rigid order in which the silica-rich components of the magma will be extruded first, followed successively by magmas of decreasing silica content. The sequence of the volcanic rocks of the Cienega area shows a general trend from acidic to basic. The intermediate rocks, which have a silica content of 55-61 percent, form the first three units. Next is the glassy latite, an acidic rock with 62-69 percent silica, followed by the most basic unit, the limburgite, with a silica content of 39-46 percent. The last unit, which followed after a considerable interval, consists of basalt flows with a silica content of about 50 percent. In order to interpret the sequence of the Cienega volcanic rocks, it seems necessary to suggest that subcrustal disturbances have shifted the parent basaltic magma and that the differentiated magmas were extruded to the surface through the same or adjacent vents in a sequence irrespective of silica content.

The possibility of the change of silica content of the rocks by magmatic assimilation is considered to be remote.

During magmatic differentiation, olivine crystals are usually formed first. If there is adequate silica in the magma, these olivine crystals will react with the magma and form pyroxene or amphibole, provided the time of this reaction is also adequate. Often these olivine crystals failed to react with the magma completely and therefore they were left in the rock as phenocrysts. Such olivine phenocrysts will exhibit various absorption rims or embayments. A modal study, together with the norm study of the rock, will reveal such incomplete reaction. Sample 85 of a basalt flow is a good example. The mode of this rock shows 7.4 percent of olivine, yet the norm of this rock (table 5) shows no olivine but, rather, a small amount of quartz. All the olivine phenocrysts have absorption embayments or absorption rims of varying width.

NORM CLASSIFICATION

A comparative study of the various rocks of the Cienega area by the method of normative classification is appropriate because many of those



rocks contain a high percentage of fine-grained and glassy groundmass. A modal analysis would not adequately reveal all the mineralogical composition of such groundmass. The mode of a rock represents its true and natural mineralogical composition, whereas the norm is only a hypothetical chemical-mineralogical composition. The great discrepancy between the mode and the norm of a rock rests on the hypothetical and natural composition of feldspars and the pyroxenes (Chayes, 1951). Further, biotite of the mode will appear as orthoclase and pyroxene in the norm. Different rules are necessary for the normative calculation of rocks of different mineral facies. The volcanic rocks of the Cienega area belong to gabbro facies, and the C.I.P.W. rules are used.

WEIGHT NORM

The C.I.P.W. system of weight normative classification was proposed by Cross, Iddings, Pirsson, and Washington (1902). It was used widely by many petrographers, until a modification of the system was proposed by Barth (1931-1932). Barth calculated the normative pyroxene minerals as three separate normative mineral molecules: Wollastonite, CaSiO_3 (wo); enstatite, MgSiO_3 (en); and hypersthene, FeSiO_3 (hy). The olivine molecule was calculated by Barth as forsterite, Mg_2SiO_4 (fo) and fayalite, Fe_2SiO_4 (fa). Tilley (1931-1932) opposed this modification on the ground that these normative minerals are not actual minerals in rocks. Data on dry melts show that CaSiO_3 and MgSiO_3 will unite to form the diopside molecule, whereas wollastonite and enstatite are an incompatible association. If the normative calculation is designed to fit the natural condition as closely as possible, it is indeed inconsistent to assume at the same time that wollastonite and enstatite can coexist as separate minerals. Such an association is unknown in nature. Nevertheless, Barth's proposal was accepted by Washington (1932-1933). Washington also proposed that the name ferrosilite, FeSiO_3 (fs), be used instead of Barth's hypersthene, FeSiO_3 (hy). This proposal was accepted by Barth. Washington also pointed out that the C.I.P.W. system of normative classification represents hypothetical chemical molecules, not actual minerals. In other words, the C.I.P.W. norm is chemical-mineralogical, whereas the word molecule used in the calculation of the norm means a normative molecule. This system was proposed primarily for comparative studies of rock analysis.

Eskola (1921), in his study of mineral facies of rocks, clearly recognized and emphasized the fact that all the rocks of a mineral facies, if congealed under similar chemical equilibria, will result in a definite chemical composition and a similar set of minerals "regardless of their mode of crystallization, whether from magma or aqueous solution or gas, and whether by direct crystallization from solution (primary crystallization) or by gradual change of earlier minerals (metamorphic recrystallization)." Barth (1931-1932) pointed out that the C.I.P.W. system fits closely the natural condition of rocks of the diabase or gabbro

facies. The rocks of the hornfels facies, the metamorphic equivalent of the gabbro facies, can be studied also by the C.I.P.W. system. There is a continuous variation of the composition of latite, monzonite, andesite, limburgite, basalt, and gabbro. These rock types are abundant in the Cienega area, and in other parts of New Mexico as well. Therefore, the application of the C.I.P.W. system for the interpretation of the chemical analyses of these rocks is not only appropriate but also logical.

By using the end-member normative mineral molecules ferrosilite, enstatite, wollastonite, forsterite, and fayalite, the C.I.P.W. norm calculation is somewhat simplified. The C.I.P.W. rules of the normative calculation which were condensed by Johannsen (1931, v. 1, p. 89) are modified accordingly. These modified rules appear in Appendix I.

MOLECULAR NORM

The molecular norm consists of the percentages of the number of molecules of the normative minerals. The difference between the molecular norm and the weight norm is that the weight norm consists of the percentages of the weight of the normative minerals.

Niggli (1933, 1936), after his study of the petrographical provinces of Bushveld, proposed the use of atomic or molecular percentages in petrographic calculation. He assumed that the fundamental compounds that existed in the magma were "basis molecules." New minerals are formed by the reaction of the basis molecules, although it is doubtful that a large quantity of these basis molecules actually exists in the magma. In petrographic calculation the basis molecules are calculated first; then normative minerals are formed by combining the basis molecules according to the mineral facies of the rock. The basis molecules are calculated to a total of 100 percent. Both H_2O^+ and H_2O^- are excluded in the calculation. The total percentage of the normative minerals is also 100. All these normative minerals constitute the molecular norm of the rock. The basis molecule is also called the equivalent molecular unit. By definition, a basis molecule has only one electropositive atom. For instance, the formula of orthoclase is $KAlSi_3O_8$. The basis molecule of orthoclase is $1/5 KAlSi_3O_8$ and is denoted by the symbol Or. There are five cations in orthoclase. Likewise, En is $1/3 MgSiO_3$, and Fo is $1/3 Mg_2SiO_4$, etc. Niggli's method of petrographic calculation was interpreted and illustrated explicitly by Muthuswami (1952). The meaning of the word "equivalent" has no connection with the meaning of "valence."

According to Barth (1945 [Eskola, 1954], 1948), calculation of the basis molecules is unnecessary; he suggests the use of the molecular percentage of the one-cation oxides. The molecular percentage of the one-cation oxides is the same as the cation percentage, because there is only one cation in each one-cation oxide molecule. The normative minerals are formed by combining the necessary number of cations. The one-cation oxides of the rock analysis are the following: SiO_2 , $FeO_{3/2}$, FeO ,

MgO, CaO, Na $0\frac{1}{2}$, K $0\frac{1}{2}$, TiO 2 , P $0\frac{5}{2}$, MnO, BaO, Cr $0\frac{3}{2}$, etc. The term "ionic percentage" (Eskola, 1954) is the general term for both cation and anion percentage.

There are advantages in using ionic percentage in petrographic calculation, especially in norm calculation. The usual procedure of analytical technique is to present the constituents of a rock in the percentages of its oxides, and rock analyses are presented traditionally as the weight norm. However, the weight-norm calculation can be substituted by molecular-norm calculation. The advantages of the molecular norm are evident:

1. The normative calculation is much simplified. In weight-norm calculation, the weight percentages of the normative minerals are derived by multiplying their molecular proportions by their respective molecular weight. The weight percentages are recalculated to a total of 100 percent, excluding H 2 O. In molecular-norm calculation this step is avoided.

2. The molecular percentage indicates the proportions of material in units more fundamental than those obtained from weight percentage (Eskola, 1954). The ions, in their various ways of combination with anions, are the essential constituents of the rock. Under definite physicochemical conditions the ions tend to react to form mineral molecules of a rock of certain mineral facies.

3. The molecular norm is more closely related to the mode than is the weight norm. The proportion in volume and the arrangement of the minerals are what one can see of a rock, either megascopically or microscopically. Usually the proportions of the volume of the minerals of a rock are measured in the modal analysis by the use of an integrating stage or a Chayes point counter (Chayes, 1949), although it is not uncommon to use weight percentage in modal analysis of rocks and meteorites. A slight increase in the number of cations will result in a large change in the volume of the normative mineral formed by such cations, because oxygen, which is combined with the cations, has a big volume. The oxygen-cations ratio of a rock is about 160:100. Barth (1948) pointed out that the oxygen of the average igneous rock amounts to 91.83 percent by volume, whereas 7 other major cations amount to only 8.16 percent. On the other hand, oxygen amounts to 46.42 percent by weight, whereas the rest of the major cations amount to 51.86 percent.

4. The discrepancy between the percentage of the weight norm and that of the molecular norm is not substantial. The percentages of quartz, apatite, wollastonite, ilmenite, magnetite, and hematite in the weight norm are usually slightly higher than those of the molecular norm. On the other hand, the percentages of the feldspars in the weight norm are usually slightly lower than in the molecular norm.

Barth (1952, p. 79) published rules for the molecular-norm calculation. These rules parallel those of C.I.P.W. weight-norm calculation. In other words, Barth's rules of molecular norm calculation will fit rocks

TABLE 4. THE C.I.P.W. WEIGHT NORMS OF SEVEN VOLCANIC ROCKS, CIENEGA AREA, NEW MEXICO
(In percent)

GLASSY LAIITE		AN DESITE BRECCIA	AUGITE MONZONITE	CALCIC LAIITE	BASALT Sample 85	OLIVINE BASALT	LIMBURGITE Sample 272	AVERAGE a IGNEOUS ROCK
Sample 92		Sample 162	Sample 84	Sample 72B	Sample 85	Sample 1421		
	Quartz	17.84	13.81	12.16	4.37	-	-	10.27
	Orthoclase	21.79	13.37	23.26	22.67	5.23	-	18.70
	Albite	40.11	34.18	33.48	34.94	21.70	-	32.59
	Anorthite	13.25	23.91	15.58	17.71	25.44	14.42	15.73
Nepheline	-	-	-	-	-	-	16.25	-
Leucite	-	-	-	-	-	-	3.45	-
Wollastonite	0.80	2.50	4.69	4.83	8.33	6.36	17.12	3.05
	Enstatite	1.19	4.66	3.15	4.53	16.73	13.52	8.78
Ferrosilite	-	-	-	-	2.50	5.33	1.67	2.85
Casilite	-	-	-	-	-	-	2.22	-
Forsterite	-	-	-	-	-	4.08	15.96	-
Fayalite	-	-	-	-	-	1.43	2.18	-
Magnetite	0.29	3.31	1.41	1.79	6.49	7.78	6.30	4.51
Hematite	3.32	2.22	4.34	6.33	-	-	-	-
Ilmenite	1.05	1.22	1.27	1.61	2.94	3.19	5.15	2.02
Chromite	-	-	-	-	-	-	0.10	0.08
Pyrite	-	-	-	-	-	-	0.06	0.10
Apatite	0.36	0.82	0.66	1.22	2.51	0.67	1.60	1.25
Calcite	-	-	-	-	-	2.06	-	0.23
Zircon	-	-	-	-	-	-	-	0.04
Halite	-	-	-	-	-	-	-	0.04
Total	100.00	100.00	100.00	100.00	100.00	100.00	100.00	100.24
<p>1. Diopside, 12.20%; hypersthene, (MgO • FeO) . SiO₂, 16.22%; olivine, 5.51%. Ratio MgO:FeO = 80.51 : 19.49. 2. Diopside, 32.31%; olivine, 18.14%; casilite, 2.22%. Ratio MgO:FeO = 91.39 : 8.61. 3. Calculated from data of Clarke and Washington (1924).</p>								

TABLE 5. THE MOLECULAR NORMS OF SEVEN VOLCANIC ROCKS, CIENEGA AREA, NEW MEXICO
(In percent)

	GLASSY LATTITE Sample 92	ANDESITE BRECCIA Sample 162	AUGITE MON ZONITE Sample 84	CALCIC LATTITE Sample 72B	BASALT Sample 85	OLIVINE BASALT Sample 1421	LIMBURGITE Sample 27 ²	AVERAGE ³ IGNEOUS ROCK
Quartz	16.54	12.87	11.35	4.09	0.38	-	-	9.58
Orthoclase	21.85	13.45	23.45	22.85	12.45	5.25	-	18.80
Albite	42.65	36.45	35.80	37.40	30.05	23.10	-	34.75
Anorthite	13.25	24.05	15.74	17.86	19.67	25.53	14.05	15.83
Nepheline	-	-	-	-	-	-	18.63	-
Leucite	-	-	-	-	-	-	3.48	-
Wollastonite	0.78	2.38	4.52	4.70	8.10	6.10	15.92	2.94
Enstatite	1.32	5.20	3.52	5.06	18.14	18.60	14.56	9.80
Ferrosilite	-	-	-	-	2.10	4.52	1.36	2.44
Casilite	-	-	-	-	-	-	2.14	-
Forsterite	-	-	-	-	-	4.86	18.50	-
Fayalite	-	-	-	-	-	1.17	1.74	-
Magnetite	0.24	2.40	1.02	1.29	4.68	5.62	4.42	3.27
Hematite	2.29	1.55	3.05	4.46	-	-	-	-
Ilmenite	0.76	0.90	0.94	1.20	2.16	2.34	3.68	1.48
Chromite	-	-	-	-	-	-	0.08	0.06
Pyrite	-	-	-	-	-	-	0.07	0.13
Apatite	0.32	0.75	0.61	1.09	2.27	0.61	1.42	0.72
Calcite	-	-	-	-	-	2.30	-	0.26
Zircon	-	-	-	-	-	-	-	0.04
Halite	-	-	-	-	-	-	-	0.16
Total	100.00	100.00	100.00	100.00	100.00	100.00	100.054	100.265

1. Diopside, 12.20%; hypersthene, (MgO • FeO) • SiO₂, 17.02%; olivine, 6.03%. Ratio Mg:Fe = 80.49: 19.51.

2. Diopside, 31.84%; olivine, 20.24%; casilite, 2.14%. Ratio Mg:Fe = 91.42 : 8.58.

3. Calculated from data of Clarke and Washington (1924).

4. Because of 0.05 percent S the total percentage of the norm exceeds 100.

5. Because of 0.08 percent Cl, 0.09 percent S, and 0.09 percent F, the total percentage of the norm exceeds 100.

of gabbro facies also. Barth omitted the step of recalculating diopside and olivine, with the formation of casilite, after the formation of leucite. Because of this omission, his rules are inadequate for the molecular-norm calculation of the limburgite of the Cienega area. Therefore, it is necessary to have the rules of molecular-norm calculation completely parallel those of the weight-norm calculation.

NORMS OF THE CIENEGA ROCKS

The weight norm and molecular norm of the Cienega rocks are listed in Tables 4 and 5 respectively. For comparison, the norm of the average igneous rock, based on the chemical data of Clarke and Washington (1924), is also listed in these tables.

GEOCHEMICAL ASPECTS

The six major units of volcanic rocks of the Cienega area — glassy latite, augite monzonite, andesite breccia, calcic latite, basalt, and limburgite — have a wide range in chemical composition, both in major constituents and in minor constituents. The silica content for 21 rock samples was determined, and after the samples had been powdered and fused to artificial glasses, the index of refraction of each glass was also determined. These data permitted the comparison of composition with the index of refraction. Seven rock types, including olivine basalt, a flow in the Cieneguilla limburgite, are represented by complete chemical analyses (table 10). From study of these analyses, the ratio of cation numbers to anion numbers has been established for the seven rock types. The rock types are also expressed in terms of the volume of the standard rock cell. The minor constituents of six of the seven rock types (andesite breccia excluded) were determined by spectrographic analysis. The following section discusses methods of analysis of data and the application of those methods to rocks of the Cienega area.

INDEX OF REFRACTION

General Discussion

Tilley (1922), George (1924), Mathews (1951), and many others have discussed the relation between (a) the chemical composition of volcanic glasses or igneous rocks and (b) the index of refraction of the volcanic glasses or the artificial glasses formed by fusing powdered igneous rocks. A general conclusion has been reached that the chemical composition of a number of rocks can be estimated on the basis of the indices of refraction of their corresponding glasses if those rocks occur in the same petrographic province. Callaghan and Sun (1956), after an extensive study of the correlation of some igneous rocks of New Mexico by this method, reached the conclusion that once a curve of composition versus index of refraction is established by means of adequate data, such a

curve can be used to estimate the approximate composition of intermediate igneous rocks of other petrographic provinces.

The properties of glass have been discussed thoroughly by Morey (1938) and Stanworth (1950). The relation between the physical properties and the chemical composition of a glass has been expressed by the Lorentz-Lorenz formula:

$$R = \frac{n^2 - 1}{n^2 - 2} \frac{M}{D},$$

where R = molecular refractivity; n = index of refraction; M = molecular weight; and D = density. This formula shows that the index of refraction of a glass is closely related to its composition, its molecular refractivity, and its density.

The relation between composition and index of refraction can best be illustrated by artificial glasses formed under controlled laboratory conditions. Generally speaking, the index of refraction of a glass is related to all of its constituents, and the relationship is not a linear one. Some constituents will affect the index of refraction more than others. The magnitude of effect of the various constituents on the index of refraction is shown in Table 6.

TABLE 6. EFFECT OF VARIOUS OXIDES ON THE INDEX OF REFRACTION OF GLASSES OF BINARY OR TERNARY SYSTEM WITH SILICA

OXIDES IN GLASSES OF BINARY OR TERNARY SYSTEM WITH SiO ₂	INCREASE OF INDEX OF REFRACTION OF THE GLASSES PER ONE PERCENT INCREASE OF THE OXIDE (APPROXIMATE) ^a
Fe ₂ O ₃	0.0068
TiO ₂	0.0063
FeO	0.0061
MgO	0.0044
CaO	0.0030
Na ₂ O	0.0013
1K ₂ O	0.0011

a. The relation between the composition and index of refraction is not a linear one; the approximate value is derived from Morey's data (1938) of the optical properties of glass.

Callaghan and Sun (1956) demonstrated that the descending order shown in Table 6 is related to the ionic density of the cations present in the glass. Table 7 shows the ionic density in grams per cubic centimeter of the common cations of the artificial glass made of rock samples. The ionic density is calculated by dividing the atomic weight of each element by Avogadro's number. The ionic size, the volume of the sphere of an ion, is here calculated according to its crystal radius as determined by Pauling (1945).

TABLE 7. THE IONIC DENSITY OF THE CATIONS WHICH OCCUR AS MODIFIERS IN SILICATE GLASS

ION	DENSITY OF ELEMENT gm/CM ³	IONIC DENSITY gm/CM ³
Fe ³⁺	7.88	73.60
Ti ⁴⁺	4.50	60.38
Fe ²⁺	7.88	52.47
Mg ²⁺	1.74	35.10
Ca ²⁺	1.54	16.37
Na ¹⁺	0.95	10.63
K ¹⁺	0.85	6.59

The molecular refractivity is directly related to the arrangement of the ions in the glass structure. The effect of an individual ion may differ according to how the ion is bonded in the glass structure. For instance, the effect of O bonded to two Si cations is different from the effect of O bonded to one Si cation and to one other cation, or from that of O bonded to cations other than Si. These differences are directly related to the change of the coordination number of the cations. In the case of soda-boric glass, when the Na₂O is introduced into the frame network of B₂O₃, some B cations will be changed from three-coordinated cations, as in pure B₂O₃, into four-coordinated cations.

The density is related to the structure and molecular weight of the glass. In artificial glass formed by fusing powdered rock samples, SiO₂ and Al₂O₃ form the frame network of the glass structure. The other cations, such as Na¹⁺, K¹⁺, Mg²⁺, Fe²⁺, Fe³⁺, and Ca²⁺, merely fill the vacant spaces or holes in the frame network. When the holes of the glass are filled with cations of large radii, such as K¹⁺ with a radius of 1.33 Å, the frame usually expands to make large holes for the large cation. Glasses of such expanded frame network have comparatively smaller density. On the other hand, if the holes are filled with smaller but heavier cations, such as Fe²⁺, the density of the glass will be higher. The exact mode of occurrence of the cations in the holes is not clear.

When there is internal stress in glass formed under unsuitable cooling conditions, the index of refraction is usually lower. If the internal stress is unevenly distributed throughout the glass, various parts of the glass will be anisotropic. If the glass is correctly annealed, so that internal stress is released, the index of refraction becomes uniform and slightly higher. The cooling conditions under which the internal stress will be raised or released are rather complicated. However, the index of refraction and the density of a glass can be slightly increased or decreased by proper heat treatment. Further discussion of the effect of heat treatment upon the index of refraction is beyond the scope of this report.

The problem of devitrification is rather important in the formation of a homogeneous glass. Devitrification usually occurs during the cool-

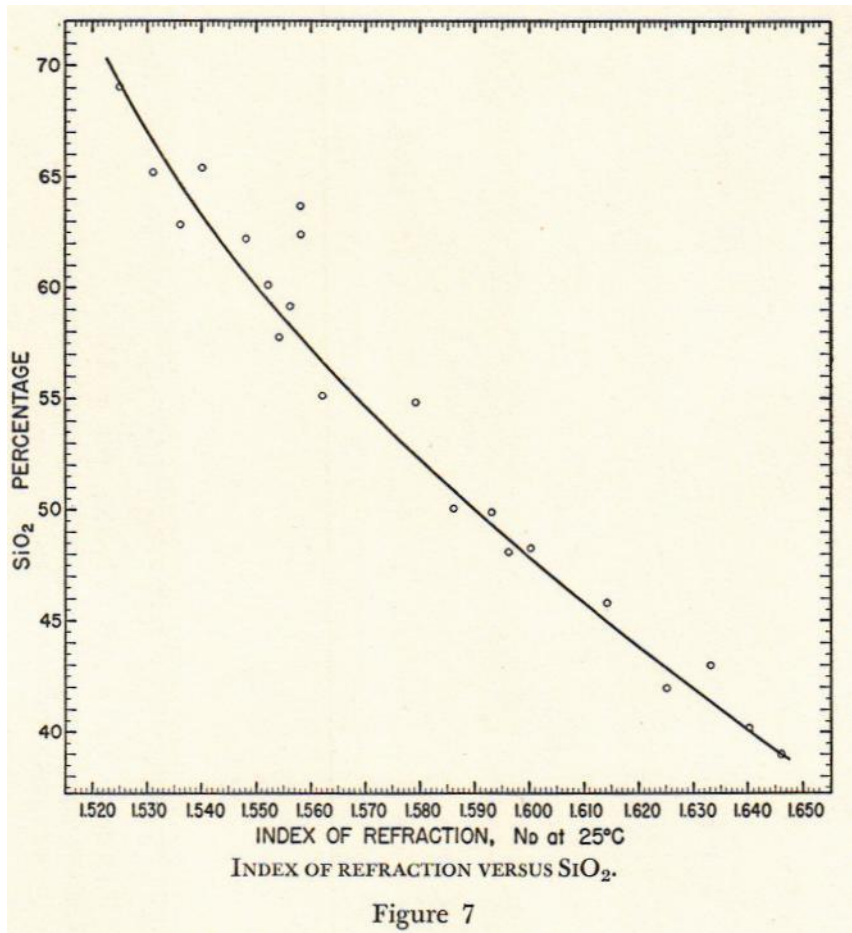
ing of a molten glass. It is also related to the composition of the glass. For instance, if there is more CaO in the melt, crystallites will grow faster during the cooling of the melt. On the other hand, if CaO is largely replaced by MgO, crystal growth or devitrification of the glass will be greatly decreased. The percentage of MgO is comparatively higher in basic than in acidic rocks. Therefore, the artificial glass formed by fusing powdered basic rocks is usually homogeneous, without appreciable devitrification; but the artificial glass of acidic rocks may show a considerable amount of devitrification. If numerous crystallites are formed during cooling, the glass will be partly anisotropic, and accurate determination of the index of refraction of such glass will be difficult.

Although it may hide the Becke line and hinder the determination by immersion method of index of refraction, the color of a glass does not affect its index of refraction. Glass formed by fusing a powdered rock sample usually shows a special color, which may reflect the composition of a particular rock. The most common coloring ingredients are chromium, cobalt, manganese, iron, and other impurities, which occur in glass as microscopic or megascopic particles or as dispersed colloidal particles.

Artificial Glasses

About 80 rock samples have been powdered and fused to form artificial glasses. The method and the accuracy of the method have been discussed by Callaghan and Sun (1956). The relation between the index of refraction and the silica content is shown in Figure 7. As a whole, the indices of refraction of the artificial glasses range from 1.525 to 1.646, whereas the silica content of the corresponding rock samples ranges from 69.04 to 38.99 percent (appendix II).

Figure 8 shows that the indices of refraction of glasses of the glassy latite range from 1.525 to 1.544. A fragment (sample 70) from the glassy latite breccia has an index of refraction of 1.564. It may represent a piece of the hornblende andesite dike included in the glassy latite unit. Glasses of augite monzonite have indices of refraction ranging from 1.544 to 1.556. Glasses of calcic latite have indices of refraction ranging from 1.550 to 1.563. This rather narrow range indicates that the composition of the calcic latite is uniform throughout the rock unit. Glasses of the andesite breccia have indices of refraction ranging from 1.545 to 1.579. The andesite breccia is rather heterogeneous in composition. The glasses of two samples of basalt have indices of refraction of 1.585 and 1.586. The glasses of the augite basalt have indices of refraction ranging from 1.600 to 1.608. On the basis of the index of refraction, the augite basalt may be assumed to be related to the olivine basalt. The glass of olivine basalt has a higher index of refraction than the other basaltic rocks. It is represented by sample 142, whose index of refraction is 1.614. Glasses of limburgite have indices of refraction ranging from 1.625 to 1.647. However, the indices of refraction of the glasses of the



limburgite flows range from 1.633 to 1.642, whereas those of the limburgite dike range from 1.625 to 1.647. The indices of refraction of other dikes, including the vent breccia, felsite dike, and the hornblende andesite dike, range from 1.532 to 1.567. The indices of refraction of the glasses of the vent breccia are similar to those of the augite monzonite. It is reasonable to assume that the composition of the vent breccia is similar to that of the augite monzonite. Miscellaneous rocks were collected from adjacent areas, such as Cerros del Rio and Arroyo Hondo. The indices of refraction of the glasses of these rocks are similar to those of the Cienega area. Figure 8 shows clearly that various rocks of the Cienega area can be grouped together according to the indices of refraction of their corresponding glasses.

The occurrence of volcanic glasses in New Mexico is common, but

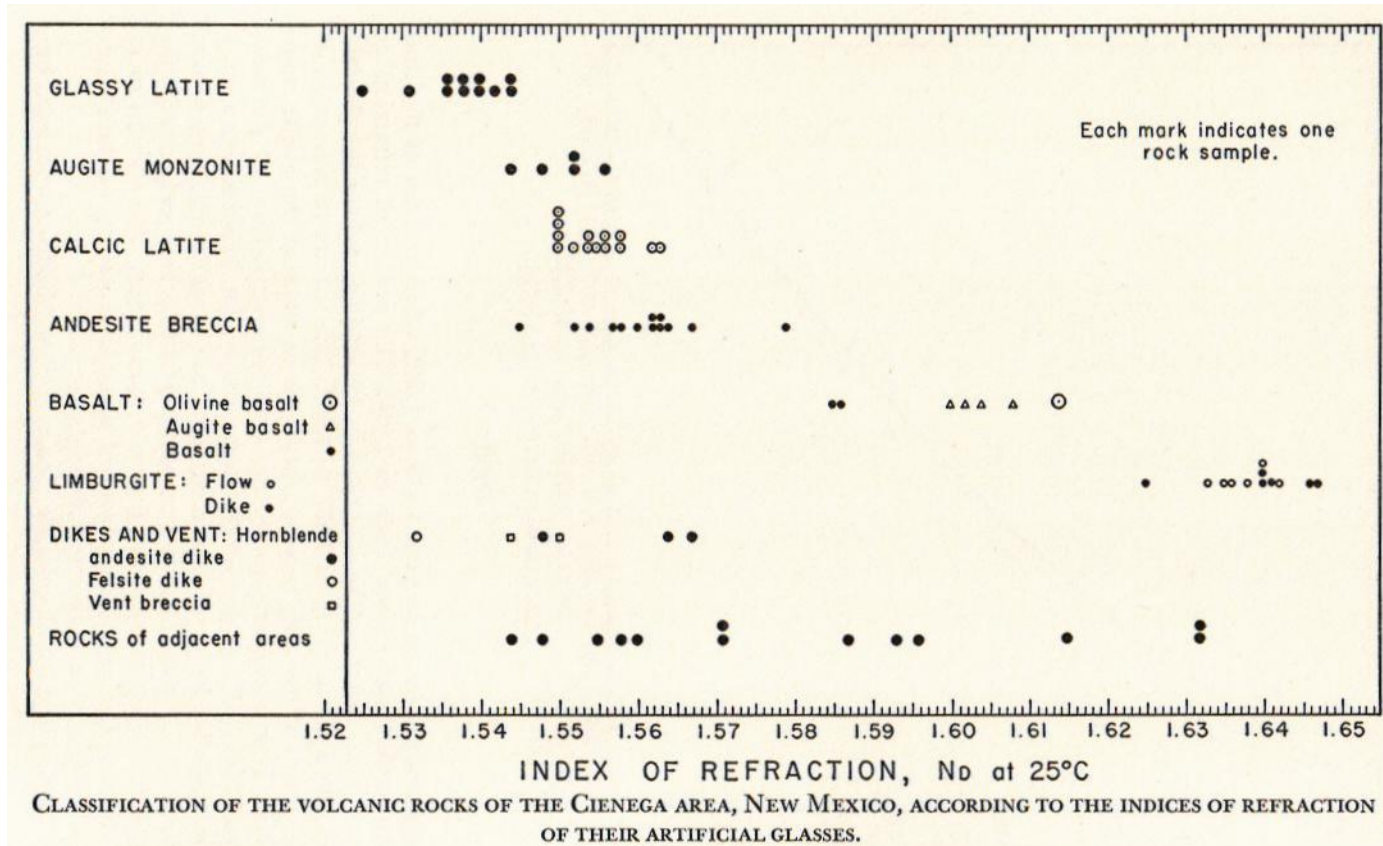


Figure 8

these glasses are acidic. Their indices of refraction range from 1.481 to 1.500, whereas their silica content ranges from about 69 percent to 75 percent. The SiO₂ percentage is referred to the whole rock, whereas the index of refraction is referred to the glassy groundmass. Most of the volcanic glasses contain a few percent of phenocrysts of plagioclase and some mica or hornblende. The artificial glass formed of glassy latite of the Cienega area may be compared with the natural volcanic glass of New Mexico, whose glassy groundmass has an index of refraction of about 1.500. On the other hand, no basic volcanic glasses which can be compared with the artificial glasses of basalt or limburgite of the Cienega area have been reported in New Mexico. Nevertheless, natural basic glasses found elsewhere, such as taiwanite (Juan et al., 1953), can be compared with the artificial glasses of basalt and olivine basalt of the Cienega area. Taiwanite contains 82-95 percent of glassy groundmass and 5-18 percent of phenocrysts of labradorite and olivine. The indices of refraction of its glassy groundmass range from 1.586 to 1.596, whereas the silica content of the entire rock ranges from about 49 to 44 percent. The index of refraction of the glass formed of powdered taiwanite will be higher than that of its glassy groundmass, because the labradorite and olivine phenocrysts will be incorporated in the glass. The CaO, MgO, and some FeO of the labradorite and olivine will increase the index of refraction of the artificial glass.

CHEMICAL COMPOSITION

Minor Constituents

Spectrographic analyses were made of samples of six of the seven rock types of the Cienega area. The data of these analyses are listed in Table 9. The precision of the spectrographic method is within 10 percent of the amount reported for each constituent. The lower limits of detection of the minor constituents by spectrographic methods employed are shown in Table 8.

TABLE 8. LOWER LIMITS OF SPECTROGRAPHIC
DETECTION (In parts per million)
Analyst: Oiva Joensuu.

Exposure No. 1	La, Cr, Sc, Co, Cu, Ag, Ni, Mo, V, Ga, Be	3-10
	Zr, Sn, Pb, Y, Sr, Ba, B	10-30
	Ce, Zn, W, Nb, Ta	110-300
Exposure No. 2	Cu, Ag	0.3
	Zn	10
	Sn, Pb, Ti, Bi	1
	As, Sb	100
Exposure No. 3	Li, Rb, Cs	0.5-1

Generally speaking, vanadium, chromium, cobalt, and nickel are inversely proportional to the silica content of the various rocks. They are directly proportional to the ferrous iron, magnesium, calcium, and titanium of these rocks. Vanadium is found to be comparatively rich in such basic rock as basalt, olivine basalt, and limburgite. Calcic latite contains more vanadium than glassy latite or monzonite. No vanadium minerals are identified in the rock samples. The amount of vanadium increases in rocks which contain more pyroxene, ilmenite, or titanium magnetite. Spectrographic analyses of olivine from kimberlite of Buell Park, Arizona, do not show any trace of vanadium. However, the V_2O_5 content of diopside of the same kimberlite is fairly high, 670 ppm. Therefore, it is likely that the vanadium of the Cienega rocks is not stored in olivine, which is rich in the basic rocks.

In the crystallization of basaltic magma, chromium is among the elements that form the earliest minerals. It occurs mainly in chromite, but also occurs in chromium-bearing magnetite, chromium spinel, and such ferromagnesian minerals as chromium diopside and olivine. No chromium spinel or chromium diopside has been identified in the Cienega rocks. The amount of chromium is directly proportional to the amount of olivine in the Cienega rocks.

There is more nickel and cobalt in basalt, olivine basalt, and limburgite than in glassy latite, monzonite, or calcic latite. The occurrence of nickel and cobalt is quite similar to that of chromium and titanium. Because the ionic radii of nickel and cobalt are similar to those of ferrous iron and magnesium, respectively, the usual inference is that nickel replaces magnesium and the cobalt replaces the ferrous iron in ferromagnesian minerals (Rankama and Sahama, 1950, p. 682). However, the ratio between the amount of nickel and magnesium and the ratio between the amount of cobalt and ferrous iron are not the same. The spectrographic data in Table 9 show that the amount of both nickel and cobalt is about the same in glassy latite, monzonite, and calcic latite, and about the same in basalt, olivine basalt, and limburgite. The Co : Ni ratio of the various rocks is as follows: Glassy latite 1; monzonite 1; calcic latite 2.67; basalt 0.25; olivine basalt 0.22; limburgite 0.20. The ratio is less than one for all the basic rocks. The ratio of the more acidic rocks is one or more than one.

There is a slight indication that gallium is richer in glassy latite and monzonite than it is in the basic rocks. Wickman (Rankama and Sahama, 1950, p. 721) suggested that gallium is associated with or camouflaged by aluminum. Aluminum is richer in acidic rocks. Barite is a common secondary mineral in igneous rocks. Spectrographic analyses show fairly high contents of barium and strontium in all of the Cienega volcanic rocks. The amount of zirconium is about the same in all the volcanic rocks. There is no apparent pattern to the occurrence of La, Sc, Cu, Pb, and Mo.

TABLE 9. MINOR CONSTITUENTS OF THE CIENEGA VOLCANIC ROCKS

(In parts per million)

Analyst: Oiva Joensuu.

Nos.*	CoO	NiO	ZrO ₂	Y ₂ O ₃	V ₂ O ₃	MoO ₃	Cr ₂ O ₃	La ₂ O ₃	Sc ₂ O ₃	SrO	BaO	CuO	Ga ₂ O ₃	PbO	Sn
1.	3	3	270	×	40	×	8	×	5	500	>1000	20	25	10	×
2.	3	3	290	×	85	×	3	×	5	520	>1000	30	20	10	×
3.	20	7	250	10	270	6	5	×	×	500	>1000	60	×	10	×
4.	47	190	340	20	200	5	220	30	×	500	>1000	60	×	10	×
5.	75	340	240	×	270	×	420	×	25	350	480	35	15	10	×
6.	55	280	270	10	340	5	600	30	×	400	>1000	80	×	×	×

- * 1. Glassy latite, sample 92
 2. Augite monzonite, sample 84
 3. Calcic latite, sample 72B
 4. Basalt, sample 85
 5. Olivine basalt, sample 142
 6. Limburgite, sample 27

Major Constituents

The volcanic rocks of the Cienega area show a wide range of chemical composition. The data of the chemical analyses are listed in Table 10.

Standard rock cell—*Holmquist formulae*. The chemical analyses may be presented by using the "standard cell of a rock" (Barth, 1948, p. 51), and also by applying the modified Holmquist formulae.

TABLE 10. CHEMICAL COMPOSITION OF SEVEN VOLCANIC ROCKS, CIENEGA AREA, NEW MEXICO*

CONSTITUENTS	GLASSY LATITE Sample 92	AUGITE MONZONITE Sample 84	ANDESITE BRECCIA Sample 162	CALCIC LATITE Sample 72B	BASALT Sample 85	OLIVINE BASALT Sample 142	LIMBURGITE Sample 27
SiO ₂	65.16	60.10	58.43	55.12	50.06	45.81	40.18
Al ₂ O ₃	16.34	16.16	17.28	17.18	14.51	14.08	11.70
Fe ₂ O ₃	3.45	5.21	4.36	7.45	4.33	5.21	4.26
FeO	0.50	0.86	1.55	1.22	4.46	7.41	6.68
MgO	0.47	1.24	1.81	1.79	6.36	8.79	14.30
CaO	3.20	5.67	6.28	6.50	9.17	9.45	13.28
Na ₂ O	4.65	3.88	3.91	4.07	3.24	2.49	3.48
K ₂ O	3.62	3.86	2.19	3.78	2.04	0.86	0.73
H ₂ O+	1.20	1.20	1.05	1.69	2.18	2.43	1.66
H ₂ O-	0.33	0.34	1.60	0.22	0.52	0.43	—
CO ₂	—	—	—	—	—	0.88	—
TiO ₂	0.54	0.66	0.62	0.84	1.50	1.63	2.66
P ₂ O ₅	0.15	0.28	0.34	0.52	1.05	0.28	0.68
MnO	0.07	0.16	tr	0.08	0.15	0.19	0.08
Cr ₂ O ₃	—	—	—	—	—	—	0.07
Total	99.68	99.62	99.42	100.46	99.57	99.94	99.76

* Analyst for samples 92, 84, 72B, 85, and 142: H. B. Wiik.

Analyst for sample 162: V. C. Juan.

Analyst for sample 27: F. E. Gonyer (see Stearns, 1953-b).

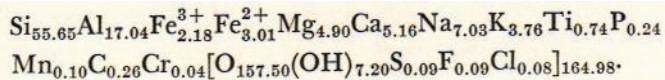
The standard cell of a rock is a rock volume containing exactly 160 oxygen ions. When the total number of oxygen ions of a rock cell (oxygen number) is calculated to be 160, then the total number of cations of that rock cell is nearly 100. Eskola (1954) proposed a new method for the presentation of rock analysis in one-cation molecular percentage. Actually, this method is a modified form of the standard rock cell of Barth. Eskola calculated the rock analysis on the basis of a total of 100 cations, and the total number of oxygen and other anions bonded to the cations was calculated accordingly. In this case, the oxygen number is nearly, but not exactly, 160. This proposal was accepted by Barth. An example of the calculation is illustrated in Table 12. The standard rock cells of the Cienega rocks are presented in the following modified Holmquist formulae:

TABLE II. MODIFIED HOLMQUIST FORMULAE

Glassy latite:	$\text{Si}_{61.59}\text{Al}_{18.20}\text{Fe}^{3+}_{2.45}\text{Fe}^{2+}_{0.40}\text{Mg}_{0.66}\text{Ca}_{3.24}\text{Na}_{8.53}\text{K}_{4.37}\text{Ti}_{0.38}\text{P}_{0.12}$
Sample 92	$\text{Mn}_{0.06}[\text{O}_{162.26}(\text{OH})_{7.56}]_{169.82}$
Augite monzonite:	$\text{Si}_{57.22}\text{Al}_{18.14}\text{Fe}^{3+}_{3.73}\text{Fe}^{2+}_{0.68}\text{Mg}_{1.76}\text{Ca}_{5.79}\text{Na}_{7.16}\text{K}_{4.69}\text{Ti}_{0.47}$
Sample 84	$\text{P}_{0.23}\text{Mn}_{0.13}[\text{O}_{159.45}(\text{OH})_{7.22}]_{166.67}$
Andesite breccia:	$\text{Si}_{56.22}\text{Al}_{19.60}\text{Fe}^{3+}_{3.15}\text{Fe}^{2+}_{1.25}\text{Mg}_{2.60}\text{Ca}_{6.47}\text{Na}_{7.29}\text{K}_{2.69}\text{Ti}_{0.45}\text{P}_{0.25}$
Sample 162	$\text{Mn}_{\text{tr.}}[\text{O}_{156.72}(\text{OH})_{13.50}]_{170.22}$
Calcic latite:	$\text{Si}_{52.26}\text{Al}_{19.20}\text{Fe}^{3+}_{5.32}\text{Fe}^{2+}_{0.97}\text{Mg}_{2.53}\text{Ca}_{6.60}\text{Na}_{7.48}\text{K}_{4.57}\text{Ti}_{0.60}\text{P}_{0.41}$
Sample 72B	$\text{Mn}_{0.06}[\text{O}_{154.38}(\text{OH})_{10.68}]_{165.06}$
Basalt:	$\text{Si}_{47.92}\text{Al}_{16.37}\text{Fe}^{3+}_{3.12}\text{Fe}^{2+}_{3.57}\text{Mg}_{9.07}\text{Ca}_{0.40}\text{Na}_{6.01}\text{K}_{2.49}\text{Ti}_{1.08}\text{P}_{0.85}$
Sample 85	$\text{Mn}_{0.12}[\text{O}_{148.83}(\text{OH})_{13.92}]_{162.75}$
Olivine basalt:	$\text{Si}_{43.84}\text{Al}_{15.88}\text{Fe}^{3+}_{3.75}\text{Fe}^{2+}_{5.93}\text{Mg}_{12.54}\text{Ca}_{9.69}\text{Na}_{4.62}\text{K}_{1.05}\text{Ti}_{1.17}$
Sample 142	$\text{P}_{0.23}\text{Mn}_{0.15}\text{C}_{1.15}[\text{O}_{145.72}(\text{OH})_{15.53}]_{161.24}$
Limburgite:	$\text{Si}_{36.97}\text{Al}_{12.69}\text{Fe}^{3+}_{2.95}\text{Fe}^{2+}_{5.14}\text{Mg}_{19.61}\text{Ca}_{13.09}\text{Na}_{6.21}\text{K}_{0.86}\text{Ti}_{1.84}$
Sample 27	$\text{P}_{0.53}\text{Mn}_{0.06}\text{Cr}_{0.05}\text{L}_{0.18}\text{S}_{0.04}[\text{O}_{138.83}(\text{OH})_{10.18}]_{149.05}$

The oxygen number is directly proportional to the silicon number. In other words, there is more oxygen in acidic rocks than in basic rocks. The total number of oxygen and hydroxyl ions of the olivine basalt is 161, whereas the number of those ions in the monzonite is 1,670. There is no relation between the hydroxyl number and the silicon number, although there is a slight indication that the hydroxyl number is greater in rocks containing more hornblende or biotite.

The modified Holmquist chemical formula of the "average igneous rock" (Clarke and Washington, 1924) is presented as follows:



A small amount of Li is added to Na; V and (Ce, Y) are added to Al; Ba and Sr are added to Ca; and Ni is added to Fe²⁺. On the basis of the silicon number, the chemical composition of the average igneous rock falls between andesite breccia and calcic latite. On the basis of the oxygen number, the chemical composition of the average igneous rock falls between monzonite and andesite breccia.

Ionic rock volume. The chemical composition of the seven volcanic rock types of the Cienega area have been expressed in terms of cation and oxygen numbers. Their composition may also be expressed by the change of ionic volume of both the cations and anions, although the total volume of the ions of a rock does not represent the total volume of the rock. The total volume of a rock is made up of at least three parts (Barth, 1955, p. 353); namely, (1) the volume of the ions as calculated from their radii, (2) the volume of the empty space between ions, and (3) the volume of the empty space between minerals. The method of calculation of the ionic volume of a rock is illustrated in Table 13. The

TABLE 12. CALCULATION OF STANDARD ROCK CELL OF
OLIVINE BASALT OF THE CIENEGA AREA
(Sample 142)

OXIDES	MOL. WT.	WT. %	MOL. WT. OF ONE-CATION OXIDE 1	CATION NUMBER 2	CATION %	OXYGEN NUMBER
SiO ₂	60.09	45.81	60.09	7623.6 Si	43.84	87.68
Al ₂ O ₃	101.96	14.08	50.98	2761.8 Al	15.88	23.82
Fe ₂ O ₃	159.70	5.21	79.85	652.4 Fe ³⁺	3.75	5.63
FeO	71.85	7.41	71.85	1031.3 Fe ²⁺	5.93	5.93
MgO	40.32	8.79	40.32	2180.1 Mg	12.54	12.54
CaO	56.08	9.45	56.08	1685.1 Ca	9.69	9.69
Na ₂ O	61.994	2.49	30.997	803.4 Na	4.62	2.31
K ₂ O	94.20	0.86	47.10	182.6 K	1.05	0.53
H ₂ O ⁺	18.016	2.43	18.016	(1348.8)	(7.76)	—
H ₂ O ⁻	18.016	0.43	18.016	(238.7)	—	—
CO ₂	44.01	0.88	44.01	200.0 C	1.15	2.30
TiO ₂	79.90	1.63	79.90	204.0 Ti	1.17	2.34
P ₂ O ₅	141.95	0.28	70.975	39.4 P	0.23	0.56
MnO	70.93	0.19	70.93	26.8 Mn	0.15	0.15
BaO	153.36	0.00	153.36	— Ba	—	—
Total		99.94		17390.5	100.00	153.48

Minus oxygen for (OH) 7.76

145.72

Oxygen for 2(OH) 15.52

Total oxygen and (OH) 161.24

1. Molecular weight of one-cation oxide is also called equivalent molecular weight.

$$2. \text{Cation number} = \frac{\text{Wt. \% of oxide}}{\text{Mol. wt. of one-cation oxide}} \times 10,000.$$

Because there is only one cation in each one-cation oxide, the cation number is the same as molecular number of one-cation oxide.

3. Oxygen number is calculated according to two oxygen ions bound to one Si, 1½ oxygen ions bound to one Al, 2½ oxygen ions bound to one P, etc.

elementary composition of the "average igneous rock" (Clarke and Washington, 1924) is taken as an example. The crystal radii (effective radii of atoms), as determined by Pauling (1945) on the basis of wave mechanics, are used in the calculation. The valence of the ions is selected on the basis of their abundance in average igneous rock. The ionic number is derived by dividing the weight percentage by the atomic weight and then multiplying the result by 10,000. The total ionic volume is derived by multiplying the volume of the sphere of an ion by its ionic number. The calculation has been carried out to the fourth decimal place, so that the ionic volume of some minor constituents of the igneous rocks could be included.

TABLE 13. CALCULATION OF THE IONIC VOLUME PERCENTAGE OF THE AVERAGE IGNEOUS ROCK OF CLARKE AND WASHINGTON (H₂O INCLUDED)

ELEMENTS	WT. %	CRYSTAL RADII			4.189 x r ³	IONIC	IONIC	IONIC VOLUME PERCENTAGE
		Val- ence	r	r				
Oxygen	46.59	2-	1.40	11.4946	29119	334711	93.5436	
Silicon	27.72	4+	0.41	.2887	9868	2849	.7962	
Aluminum	8.13	3+	0.50	.5236	3013	1578	.4410	
Iron	5.01	2+	0.75	1.7672	897	1585	.4430	
Calcium	3.63	2+	0.99	4.0646	906	3683	1.0293	
Sodium	2.85	1+	0.95	3.5915	1239	4450	1.2437	
Potassium	2.60	1+	1.33	9.8552	665	6554	1.8317	
Magnesium	2.09	2+	0.65	1.1504	859	988	.2761	
Titanium	.63	4+	0.68	1.3172	132	174	.0486	
Phosphorus	.13	5+	0.34	.1646	42	7	.0020	
Hydrogen	.13	1+	0.31	.1248	1290	161	.0450	
Manganese	.10	2+	0.80a	2.1448	18	39	.0109	
Sulfur	.052	2-	1.84	26.0954	16	418	.1168	
Barium	.050	2+	1.35	10.3065	4	41	.0115	
Chlorine	.048	1-	1.81	24.8397	14	348	.0973	
Chromium	.037	3+	0.64a	1.0981	7	8	.0022	
Carbon	.032	4+	0.15	.0141	27	0.38	.0001	
Fluorine	.030	1-	1.36	10.5372	16	169	.0472	
Zirconium	.026	4+	0.80	2.1448	3	6	.0017	
Nickel	.020	2+	0.69	1.3761	3	4	.0011	
Strontium	.019	2+	1.13	6.0443	2	12	.0034	
Vanadium	.017	4+	0.59	.8603	3	3	.0008	
Cerium (Yttrium)	.815	4+	1.01	4.3159	1	4	.0011	
Copper	.010	1+	0.96	3.7062	2	7	.0020	
Uranium	.008	4+	0.97	3.8232	0.33	1	.0003	
Tungsten	.005	4+	0.66	1.2043	0.27	0.32	.0001	
Lithium	.004	1+	0.60	.9048	6	5	.0014	
Zinc	.004	2+	0.74	1.6975	1	2	.0006	
Niobium (Tantalum)	.003	4+	0.67	1.2599	0.3	0.4	.0001	
Hafnium	.003	0	1.66	19.1617	0.16	3	.0008	
Thorium	.002	4+	1.02	4.4454	0.08	0.36	.0001	
Lead	.002	2+	1.21	7.4211	0.1	0.74	.0002	
Cobalt	.001	2+	0.72	1.5635	0.17	0.26	.0001	
Boron	.001	3+	0.20	.0335	0.92	0.03	.0000	
Beryllium	.001	2+	0.31	.1248	1.1	0.14	.0000	
Total							100.0000	

a. Empirical crystal radii.

The ionic composition by volume of six of the seven volcanic rock types (andesite breccia excluded) of the Cienega area is listed in Table 14. The volume of oxygen ranges from 94.1959 to 93.0236 percent. The volume of oxygen decreases about 1 percent from glassy lathe toward limburgite. This decrease is not a gradual one, because olivine basalt and basalt have higher water content. The total volume of oxygen of

TABLE 14. IONIC (ELEMENTARY) COMPOSITION BY
VOLUME OF THE VOLCANIC ROCKS OF THE
CIENEGA AREA, NEW MEXICO
(In percent)

IONS	GLASSY	AUGITE	CALCIC	OLIVINE		LIMBURGITE
	LATITE	MONZONITE	LATITE	BASALT	BASALT	
	Sample 92	Sample 84	Sample 72B	Sample 85	Sample 142	Sample 27
O ²⁻	94.1959	93.5938	93.2407	93.4555	93.9525	93.0236
Si ⁴⁺	.8580	.8061	.7414	.6910	.5658	.5269
Al ³⁺	.4599	.4634	.4940	.4282	.4215	.3280
Fe ³⁺	.1492	.2295	.3291	.1963	.2396	.1835
Fe ²⁺	.0337	.0591	.0840	.3151	.5313	.4484
Mg ²⁺	.0368	.0987	.1430	.5213	.7311	1.1136
Ca ²⁺	.6357	1.1473	1.3189	1.9096	1.9966	2.6270
Na ⁺	1.4779	1.2551	1.3202	1.0785	.8411	1.1004
K ⁺	2.0761	2.2549	2.2143	1.2266	.5246	.4169
H ¹⁺	.0456	.0464	.0655	.0868	.0981	.0628
C ⁴⁺	-	-	-	-	.0008	-
Ti ^{4±}	.0244	.0304	.0387	.0710	.0783	.1197
P ⁵⁺	.0010	.0018	.0034	.0070	.0019	.0043
Mn ²⁺	.0058	.0135	.0068	.0131	.0168	.0066
Ba ²⁺	-	-	-	-	-	-
Cr ³⁺	-	-	-	-	-	.0027
S ²⁻	-	-	-	-	-	.0356
Total	100.0000	100.0000	100.0000	100.0000	100.0000	100.0000

these two rocks is increased by their hydroxyls. If the oxygen of water is not included, there is a gradual decrease of the volume of oxygen from the acidic toward the basic rocks. The ionic volume of silicon decreases from glassy latite toward limburgite. The increase of the ionic volume of ferrous iron, magnesium, calcium, and titanium is also shown.

On the basis of the ionic volume of all the ions, it is shown that the average igneous rock is about equivalent to the calcic latite of the Cienega area.

Appendix I

RULES FOR THE CALCULATION OF NORMS (Modified from C.I.P.W. system)

The theoretical mineral composition of a rock can be calculated from a chemical analysis of the rock in terms of its weight norm or in terms of its molecular norm (norm classification, p. 38-45). The weight norm is calculated from molecular weights of the oxides. The molecular norm is calculated from the one-cation percentages. Parallel rules, modified from the C.I.P.W. system, are here set forth for each set of calculations.

The molecular weights of the oxides and normative molecules, calculated according to the revised international atomic weights of 1952, are listed in the following table:

OXIDES	MOLECULAR		NORMATIVE MOLECULES	MOLECULAR
	MOLECULAR WT.	WT. OF ONE- CATION OXIDE		
SiO ₂	60.09	60.09	Quartz, SiO ₂	60.09
Al ₂ O ₃	101.96	50.98	Orthoclase, K ₂ O·Al ₂ O ₃ ·6SiO ₂	556.70
Fe ₂ O ₃	159.70	79.85	Albite, Na ₂ O·Al ₂ O ₃ ·6SiO ₂	524.49
FeO	71.85	71.85	Anorthite, CaO·Al ₂ O ₃ ·2SiO ₂	278.22
MgO	40.32	40.32	Leucite, K ₂ O·Al ₂ O ₃ ·4SiO ₂	436.52
CaO	56.08	56.08	Nepheline, Na ₂ O·Al ₂ O ₃ ·2SiO ₂	284.13
			Kaliophilite, K ₂ O·Al ₂ O ₃ ·2SiO ₂	316.34
Na ₂ O	61.99	31.00	Corundum, Al ₂ O ₃	101.96
K ₂ O	94.20	47.10	Acmite, Na ₂ O·Fe ₂ O ₃ ·4SiO ₂	462.05
			Sodium metasilicate, Na ₂ O·SiO ₂	122.08
			Potassium metasilicate, K ₂ O·SiO ₂	154.29
H ₂ O	18.02		Wollastonite, CaO·SiO ₂	116.17
CO ₂	44.01	44.01	Enstatite, MgO·SiO ₂	100.41
TiO ₂	79.90	79.90	Ferrosilite, FeO·SiO ₂	131.94
			Hypersthene, (Mg,Fe)O·SiO ₂	—*
			Diopside, CaO·(Mg,Fe)O·2SiO ₂	—*
			Casilite, cs, 2CaO·SiO ₂	172.25
P ₂ O ₅	141.95	70.98	Forsterite, 2MgO·SiO ₂	140.73
MnO	70.93	70.93	Fayalite, 2FeO·SiO ₂	203.79
BaO	153.36	153.36	Magnetite, FeO·Fe ₂ O ₃	231.55
SrO	103.63	103.63	Hematite, Fe ₂ O ₃	159.70
V ₂ O ₃	149.90	74.95	Ilmenite, FeO·TiO ₂	151.75
Li ₂ O	29.88	14.94	Apatite, 3.33CaO·P ₂ O ₅	328.70
SO ₃	80.07	80.07	or 3CaO·P ₂ O ₅ ·O·33CaO·F ₂	366.70
Cl ₂	70.91		Calcite, CaO·CO ₂	100.09
			Chromite, Cr ₂ O ₃ ·FeO	223.87
			Pyrite, FeS ₂	119.98
			Sphene, CaO·TiO ₂ ·SiO	196.07
			Perovskite, CaO·TiO ₂	135.98
			Zircon, ZrO ₂ ·SiO ₂	123.22
			Thenardite, Na ₂ O·SO ₃	142.06
			Halite, NaCl	58.45

* Molecular wt. varies with the Mg:Fe ratio.

WEIGHT NORM

The molecular number of each oxide of the rock analysis is derived by dividing the percentage weight of the oxide by its molecular weight. The molecular numbers of MnO and NiO are added to that of FeO, that of Li₂O to that of Na₂O, that of V₂O₃ to that of Al₂O₃, and those of BaO and SrO to that of CaO. H₂O is not included in the normative calculation. The weight percentages of the normative minerals are recalculated to total 100 percent.

- Rule 1a. *Apatite*. A molecular number of CaO equal to 3.33 times that of P₂O₅ is allotted for apatite. If F is present, allot CaO equal to 3.00P₂O₅ and 0.33F.
- Rule 2a. *Pyrite*. A molecular number of FeO equal to half that of SO₃ is allotted for pyrite. If there is Cl₂ in the analysis, a molecular number of Na₂O equal to that of Cl₂ is allotted to form halite. If there are any hauynite-group minerals in the rock, as determined by microscopic examination, a molecular number of Na₂O equal to that of SO₃ is allotted for thenardite. In this case, thenardite is calculated before pyrite.
- Rule 3a. *Chromite*. Allot a molecular number of FeO equal to that of Cr₂O₃ for chromite.
- Rule 4a. *Ilmenite*. Allot a molecular number of FeO equal to that of TiO₂ for ilmenite. If there is an excess of TiO₂, see Rule 5a.
- Rule 5a. *Sphene*. Allot a molecular number of CaO equal to that of the excess of TiO₂ in Rule 4a to form sphene. This is done only after the allotment of CaO to Al₂O₃ for anorthite in Rule 10a. Any excess of TiO₂ over CaO is calculated as rutile.
- Rule 6a. *Calcite*. Allot a molecular number of CaO equal to that of CO₂ for calcite.
- Rule 7a. *Zircon*. The molecular number of ZrO₂ is calculated as zircon.
- Rule 8a. *Orthoclase*. Allot a molecular number of Al₂O₃ equal to that of K₂O to form orthoclase. In extremely rare cases an excess of K₂O over Al₂O₃ is calculated as potassium metasilicate.
- Rule 9a. *Albite*. Allot a molecular number of Al₂O₃ equal to that of Na₂O to form albite. If there is an excess of Na₂O over Al₂O₃, see Rule 12a. In this case there will be no anorthite in the norm.
- Rule 10a. *Anorthite*. The molecular number of Al₂O₃, left over after Rule 9a, is allotted to an equal molecular number of CaO for anorthite. See Rule 15a if there is excess of CaO over Al₂O₃.
- Rule 11a. *Corundum*. An excess of Al₂O₃ after Rule 10a is calculated as corundum.
- Rule 12a. *Acmite*. The excess of Na₂O in Rule 9a is combined with an equal molecular number of Fe₂O₃ to form acmite. In very

- rare cases an excess of Na_2O over Fe_2O_3 is calculated as sodium metasilicate.
- Rule 13a. *Magnetite*. The remaining Fe_2O_3 is allotted an equal molecular number of the remaining FeO to form magnetite.
- Rule 14a. *Hematite*. If there is an excess of Fe_2O_3 in Rule 13a, it is calculated as hematite.
- Rule 15a. *Wollastonite*. The remaining CaO is calculated as wollastonite.
- Rule 16a. *Enstatite*. The remaining MgO is calculated as enstatite.
- Rule 17a. *Ferrosilite*. The remaining FeO is calculated as ferrosilite.
- Rule 18a. *Quartz*. Allot a molecular number of SiO_2 equal to that of ZrO_2 for zircon in Rule 7a; to that of TiO_2 for sphene in Rule 5a; to four times that of Na_2O for acmite in Rule 12a; to six times that of K_2O for orthoclase in Rule 8a; to six times that of Na_2O for albite in Rule 9a; to twice that of CaO for anorthite in Rule 10a; to that of CaO for wollastonite in Rule 15a; to that of MgO for enstatite in Rule 16a; to that of FeO for ferrosilite in Rule 17a; or to that of K_2O or Na_2O for potassium metasilicate or sodium metasilicate in Rule 8a or 12a. After these allotments, the excess of SiO_2 is calculated as quartz. If there is a deficiency of SiO_2 , the previously calculated wollastonite, enstatite, and ferrosilite will be changed to diopside, hypersthene (enstatite, ferrosilite), and olivine (forsterite and fayalite) according to the following rules:
- Rule 19a. *Diopside*. The CaO of wollastonite in Rule 15a is combined with an equal molecular number of $\text{MgO} \pm \text{FeO}$ to form diopside. A molecular number of SiO_2 equal to that of CaO ($\text{MgO} \text{ FeO}$) is allotted for diopside. The ratio $\text{MgO} : \text{FeO}$ in this normative diopside is the same as the ratio of MgO of Rule 16a to FeO of Rule 17a, which are used to form enstatite and ferrosilite. If there is an excess of CaO , see Rule 21a. If there is an excess of FeO MgO , see Rule 20a.
- Rule 20a. *Olivine and hypersthene, (Mg, Fe)O • SiO₂*. If the remaining SiO_2 after diopside in Rule 19a is more than half, but less than, the remaining MgO FeO , this remaining MgO - } FeO will be distributed between olivine and hypersthene according to the following equations:

$$\begin{aligned} x y &= M, \\ \text{and } 2x y &= 2S, \end{aligned}$$

where x = molecular number of Mg Fe in hypersthene,
 y = molecular number of Mg Fe in olivine,
 S = the remaining molecular number of SiO_2 after diopside,
and M = the remaining molecular number of MgO FeO after diopside.

Olivine and hypersthene may be listed separately in terms of their end members: forsterite, fayalite, enstatite, and ferrosilite. The MgO : FeO ratio of the hypersthene and olivine is the same as that of diopside in Rule 19a.

- Rule 21a. *Casilite*. If the remaining SiO₂ after diopside is more than half, but less than, the remaining CaO, this remaining CaO will be distributed between wollastonite and casilite (2CaO • SiO₂) according to the same equations in Rule 20a. In this case, x equals the molecular number of CaO of wollastonite, y equals the molecular number of CaO of casilite, and M equals the remaining molecular number of CaO after diopside.
- Rule 22a. *Perovskite and olivine*. If the remaining SiO₂ after diopside in Rule 19a is less than half the remaining MgO FeO, there will be no hypersthene in the norm. All or part of the sphene calculated in Rule 5a is changed to perovskite. The SiO₂ obtained from this change is allotted to satisfy the olivine of Rule 20a. If this additional SiO₂ is still not enough to satisfy the olivine of Rule 20a, see Rule 23a below. In case of an excess of CaO in Rule 19a, treat casilite of Rule 21a the same as the olivine in this rule.
- Rule 23a. *Nepheline and albite*. Sum up the molecular numbers of SiO₂ allotted to zircon, orthoclase, anorthite, diopside, acmite, sodium and potassium metasilite, casilite, and olivine; subtract this sum from the total molecular number of SiO₂ of the rock analysis; if the remainder is more than twice but less than six times that of the Na₂O of the albite of Rule 9a, this remainder of the molecular number of SiO₂ is distributed between albite and nepheline according to the following equations:
- $$\begin{aligned} x \ y &= N, \\ \text{and } 6x \ 2y &= S, \end{aligned}$$
- where x = molecular number of Na₂O in albite,
 y = molecular number of Na₂O in nepheline,
 N = molecular number of Na₂O of the albite in Rule 9a,
 and S = the remainder of the molecular number of SiO₂.
- Rule 24a. *Leucite and orthoclase*. If the remainder of the molecular number of SiO₂ mentioned in Rule 23a is less than twice that of Na₂O of the albite of Rule 9a, there will be no albite in the norm. Allot all the Na₂O to form nepheline. The deficient molecular number of SiO₂ needed for the nepheline will be made up by changing all or part of the orthoclase of Rule 8a to leucite according to the following equations:

$$\begin{aligned}x y &= K, \\ \text{and } 6x - 4y &= S,\end{aligned}$$

where x = molecular number of K_2O in orthoclase,
 y = molecular number of K_2O in leucite,
 K = molecular number of K_2O of the orthoclase in Rule 8a,
and S = molecular number of SiO_2 allotted to orthoclase in Rule 18a, minus the deficient SiO_2 mentioned above.

If the SiO_2 derived by changing all the orthoclase to leucite is still not enough to satisfy both the nepheline and leucite, see Rule 25a below.

Rule 25a. *Diopside, casilite, and olivine.* There will be no albite and orthoclase in the norm. Allot all the Na_2O to form nepheline, and then all the K_2O to form leucite. Allot enough SiO_2 to nepheline first. Then the remaining SiO_2 will not be enough to satisfy leucite. The deficient SiO_2 will be derived by changing part of the diopside calculated in Rule 19a into casilite and olivine according to the following equations:

$$\begin{aligned}x y &= MC, \\ \text{and } 2x - y &= 2S,\end{aligned}$$

where x = the total molecular number of CaO and MgO FeO of the new diopside, or the SiO_2 of the new diopside (the molecular number of the CaO and the MgO FeO of diopside are equal),
 y = the total molecular number of CaO and MgO FeO of the casilite and olivine, or twice the total SiO_2 of the casilite and the olivine (the CaO molecular number of the casilite and the MgO - } FeO molecular number of the olivine are equal),
 MC = the total molecular number of CaO and MgO FeO of the diopside of Rule 19a,
and
 S = the molecular number of the SiO_2 of the rock analysis, minus the total SiO_2 allotted to zircon, anorthite, nepheline, leucite, acmite, sodium and potassium metasilite, olivine of Rule 20a, and casilite of Rule 21a.

Note: (1) The total casilite of the norm is the sum of the casilite calculated in Rules 21a and 25a. The total olivine of the norm is the sum of the olivine calculated in Rules 20a and 25a.
(2) The MgO : FeO ratio of the diopside and olivine remains the same as that of the diopside of Rule 19a.

Rule 26a. *Kaliophilite*. If the SiO_2 (S) in Rule 25a is not sufficient to satisfy the olivine and casilite, there will be no diopside in the norm. Change part of the leucite to kaliophilite in order to derive additional SiO_2 to satisfy the olivine and casilite according to the following equations:

$$\begin{aligned}x y &= K, \\ \text{and } 4x + 2y &= S,\end{aligned}$$

where x = molecular number of K_2O in leucite,
 y = molecular number of K_2O in kaliophilite,
 K = molecular number of K_2O of the orthoclase in Rule 8a,
 and S = molecular number of SiO_2 to satisfy leucite, minus the deficient molecular number of SiO_2 to satisfy olivine and casilite in Rule 25a.

MOLECULAR NORM

The weight percentages of the oxides of the rock analysis are divided by the molecular weights of their respective one-cation oxides. The quotient is called the cation number, or the equivalent molecular number of one-cation oxide. Recalculate the cation number into a total 100 percent. The percentages of Mn and Ni are added to Fe^{2+} , of Ba and Sr to Ca, of Li to Na, and of V to Al. Thus the percentages of the cations are obtained. These cation percentages are used in the molecular-norm calculation as follows (apatite is the first normative mineral to be calculated):

- Rule 1b. *Apatite*. A percentage of Ca equal to 1.67 that of P is allotted to form apatite. If F is present, allot Ca equal to 1.50 P and half of F. Allot a percentage of Na equal to that of Cl to form halite.
- Rule 2b. *Pyrite*. A percentage of Fe^{2+} equal to half that of S is allotted to form pyrite. If there are any häüynite-group minerals in the rock, as determined by microscopic examination, a percentage of Na equal to twice that of S is allotted to form thenardite. In this case thenardite is calculated before pyrite.
- Rule 3b. *Chromite*. A percentage of Fe^{2+} equal to half that of Cr is allotted to form chromite.
- Rule 4b. *Ilmenite*. Equal percentages of Ti and Fe^{2+} are combined to form ilmenite. If there is an excess of Ti, see Rule 5b.
- Rule 5b. *Sphene*. Allot a percentage of Ca equal to the excess of Ti in Rule 4b to form sphene. This is done only after the allotment of Ca to Al for anorthite in Rule 10b.
- Rule 6b. *Calcite*. Allot a percentage of Ca equal to that of C for calcite.
- Rule 7b. *Zircon*. The percentage of Zr is allotted for zircon.

- Rule 8b. *Orthoclase*. Allot a percentage of Al equal to that of K to form orthoclase. If there is an excess of K over Al, the excess of K is allotted to form potassium metasilicate.
- Rule 9b. *Albite*. Allot a percentage of Al equal to that of Na to form albite. If there is an excess of Na over Al, see Rule 12b. In this case there will be no anorthite in the norm.
- Rule 10b. *Anorthite*. A percentage of Ca equal to half the percentage of Al after Rule 9b is allotted to form anorthite. See Rule 15b if there is an excess of Ca over Al.
- Rule 11b. *Corundum*. Any excess of Al after anorthite is calculated as corundum.
- Rule 12b. *Acmite*. The excess of Na in Rule 9b is combined with an equal percentage of Fe^{3+} to form acmite. In very rare cases any excess of Na over Fe^{3+} is allotted to form sodium metasilicate.
- Rule 13b. *Magnetite*. A percentage of the remaining Fe^{2+} equal to half that of the remaining Fe^{3+} is allotted to form magnetite. Rule 14b. *Hematite*. Any excess of Fe^{3+} in Rule 13b is calculated as hematite.
- Rule 15b. *Wollastonite*. The remaining percentage of Ca is calculated as wollastonite.
- Rule 16b. *Enstatite*. The remaining percentage of Mg is calculated as enstatite.
- Rule 17b. *Ferrosilite*. The remaining percentage of Fe^{2+} is calculated as ferrosilite.
- Rule 18b. *Quartz*. Allot a percentage of Si equal to that of Zr to form zircon in Rule 7b; to that of Ti to form sphene in Rule 5b; to three times that of K to form orthoclase in Rule 8b; to three times that of Na to form albite in Rule 9b; to twice that of Ca to form anorthite in Rule 10b; to that of Ca to form wollastonite in Rule 15b; to that of Mg to form enstatite in Rule 16b; to that of Fe to form ferrosilite in Rule 17b; or to that of K or Na to form potassium or sodium metasilicate in Rules 8b and 12b. After these allotments the excess of Si is calculated as quartz. If there is a deficiency of Si, the previously calculated wollastonite, enstatite, and ferrosilite will be recalculated into diopside, hypersthene (enstatite, ferrosilite), and olivine (forsterite and fayalite) according to the following rules:
- Rule 19b. *Diopside*. The Ca of wollastonite in Rule 15b is combined with an equal percentage of Mg + Fe to form diopside. A percentage of Si equal to that of Ca + (Mg + Fe) is allotted for diopside. The ratio Mg : Fe in this normative diopside is the same as the ratio of Mg of Rule 16b to Fe of Rule 17b. If there is an excess of Mg + Fe, see Rule 20b. If there is an excess of Ca, see Rule 21b.

Rule 20b. *Olivine and hypersthene*. If the remaining percentage of Si after diopside in Rule 19b is more than half, but less than, the remaining Mg + Fe, this remaining Mg + Fe will be distributed between olivine and hypersthene according to the following equations:

$$\begin{aligned}x + y &= M, \\ \text{and } 2x + y &= 2S,\end{aligned}$$

where x = percentage of Mg + Fe of hypersthene,
y = percentage of Mg + Fe of olivine,
M = the remaining percentage of Mg + Fe,
and S = the remaining percentage of Si.

The ratio Mg : Fe of the olivine and hypersthene is the same as that of diopside in Rule 19b. Both olivine and hypersthene may be listed separately in terms of their end members: forsterite, fayalite, enstatite, and ferrosilite.

Rule 21b. *Casilite*. If the remaining Si after diopside in Rule 19b is more than half, but less than, the remaining Ca, this remaining Ca will be distributed between wollastonite and casilite according to the same equations as in Rule 20b. In this case x is the percentage of Ca of wollastonite, y is the percentage of Ca of casilite, and M is the remaining percentage of Ca.

Rule 22b. *Perovskite and olivine*. If the remaining Si after diopside of Rule 19b is less than half the remaining Mg + Fe, there will be no hypersthene in the norm. All or part of the sphere of Rule 5b is changed to perovskite. The Si obtained from this change is allotted to satisfy olivine of Rule 20b. If this additional Si is still not enough to satisfy the olivine of Rule 20b, see Rule 23b. In case of an excess of Ca in Rule 19b, treat casilite of Rule 21b the same as the olivine in this rule.

Rule 23b. *Nepheline and albite*. Sum up the percentage of Si allotted to zircon, orthoclase, anorthite, acmite, sodium and potassium metasilicate, diopside of Rule 19b, casilite of Rule 21b, and olivine of Rule 22b. Subtract this sum from the total Si of the rock analysis. If the remainder is more than, but less than three times that of the Na of the albite in Rule 9b, this remainder of the Si percentage is distributed between albite and nepheline according to the following equations:

$$\begin{aligned}x + y &= N, \\ \text{and } 3x + y &= S,\end{aligned}$$

where x = percentage of Na of the new albite,
y = percentage of Na of the nepheline,
N = percentage of Na used for albite in Rule 9b,
and S = the remainder of the Si percentage.

Rule 24b. *Leucite*. If the remainder of the Si percentage mentioned in Rule 23b is less than that of Na, allot all the Na to form nepheline. In this case there will be no albite in the norm. The deficient percentage of Si needed for the nepheline will be made up by changing all or part of the orthoclase of Rule 8b to leucite according to the following equations:

$$\begin{aligned}x y &= K, \\ \text{and } 3x + 2y &= 5,\end{aligned}$$

where x = percentage of K of the new orthoclase,

y = percentage of K of leucite,

K = percentage of K used for orthoclase in Rule 8b,

and S = the remainder of the Si percentage (Si for orthoclase in Rule 8b, minus the deficient Si needed for the nepheline).

If the Si percentage derived by changing all the orthoclase to leucite is still not enough to satisfy both the nepheline and leucite, see Rule 25b.

Rule 25b. *Diopside, casilite, and olivine*. There will be no albite and orthoclase in the norm. Allot all Na to nepheline and all K to leucite. Allot enough Si to nepheline first. Then the remaining Si will not be enough to satisfy the leucite. The deficient Si needed for the leucite will be derived by changing part of the diopside calculated in Rule 19b into casilite and olivine according to the following equations:

$$\begin{aligned}x + y &= MC, \\ \text{and } 2x + y &= 2S,\end{aligned}$$

where x = the total percentage of Ca and Mg + Fe of the new diopside, or the Si percentage of the new diopside (the percentage of the Ca and the Mg + Fe of the new diopside are equal), y = the total percentage of Ca and Mg + Fe of the casilite and the olivine, or twice the total Si percentage of the casilite and the olivine (the Ca percentage of the casilite and the Mg + Fe percentage of the olivine are equal),

MC = the total percentage of Ca and Mg + Fe of the diopside of Rule 19b,

and S = the percentage of Si of the rock analysis, minus the total Si allotted to zircon, anorthite, nepheline, leucite, acmite, sodium and potassium metasilicate, olivine of Rule 20b, and casilite of Rule 21b.

Note: (1) The total casilite of the norm is the sum of the casilite calculated in Rules 21b and 25b. The total olivine of the norm is the sum of the olivine calculated in Rules 20b and 25b.

(2) The Mg : Fe ratio of the diopside and olivine remains the same as that of the diopside of Rule 19b. Rule 26b.

Kaliophilite. If the percentage of Si (S) in Rule 25b is not sufficient to satisfy the casilite and olivine, there will be no diopside in the norm. Change part of the leucite of Rule 24b to kaliophilite in order to obtain additional Si to satisfy the olivine and casilite according to the following equations:

$$\begin{aligned} x y &= K, \\ \text{and } 2x + y &= S, \end{aligned}$$

where x = cation percentage of K of the new leucite,

y = cation percentage of K of kaliophilite,

and S = the Si percentage to satisfy leucite, minus the deficient Si to satisfy olivine and casilite.

Appendix II

SUMMARY OF DATA FROM ROCK SAMPLES,
CIENEGA AREA, NEW MEXICO

SAMPLE NO. ¹	COLOR ²	INDEX OF REFRACTION ³	SILICA PERCENTAGE ⁴	THIN SECTION	REMARKS
BASALT					
2	N4	1.585	_____	x	Base of flow; some vesicles.
85	N5	1.586	50.06	X	Flow; 12 ft below top of cliff; some vesicles.
CIENEGUILLA LIMBURGITE					
27	N3	1.640	90.18	X	Top of Cerro de la Cruz; analysis is for sample collected by Stearns (1953-b); olivines are fresh.
48	N3	1.625	41.99	—	Dike 8 in. thick; cuts andesite breccia.
49	N3	1.633	43.05	X	Flow(?); contains monzonite inclusions.
73	N4	1.646	38.99	—	Dike.
79	N3	1.647	_____	—	Dike cutting andesite breccia; somewhat altered.
80	N3	1.641	_____	—	One of 4 parallel dikes.
86	N3	1.635	_____	X	Block in fault breccia; adjacent blocks have meager matrix of red sandstone.
87	N3	1.638	_____	X	Flow no. 2.
95	N4	1.640	_____	—	Dike; somewhat altered.
109	N2	1.640	_____	—	Dike about 10 ft wide along fault that offsets hornblende andesite dike about 10 ft; horizontal columnar jointing.
141	N3	1.636	_____	—	Lower, nonvesicular part of flow just above tuff-breccia.
142	N4	1.619	45.81	X	Flow no. 1; olivine basalt.
147	N3	1.642	_____	—	Flow no. 2.
FELSITE DIKE					
3	5R7/2	1.532	_____	X	Finely vesicular.
VENT BRECCIA					
187	N5	1.550	_____	X	Abundant tiny light-colored spots.
189	N5	1.594	_____	X	Similar to 187, but with flow bands.
190	N4	_____	_____	X	Flow bands, small vesicles; part of block 3 ft in diameter.

SAMPLE NO.1	COLOR ²	INDEX OF REFRACTION ³	SILICA PERCENTAGE ⁴	THINSECTION	REMARKS
HORNBLLENDE ANDESITE DIKE					
4	N4	1.567	—	—	Scattered inclusions, including 2-in. piece of granitoid rock.
8	5YR5/1	1.548	62.22	×	Moderate flow alinement of hornblende crystals.
70	5YR3/1	1.564	—	—	Pebble of hornblende andesite, possibly from dike; in upper part of glassy latite.
AUGITE BASALT					
20	N5	1.604	—	×	Altered.
83	N4	1.600	48.28	—	Probably continuous with 118; slightly altered.
118	N4	1.602	—	—	Probably continuous with 83; slightly altered.
123	N6	1.608	—	—	Altered; brownish tint.
VOLCANIC CONGLOMERATE NEAR GALLEGOS RANCH— included pebbles					
173	5YR5/1	1.566	—	×	Andesite similar to 171.
174	5YR5/1	1.558	—	×	Andesite similar to 171; identical(?) to 173.
176	5YR4/1	1.552	—	—	Calcic latite(?) somewhat similar to 7; fairly fine grained.
177	5YR5/1	1.552	—	—	Calcic latite(?); feldspars measure 2 mm in aphanitic groundmass.
180	N4	1.541	—	×	Similar to 189 (vent breccia).
181	5YR5/1	1.552	—	—	Glassy latite(?); similar to 106.
182	(N5)	1.596	—	—	Fine-grained, altered rock.
GLASSY LATITE					
14	N7	1.536	62.84	×	Tuffaceous matrix; upper part of glassy latite.
19	N7	1.536	—	×	Matrix of breccia; flow structure; upper part of glassy latite.
21	10YR7/2	{ (1.530) (1.540)	—	×	{ Fragment; Mostly matrix; } upper part of glassy latite.
71	10R7/5	1.538	—	×	Matrix; lower part of glassy latite.
89	5YR4/1	1.540	65.43	—	Fragment in breccia; lower part of glassy latite.
91	N3	1.542	—	×	Fragment of welded tuff in breccia; upper part of glassy latite.

SAMPLE NO.1	COLOR 2	INDEX OF REFRACTION 3	SILICA PERCENTAGE 4	THINSECTION	REMARKS
92		1.531	65.16	×	Fragment in breccia; 5 ft above base of glassy latite.
106	5YR4/1	1.525	69.04	—	Loose block near base of glassy latite; feldspars measure 2-3 mm.
199	5YR8/1	1.544	—	—	Tuff; upper part of glassy latite; from base of cliff in Plate 3B.
CALCIC LATITE					
6	5YR5/2	—	—	×	Angular breccia; fragments similar to 13.
7	5YR4/1	1.558	—	×	Part of flow or piece of large block in breccia; fine-grained.
10	N6	1.550	—	—	Flow; vesicular; slightly altered.
13	5YR6/1	—	—	×	Flow; aphanitic with a few small feldspar phenocrysts; one piece abundantly vesicular.
17a	5YR6/1	1.556	—	×	Fine- to medium-grained phenocrysts of feldspar and some augite.
17b	5YR6/1	—	—	×	Flow breccia; similar to 72a.
17c	10Y6/2	—	—	×	Somewhat altered; feldspar phenocrysts 1 x 2 mm maximum.
18	5YR5/1	{ 1.538 1.554	—	×	{ Matrix. { Possibly calcic latite fragments in matrix of glassy latite; similar to 170, but plagioclase more sodic.
18a	5YR5/1	1.558	63.71	—	Fragments and matrix.
72a	5YR5/1	1.558	—	×	Flow breccia; above a 3-ft red oxidized zone.
72b	5YR5/1	1.562	55.12	×	Block in faintly brecciated flow; below 3-ft red oxidized zone.
74	5YR6/1	1.554	57.76	—	Flow; vesicles elongated horizontally N.-S.; similar to 13.
96	10YR6/2	1.550	—	—	Similar to 17a.
97	N4	1.552	—	—	Augite phenocrysts; somewhat altered; similar to augite basalt.
99	5YR7/1	1.554	—	—	Tuffaceous rock; just below contact with overlying glassy latite.
103	N5	1.555	—	—	Block in breccia; augite and feldspar phenocrysts generally less than 1 mm in glassy(?) groundmass; unlike other calcic latite; somewhat similar to 187 (vent breccia).
114	N6	1.556	59.17	—	Flow breccia; similar to 72a.
120	(5YR5/1)	1.550	—	—	Similar to 17a.
121	5YR6/1	1.544	—	—	Fragment in breccia; flow structure; aphanitic like 13.
122	N8	1.563	—	—	Tuff; faintly pink.
124	5YR4/1	1.550	—	—	Block in breccia; similar to 17a but finer grained.
125	5YR8/1	1.544	—	—	Tuff-breccia; possibly not calcic latite.

SAMPLE NO.1	COLOR 2	INDEX OF REFRACTION 3	SILICA PERCENTAGE 4	THINSECTION	REMARKS
AUGITE MONZONITE					
5	N7	1.548	—	×	
49		—	—	×	Monzonite inclusions in limburgite.
84	5Y7/2	1.552	<i>60.10</i>	×	
134	5Y7/2	1.544	—	—	In canyon 4 miles west of Cienega; possibly from outcrop represented by analysis "AA" of Wells (1937, p. 34).
139	5YR4/1	1.552	—	—	
185	N6	1.556	—	×	Monzonite block in basal calcic latite breccia.
ANDESITE BRECCIA					
39	5Y7/2	1.563	—	×	{ Fragments and matrix from crudely bedded basal soft zone. Matrix.
119	5YR5/1	1.552	—	—	
149	(N7)	1.579	54.81	—	Hornblende monzonite; forms 10- x 20-ft outcrop; possibly a dike. Fragment from tuff-breccia.
150	5YR5/1	1.567	—	—	Fragments and matrix of tuff-breccia.
161	5YR8/1	1.557	—	×	Block of hornblende monzonite(?) in breccia; somewhat altered.
162	5YR7/1	1.564	<i>58.43</i>	×	Block of hornblende monzonite(?) in breccia.
167	(N6)	1.558	—	×	Block of hornblende monzonite(?) in breccia.
168	5YR7/1	1.560	—	×	Block of hornblende andesite(?) in breccia; somewhat altered.
169	5YR7/2	1.562	—	×	Tuffaceous matrix of breccia.
170	5YR6/1	1.554	—	×	Tuff-breccia matrix; similar to 18 (calcic latite).
171	(N5)	1.563	—	×	Block in breccia; fine grained, with flow structure.
172	5YR7/1	1.562	—	×	Tuff-breccia.
201	—	—	—	—	Disintegrated andesite breccia (table 3).
202	N6	1.545	—	×	{ Fragments. Matrix.
	5R5/1				

1. Field samples from the Cienega area were given 132-D as a prefix; prefix is omitted in this report. Sample localities are shown on Plate 1.
2. Color symbols are the Munsell designations given on the Rock Color Chart distributed by the Geological Society of America, 1951. Colors are given for broken surfaces of rocks. Symbols in parentheses are less satisfactory approximations than the other symbols.
3. Italicized values are averages of two determinations of the same sample.
4. Silica analyses by H. B. Wiik, except sample 27 (by F. E. Gonyer) and sample 162 (by V. C. Juan). Italicized values represent complete chemical analyses.

References

- Barth, T. F. W. (1931-1932) *Proposed change in calculation of norms of rocks*, *Min. pet. Mitt.*, v. 42, 1-7.
- (1948) *Oxygen in rocks*, *Jour. Geology*, v. 56, 50-60.
- (1952) *Theoretical petrology*, New York, John Wiley & Sons, Inc.
- (1955) *Presentation of rock analysis*, *Jour. Geology*, v. 63, 348-363.
- Callaghan, E., and Sun, M.-S. (1956) *Correlation of some igneous rocks of New Mexico by fusion method*, *Am. Geophys. Union Trans.*, v. 37, 761-766.
- Chayes, F. (1949) *A simple point counter for thin-section analysis*, *Am. Mineralogist*, v. 34, 1-11.
- (1951) *Modal analyses of the granite and diabase test rocks*, U. S. Geol. Survey Bull. 980, pt. 5.
- Clarke, F. W., and Washington, H. S. (1924) *The composition of the earth's crust*, U.S. Geol. Survey Prof. Paper 127.
- Cross, C. W., Iddings, J. P., Pirsson, L. V., and Washington, H. S. (1902) *A quantitative chemico-mineralogical classification and nomenclature of igneous rocks*, *Jour. Geology*, v. 10, 555-690.
- Daly, R. A. (1933) *Igneous rocks and the depths of the earth*, 2d ed., New York, McGraw-Hill Book Co., Inc.
- Disbrow, A. E., and Stoll, W. C. (1957) *Geology of the Cerrillos area, Santa Fe County, New Mexico*, N. Mex. Inst. Min. and Technology, State Bur. Mines and Mineral Res. Bull. 48.
- Eskola, P. (1921) *The mineral facies of rocks*, *Norsk geol. tidsskr.*, v. 6, 143.
- (1954) *A proposal for the presentation of rock analyses in ionic percentage*, *Ann. Acad. Sci. Fennicae, ser. A, III (geol.-geogr.)*, n. 38.
- George, W. O. (1924) *The relation of physical properties of natural glasses to their chemical composition*, *Jour. Geology*, v. 32, 353-372.
- Hayden, F. V. (1869) *Preliminary field report [third annual] of the U. S. Geological Survey of Colorado and New Mexico*, Washington, D. C.
- Iddings, J. P. (1920) *Igneous rocks*, 2d ed. rev., v. 1, New York, John Wiley & Sons. Johannsen, A. (1931) *A descriptive petrography of the igneous rocks*, v. 1, Chicago, Chicago Univ. Press.
- (1937) *A descriptive petrography of the igneous rocks*, v. 3, Chicago, Chicago Univ. Press.
- Juan, V. C., Tai, H., and Chang, F. H. (1953) *Taiwanite, a new basaltic glassy rock of East Coastal Range, Taiwan, and its bearing on the parental magma-type*, *Acta Geologica Taiwanica*, National Taiwan University, Taipei, Taiwan, China, n. 5, 1-25.
- Kelley, V. C. (1952) *Tectonics of the Rio Grande depression of central New Mexico*, N. Mex. Geol. Soc. Guidebook, 3d Field Conf., 93-105.
- (1954) *Tectonic map of a part of the upper Rio Grande area, New Mexico*, U. S. Geol. Survey Oil and Gas Inv. Map OM 157.
- Mathews, W. H. (1951) *A useful method for determining approximate composition of fine grained igneous rocks*, *Am. Mineralogist*, v. 36, 92-101.
- Morey, G. W. (1938) *The properties of glass*, New York, Reinhold Pub. Corp. Muthuswami, T. N. (1952) *Niggli's principles of igneous petrogenesis*, *Proc. Indian Acad. Sci.*, v. 36, n. 1, sec. A, 1-40.
- Niggli, P., and Lombaard, B. (1933) *Das Bushveld als petrographische Provinz*, *Schweiz. min. pet. Mitt.*, v. 13, 110.
- (1936) *Molekularmormen zu Gesteinsberechnung*, *Schweiz. min. pet. Mitt.*, v. 16, 295-317.
- Pauling, L. (1945) *The nature of chemical bond*, Ithaca, Cornell Univ. Press.
- Rankama, K., and Sahama, T. G. (1950) *Geochemistry*, Chicago, Chicago Univ. Press.

- Robinson, P. (1957) *Age of Galisteo formation, Santa Fe County, New Mexico*, Am. Assoc. Petrol. Geol. Bull., v. 41, 757.
- Smith, H. T. U. (1938) *Tertiary geology of the Abiquiu quadrangle, New Mexico*, Jour. Geology, v. 46, 933-965.
- Spiegel, Z., and Baldwin, B. (1957) *Geology and water resources of the Santa Fe area, New Mexico*, unpublished manuscript, N. Mex. Inst. Min. and Technology, State Bur. Mines and Mineral Res.
- Stanworth, J. E. (1950) *Physical properties of glass*, London, Oxford Univ. Press. Stearns, C. E. (1943) *The Galisteo formation of north-central New Mexico*, Jour. Geology, v. 51, 301-319.
- (1953-a) *Tertiary geology of the Galisteo-Tonque area, New Mexico*, Geol. Soc. Am. Bull., v. 64, 459-508.
- (1953-b) *Early Tertiary vulcanism in the Galisteo-Tonque area, north-central New Mexico*, Am. Jour. Sci., v. 251, 415-452.
- Sun, M.-S. (1957) *The nature of iddingsite in some basaltic rocks of New Mexico*, Am. Mineralogist, v. 42, 525-533.
- Tilley, C. E. (1922) *Density, refractivity, and composition relations of some natural glasses*. Mineralogical Mag., v. 19, 275-294.
- (1932-1933) *On the proposed "doctoring" of the norm*, Min. pet. Mitt., v. 43, 67-68.
- Washington, H. S. (1932-1933) *The use of "ferrosilite" as a name for the normative molecule FeSiO_3* , Min. pet. Mitt., v. 43, 63-66.
- Wells, R. C. (1937) *Analyses of rocks and minerals from the laboratory of the U. S. Geological Survey, 1914-36*, U. S. Geol. Survey Bull. 878.

Index

Numbers in *italics* indicate figures and plates; **boldface** *indicates* main references.

- Abiquiu(?) formation, 22
Alamo Creek, 4, *p1.1*
Alluvium, 5, **19**, *p1.1*
Analyses, *see* Chemical analysis; Modal analysis; Normative analysis; Spectrographic analysis
Ancha formation, 7,18, *p1.1*
 age, 22-23
 basal contact, 18, 22
 upper contact, 18
Andesite (*see also* Andesite breccia; Hornblende andesite dike), 26-27
 orthoclase-plagioclase ratio of Daly's average, 26-27
Andesite breccia, 7, 10-11, 14, 22, 36, *p1.1*
 alteration, 37
 basal contact, 10, 20
 chemical analysis, 54
 correlation with Cerrillos units, 22
 Holmquist formula, 55
 index of refraction, 48, *50*
 norms, 43, 44
 orthoclase-plagioclase ratio, 27
 petrographic description, 27-29
 samples, 73
 soft zone at base, 10, 22, 27-28
 upper contact, 11,13
Arroyo Hondo, 49, *p1.1*
Arroyo Pinovetito, 20, 22, *p1.1*
Artificial glass, 45, 48-51
Augite basalt, 14, *p1.1*
 index of refraction, 48, *50*
 samples, 71
Augite monzonite, 7, 9, 11-12, 15, 36, *p1.1*
 chemical analysis, 54
 correlation with Cerrillos units, 22
 flow structure, 11
 "fossil" weathered mantle, 11
 Holmquist formula, 55
 index of refraction, 48, *50*
 intrusion breccia, 11
 intrusive effect, 8, 11, 23, 24
 ionic composition, 58
 minor constituents, 52, 53
 norms, 43, 44
 orthoclase-plagioclase ratio of Daly's average, 27
 petrographic description, 29.30
 samples, 73
 upper contact, 11-12
Average igneous rock, 58
 Holmquist formula, 55
 ionic volume, 57
 norms, 43, 44
 oxygen, 42
Avogadro's number, 46

Baldwin, B., *see* Spiegel, Z.
Barth, T. F. W., 40, 41, 42, 54
Basalt, 7, 14, 18-19, 24, 36, *p1.1*
 age, 22-23
 chemical analysis, 54
 Holmquist formula, 55
 index of refraction, 48, *50*
 ionic composition, 58
 minor constituents, 52, 53
 norms, 43, 44
 petrographic description, 35
 samples, 70
Basalt tuff, 18
Basis molecule, 41
Becke line, 48
Bedrock floor, 5
Bernalillo, *p1.1*
Bonanza Hill, *pl. 2*
Breccia, 12
 angular, 12-13
 fault, 24
 flow, 12
 intrusion, 11
Bryan, K., and Upson, J. E., 21
Buell Park, Arizona, 52
Bundy, W. M., 6, 16
Burand, W. M., 6

Calcic latite, 7, 12-13, 14, 15, 22, 36, 58, *p1.1*
 angular breccia, 12, 13
 basal contact, 11-12,13
 chemical analysis, 54
 correlation with Cerrillos units, 22
 flow breccia, 12-13
 Holmquist formula, 55
 index of refraction, 48, *50*
 ionic composition, 58
 minor constituents, 52, 53
 norms, 43, 44
 petrographic description, 30-31
 samples, 72

- tuff-breccia, 13
 upper contact, 13, *pl.* 3C
 vesicular flow, 12
- Callaghan, E., 6
 and Sun, M.-S., 45, 46, 48
- Calvary Butte, 16
- Canyon, 3, 4, 16, *p1.1*
- Cerrillos, 5, 8, 23, *p1.1*
 area, 5, *p1.1*
 uplift, 23
- Cerro de la Cruz**, 16, *pl.* 1, *pl.* 2
- Cerros del Rio, 49
- Cerro Seguro**, 4, 16, 18, 21, *p1.1*, *pl.* 2
- Chayes, F., 40, 42
- Chemical analysis**, 54
 used for weight norm, 41
- Cienega**:
 area, 3, 4, 5, 7, *p1.1*
 Creek, 3, 4, 5, 19, *pl.* 1
 dam, 4
 fault, 23
 La Cienega, 3, 4, *p1.1*
 school, 4, 8, 15, *pl.* 2
- Cieneguilla, 3, 4, 5, 15, *p1.1*
- Cieneguilla limburgite** (*see also* Limburgite dikes; Olivine basalt), 7, 14, 15-18, 36, *p1.1*
 age, 22
 basal contact, 14
 chemical analysis, 54
 dikes, 25
 Holmquist formula, 55
 index of refraction, 48, 50
 ionic composition, 58
 minor constituents, 52, 53
 norms, 43, 44
 petrographic description, 33-35
 samples, 70
 vesicular, 16
- C.I.P.W. system (*see also* Norm classification), 40-41
- Clarke, F. W., and Washington, H. S., 43, 44, 45, 55, 56, 57
- Correlation of volcanic units, 21-22
- Coryphodon*, 20
- Cover, 19, *p1.1*
- Cretaceous mudstone, 7, 8, 9, 24, *p1.1*
- Cross, C. W., Iddings, J. P., Pirsson, L. V., and Washington, H. S., 40
- Crystal radius, 46, 56, 57
- Cuerbio basalt, 18
- Daly, R. A., 26
- Devitrification, 47-48
- Diorite, 26-27
 orthoclase-plagioclase ratio of Daly's average, 26-27
- Disbrow, A. E., and Stoll, W. C.**, 5, 19-22
 summary, 21
- Duchesnean, 20
- Eocene, 5, 7
- Equivalent molecular unit, *see* Basis molecule
- Eskola, P., 40, 41, 42, 54
- Espanola, *p1.1*
 basin, 5, 23
- Espinaso volcanics**, 3, 20-22
 age, 22
 name, 21
 summary of Disbrow's subdivisions, 21
 type section, 20
- Felsite dike**, 11, 15, *pl.* 1 index
 of refraction, 49, 50
 petrographic description, 32-33
 samples, 70
- Flow structure, 11
- "Fossil" weathered mantle, 11
- Galisteo, *p1.1*
 Creek, *p1.1*
 structural basin, 24, 25
- Galisteo formation**, 7, 8-10, 9, 13, *pl.* 1
 age, 20
 basal contact, 8, 20
 name, 19-20
 summary of Stearn's description, 20
 upper contact, 10, 20
- Gallegos ranch, 4, 23
- George, W. O., 45
- Glassy latite**, 7, 13-14, 15, 22, 36, *pl.* 1
 basal contact, 13
 chemical analysis, 54
 correlation with Cerrillos units, 22
 Holmquist formula, 55
 index of refraction, 48, 50
 ionic composition, 58
 minor constituents, 52, 53
 norms, 43, 44
 orthoclase-plagioclase ratio, 27
 petrographic description, 31-32
 samples, 71-72
 upper contact, 14
- Ground water, 5
- Hagan, 20, *pl.* 1
- Hayden, F. V., 20
- Holmquist formula (*see also* Standard rock cell), 37, 54-55
- Hornblende andesite dike**, 8, 14-15, 22, 25, 36, *p1.1*
 index of refraction, 48, 49, 50

- petrographic description, 31 samples, 71
 - Hornblende monzonite, 11
 - Hydrothermal alteration, 24
- Iddings, J. P., 26
- Index of refraction, Cienega vol-**
 - canic rocks** (*see also* Appendix H) , 3, 48-51
 - compared with other artificial glasses, 51
 - composition curve, 49
 - range for each volcanic unit, 50
- Index of refraction of fused samples,**
 - theory, 45-48
 - composition curve, 45-46
 - devitrification, 47-48
 - effect of color, 48
 - method of artificial fusion, 48
 - properties of glass, 46
 - related to composition, 46
 - related to internal stress, 47
 - related to ionic density, 46-47
 - 1 noceram* us, 8
 - Internal stress in glass, 47
 - Ionic density, 46, 47
 - Ionic number, calculation, 56
 - Ionic percentage, 42
 - Ionic volume,** 55-58
 - calculation, 57
 - Cienega volcanic rocks, 58
- Jemez Mountains, *pl. 1, pl. 2*
- Johannsen, A., 41
- Juan, V. C., Tai, H., and Chang, F. H., 51
- Kelley, V. C., 5, 23
- Kimberlite, 52
- Kottowski, F. E., 22
- La Bajada, *pl. 1*
 - constriction, 5, 22, 23
 - fault, 23
 - Mesa, *pl. 1*
- Lamy*, 20, *pl. 1*
- Laramide orogeny, 20
- Las Tetillitas, 11, 18, 21, *pl. 1, pl. 2*
- Latite (*see also* Calcic latite; Glassy latite), 26-27
- Limburgite dikes,** 11, 16, 18
 - index of refraction, 49, 50
 - samples, 70
- Lorentz-Lorenz formula, 46
- Los Alamos, *pl. 1*
- Magmatic differentiation, 38 Mancos shale, 8, 19

Manganese oxide, 12
 Mathews, W. H., 45
 Mesa Negra, 3, 4, 18, *pl. 1*
 Mesozoic, 8
 Minor constituents, 51-53
 Miocene, 5, 7
 Modal analysis, 26, 40, 42
Molecular norm, 37, **41-45**
 advantages, compared with weight norm, 42
 average igneous rock, 44
 Barth's rules for calculation, 42, 45
 Cienega volcanic rocks, 44
 rules for calculation, 62-66
 Molecular refractivity, 47
 Molecular weights, 59
 Monzonite (*see also* Augite monzonite; Hornblende monzonite), 26-27
 orthoclase-plagioclase ratio of Daly's average, 26-27
 Morey, G. W., 46
 Muthuswami, T. N., 41

 Niggli, P., 41
 and Lombaard, B., 41
 Normative analysis, 26, 40
Norm classification (*see also* Weight norm; Molecular norm), 38-40
 rules for calculation, 59

 Oligocene, 5, 7
Olivine basalt (in Cieneguilla limburgite), 15, **33-34**, 36
 calculation of standard rock cell, 56
 chemical analysis, 54
 Holmquist formula, 55
 index of refraction, 48, 50
 ionic composition, 58
 minor constituents, 52, 53
 norms, 43, 44
 petrographic description, 34
 standard rock cell, 56
 One-cation oxide, 41, 61
 Orthoclase-plagioclase ratio, 26-27
 Ortiz Mountains, 5, 23, *pl. 1*
 Oxygen number, 54

 Pauling, L., 46, 56 Petrified wood, 8, 20 Petrographic descriptions, 27-35
 Pleistocene, 5, 7, 22-23
 Pliocene, 5, 7, 22-23
 Precambrian pebbles, 10

 Rankama, K., and Sahama, T. G., 52 Reed Research, Inc., 6
Regional structure, 5, 23

- Rio Grande, 3, *p1.1*
 structural trough, 5, 23
- Robinson, P., 20
- Rosario fault, 23
- Sample localities**, 69-73, *pl. 1*
- Sandía Mountains, *pl. I*
- Sangre de Cristo Mountains, 18, *p1.1*
- Santa Fe**, 3, *p1.1*
 ancestral river, 18, 19
 area, 3, 5, 18
 County, 4
 embayment, 5, 23
 formation, 22
 River, 3, 4, 5, 18, 19, *pl. 1*
- Santo Domingo, *pl. 1*
 structural basin, 5, 23
 Valley, 21
- Sequence of magmas, 38
- Smith, H. T. U., 22
- Spectrographic analysis** (*see also* Minor constituents), 45, **51**
- Spiegel, Z., and Baldwin, B., 3, 5, 18, 22, 23
- Standard rock cell**, 54
 calculation, 56
- Stanworth, J. E., 46
- Stearns, C. E.**, 3, 5, 6, 8, 10, 15, 16,
 19-22, 23
 summary, 20
- Structure of Cienega area**, 11, 16, **23-25**
 minor Quaternary faulting, 25
- Sun, M.-S. (*see also* Callaghan, E.), 34
- Taiwanite, 51
- Terrace gravel, 19
- Tertiary, 23
- Tesuque formation, 22
- Tetilla Peak, *p1.1*, *p1.2* quadrangle, 3, 5, *p1.1*
 Tilley, C. E., 40, 45
- Titanothera, 26
- Treseder, C. S., 6
- Turquoise Hill, *pl. 2*
 quadrangle, 3, 5, *p1.1*
- Turquoise Trading Post, *p1.1*
- Variation diagram:**
cation, 37, 37
oxide, 36, 36-37
 total oxygen versus cations, 38, 39
- Vent breccia**, 14, **15**, *p1.1*
 index of refraction, 49, 50
 petrographic description, 33 samples, 70
- Volcanic conglomerate**,
 14 samples, 71
- Volcanic glass, natural, 49,
 51 Volume of a rock, 55
- Washington, H. S., 40
- Weight norm**, **40-41**
 average igneous rock, 43
 Cienega volcanic rocks, 43
 compared with molecular norm, 42
 rules for calculation, 60-64
- Wells, R. C., 73
- White Rock Canyon, *p1.1*
- Wickman, 52
- Winkler, H. A., 18